Aplicación de la Aritmética por Intervalos para formular un método en Detección y Aislamiento de Fallas (FDI).

Eduardo Cortés Cruz

Universidad Nacional de Colombia
Facultad de Ingeniería, Departamento de Ingeniería Mecánica y Mecatrónica
Bogotá D.C, Colombia
Año 2025

Aplicación de la Aritmética por Intervalos para formular un método en Detección y Aislamiento de Fallas (FDI)

Eduardo Cortés Cruz

Una disertación presentada para cumplir con los requisitos de
el grado de Doctor en Filosofía en Ingeniería Mecánica y Mecatrónica.

Director:
Ph.D. Jorge Ivan Sofrony Esmeral

Co-Director:
Ph.D. Jesús David Avilés Velázquez

Area de investigación:
Ingeniería de Automatización, Control y Mecatrónica.
Universidad Nacional de Colombia
Facultad de Ingeniería, Departamento de Ingeniería Mecánica y Mecatrónica
Bogotá D.C, Colombia
Año 2025

Resumen

Esta tesis doctoral introduce una propuesta novedosa en el ámbito de la detección y aislamiento de fallos FDI en sistemas de transporte de fluidos a través de tuberías horizontales, al emplear la aritmética por intervalos como referente analítico. El enfoque desarrollado destaca por su confiabilidad y precisión, haciendo uso de los principios fundamentales de la aritmética por intervalos para mejorar la eficiencia en la identificación de fugas en tuberías horizontales cuando un fluido circula a través de ellas. El estudio se adentra en la formulación de un método integral que busca superar las limitaciones convencionales al abordar de manera efectiva la incertidumbre inherente en las mediciones y los errores de modelado presentes al utilizar modelos analíticos para describir el movimiento de un fluido en una tubería horizontal.

En este contexto, la aritmética por intervalos proporciona un marco analítico para gestionar las variabilidades numéricas y expresiones algebraicas surgidas durante la obtención del modelo analítico tipo intervalo y posteriormente diseñar sobre este modelo intervalo un estimador de estados analítico denominado observador intervalo, para tener una descripción total del fenómeno físico y posteriormente validar estos modelos analíticos tipo intervalo para obtener una validación FDI que va permitir realizar análisis FDI de fugas.

Este enfoque analítico se revela como un elemento clave para obtener resultados más estructurados y confiables en la detección de fugas cuando un fluido circula por una tubería horizontal.

La relevancia práctica de esta investigación resalta en la capacidad del método propuesto para lograr una detección confiable de fugas. Este logro no solo impulsa el avance en la investigación académica, sino que también busca establecer aplicaciones tangibles y valiosas en el ámbito industrial. La implementación de esta innovación contribuye directamente a mejorar la seguridad y la gestión de recursos en infraestructuras críticas, marcando un hito en la convergencia entre la investigación teórica y la solución de problemas prácticos en el sector del transporte de fluidos. Este enfoque integral promete generar un impacto positivo y duradero en la integridad y operación de sistemas de transporte de fluidos a través de tuberías a nivel global.

key words: Aritmética por Intervalos, modelo intervalar, observador por intervalos,Análisis FDI, transporte de fluidos

Application of Interval Arithmetic to formulate a method in Fault Detection and Isolation (FDI).

Eduardo Cortés Cruz

Universidad Nacional de Colombia
Facultad de Ingeniería, Departamento de Ingeniería Mecánica y Mecatrónica
Bogotá D.C, Colombia
Año 2025

Application of Interval Arithmetic to formulate a method in Fault Detection and Isolation (FDI).

Eduardo Cortés Cruz

A dissertation submitted to satisfy the prerequisites for
the degree of Doctor of Philosophy in Mechanical & Mechatronic Engineering.

Adviser:
Ph.D. Jorge Ivan Sofrony Esmeral

Co-Adviser:
Ph.D. Jesús David Avilés Velázquez

Research Area:
Automatization Engineering, Control and Mechatronic
Universidad Nacional de Colombia
Facultad de Ingeniería, Departamento de Ingeniería Mecánica y Mecatrónica
Bogotá D.C, Colombia
Año 2025

Abstract

This doctoral thesis presents the use of interval observers in the field of Fault Detection and Isolation (FDI), with application to fluid transportation systems through horizontal pipelines. Employing interval arithmetic as the theoretical basis, the developed approach stands out for its reliability and precision, leveraging the fundamental principles of interval arithmetic to enhance efficiency in identifying system faults.

The study delves into the formulation of a comprehensive method aiming to overcome conventional limitations by effectively addressing the inherent uncertainty in measurements and modeling errors encountered when using analytical models to describe fluid movement in a horizontal pipeline. System and signal uncertainty complicates the identification of faults, reducing accuracy.

In this context, interval arithmetic provides an analytical framework for managing numerical variability and algebraic expressions that arise during the acquisition of the interval-type analytical model. An observer is designed using an interval model to provide enhanced fault detection and uncertainty rejection. The interval-type analytical models are then validated on a reals life example to obtain an FDI validation, enabling FDI analysis of faults. This analytical approach proves to be a key element in obtaining more structured and reliable results in fault detection under the presence of system uncertainty and signal perturbation.

The practical relevance of this research is highlighted by the proposed method's capability to achieve reliable leak detection. This achievement not only contributes to the advancement in academic research but also seeks to establish tangible and valuable applications in the industrial sector. The results if this research directly contribute to enhancing safety and resource management in critical infrastructures, marking a milestone in the convergence between theoretical research and the practical problem-solving in the fluid transportation sector. This approach promises to generate a positive impact on the integrity and operation of fluid transportation systems through pipelines.

Keywords: *Interval arithmetic, interval models, interval observers, FDI analysis, fluid transport*

Les lois de l'aérodynamique n'autorisent pas le scarabée à voler ; mais les lois de Dieu permettent au scarabée de voler

A Dios .

A la Memoria de Mi Padre.

A Mi Mamá.

A Sandra

No pienses que no pasa nada, simplemente porque no ves tu crecimiento... las grandes cosas crecen en silencio.

Buda

Acknowledgments

Firstly, I want to thank God and Mother Mary for allowing me to conclude this life experience at my current age. To my mother, Sandra, and all those individuals who have always been with me unconditionally. To all the wonderful people I have met during my time at the National University of Colombia, a university that will always hold a special place in my heart. Likewise, to all the teaching and administrative staff at the National University of Colombia, individuals who consistently collaborated and instilled in me encouragement and determination.

I express my gratitude to my thesis advisor, Dr. Jorge Sofrony Esmeral, for his endless patience, and to my thesis co-advisor, Dr. Jesús David Avilés Velázquez, a professor at the University of Baja California, whom I always felt as an unwavering guide. To the TURIX group in Mexico for inviting me as a student to participate in various international courses, where beyond the academic involvement, I deeply appreciated the welcome received from the instructors.

I also want to thank Dr. Cristina Verde, Dr. Lizeth Torres, Dr. Gloria Gordillo, Dr. Carlos Astorga, Dr. Filippo Cacace, and Dr. Nacim Meslem for the valuable recommendations provided during academic consultations for this doctoral thesis. In advance, I express my gratitude to the committee members who will review this document; I am confident that their important comments will serve as positive feedback for this doctoral thesis, which I endeavored to create with utmost originality and effort.

I apologize for not mentioning many individuals and entities that, in various ways, have contributed to my journey thus far. To everyone: Thank you very much.

Statement of Originality

I affirm that I have carried out this thesis independently and with the only assistance of the permitted resources, as specified in the thesis itself. Any passages taken directly or figuratively from published and unpublished texts have been acknowledged in this work. No part of this thesis has been used in any other type of thesis.

Bogotá, June 2025 _____
Eduardo Cortés Cruz

Contents

List of Figures

List of Tables

Notation and Glossary

The symbol $\succeq$ denotes a partial order for two vectors $x, z \in \mathbb{R}^n$; if $x_i \geq z_i$ for all $i = 1, ..., n$ then $x \succeq z$. Also, the partial order is expressed for two matrices $A, B \in \mathbb{R}^{n\times m}$, if $A_{ij} \geq B_{ij}$ then $A \succeq B$. In particular, if $x \succeq 0$ then x is a nonnegative vector, i.e. $x_i \geq 0$ for all $i = 1, ..., n$. A nonnegative matrix $A \in \mathbb{R}^{n\times m}$ will denoted as $A \succeq 0$, iff $A_{ij} \geq 0$ with $1 \leq \{i, j\} \leq n$. This notation should not be confused with that of a positive definite matrix P (resp. positive semi-definite), which is represented by $P = P^T > 0$ (resp. $P = P^T \geq 0$). Similarly, $P = P^T < 0$ (resp. $P = P^T \leq 0$) is a negative definite matrix P (resp. negative semi-definite). Furthermore, $M = \max\{A, B\}$ is the matrix where each entry is $m_{ij} = \max\{a_{ij}, b_{ij}\}$. The positive decomposition of a matrix $N \in \mathbb{R}^{n\times m}$ is given by $N^+ = \max\{N, 0_{p\times m}\}$ and $N^- = \max\{-N, 0_{n\times m}\}$, such that $N = N^+ - N^-$ and the element-wise absolute value is $|N| = N^+ + N^-$.

Definition 1. *The positive representation of vectors, matrices, and other expressions is defined by the following items (Cacace et al., 2015):*

1. *The positive representation for any vector $x \in \mathbb{R}^n$ is defined as:*

$$X = \begin{bmatrix} x^+ \\ x^- \end{bmatrix} \in \mathbb{R}^{2n}, \qquad x^+ = \max\{x, 0\}, \quad x^- = \max\{-x, 0\}.$$

2. *For any matrix $N \in \mathbb{R}^{n\times m}$,*

$$\tilde{N} = \begin{bmatrix} N^+ & N^- \\ N^- & N^+ \end{bmatrix},$$

3. *For any square matrix $N \in \mathbb{R}^{n\times n}$,*

$$[N] = \begin{bmatrix} d^N - (N - d^N)^+ & (N - d^N)^- \\ (N - d^N)^- & d^N - (N - d^N)^+ \end{bmatrix},$$

   where $(N - d^N)^+ = \max\{N - d^N, 0\}$, $(N - d^N)^- = \max\{-(N - d^N), 0\}$, and d^N is the diagonal matrix $d^N = diag\Big(N_{11}, N_{22}, \ldots, N_{nn}\Big)$.

4. *A positive representation of a vector $x \in \mathbb{R}^n$ is a positive vector $X \in \mathbb{R}^{2n}_+$ such that $x = \Delta_n X$, where $\Delta_n = \begin{bmatrix} I_n & -I_n \end{bmatrix}$.*

5. *The min-positive representation of a vector $x \in \mathbb{R}^n$ is the positive vector $\pi(x) \in \mathbb{R}^{2n}_+$ defined as $\pi(x) = \begin{bmatrix} (x^+)^T & (x^-)^T \end{bmatrix}^T$*

6. *For a given $a \in \mathbb{R}^n$, the positive representation function is*

$$\phi_a(x) = \begin{bmatrix} x + a^- \\ a^- \end{bmatrix}$$

7. *The function* $\phi_a(x)$ *is such that* $\Delta_n \phi_a(x) = x$, $\forall x \in \mathbb{R}^n$, *and for any three vectors* a, x, b *in* $\mathbb{R}^n$ *such that* $a \preceq x \preceq b$ *it follows* $0 \preceq \phi_a(a) \preceq \phi_a(x) \preceq \phi_b(b)$.

8. *Defining* $\tilde{\phi}_A(N)$ *as*

$$\tilde{\phi}_A(N) = \begin{bmatrix} N + A^- & A^- \\ A & N + A^- \end{bmatrix}$$

If $A \preceq N$, $\tilde{\phi}_A(N)$ *is nonnegative. Moreover if* $\Delta_n X = x$ *then* $\Delta_n \tilde{\phi}_A(N) X = Nx$

9. *Given a nonsingular matrix* $T \in \mathbb{R}^{n \times n}$ *and a vector* a *in* $\mathbb{R}^n$, *and defining* $U = T^{-1}$, *the function* $\psi_{T,a}$*:* $\mathbb{R}^n \to \mathbb{R}^{2n}$, *therefore*

$$\psi_{T,a}(x) = \tilde{U}\phi_a(x) = \begin{bmatrix} U^+ & U^- \\ U^- & U^+ \end{bmatrix} \begin{bmatrix} x + a^- \\ a^- \end{bmatrix}$$

The function $\psi_{T,a}(x)$ *is such that*

$$\Delta_n \tilde{T} \psi_{T,a}(x) = x \qquad \forall x \in \mathbb{R}^n$$

and, for any three vectors a, x, b *in* $\mathbb{R}^n$*such that* $a \preceq x \preceq b$ *we have* $0 \preceq \psi_{T,a}(a) \preceq \psi_{T,a}(x) \preceq \psi_{T,a}(b)$.

Table 0-1: Glossary of symbols commonly used in this work.

$\mathbb{A}^I$	Interval matrix
$\mathbb{IR}^n$	The set of real interval vectors of dimension n
$\mathbb{IR}^{n \times m}$	The set of interval real matrices of dimension $n \times m$
$\mathbf{A}^\dagger$	Pseudo-inverse matrix
$\mathbb{R}$	Set of real numbers
$\mathbb{R}^n$	Set of real vectors of dimension n
$\mathbb{R}^{n \times m}$	Set of real matrices of dimension $n \times m$
$\mathbb{C}$	Set of complex numbers
r^I	interval residue
$\mathbf{R}_+$	Set of positive real numbers
$\mathbf{R}_-$	Set of negative real numbers

1 Introduction

Currently, industrial processes demand increasing efficiency and reliability, driving a constant evolution of associated technologies. These processes can be highly complex, composed of numerous interconnected devices and subsystems controlled by computers with schemes designed to function in diverse and often unpredictable environments.

For example, in a power plant, more than a thousand data points are generated per minute and sent to the control center, which must respond automatically (real-time), continuously, and quickly to the variable demand of the grid. Similarly, the automobile efficiency of engines has improved, and pollution has been reduced by increasing the number of automatic control loops for these complex tasks. Control theory must advance in parallel with the growing complexity of systems, requiring more elaborate monitoring schemes for larger-scale processes. Thus, the goal of this work is to contribute to the design of sophisticated, safe, and measurable systems thanks to current technological advancements(Verde et al., 2013). In the current global context, the performance and reliability of these technologies have a direct impact on the environmental setting in which they are implemented. Therefore, any fault (or loss of efficiency) in their performance will directly affect the social and environmental context in ways not considered before. These implications require that any unforeseen condition impacting the normal operation of a system must be detected and corrected (or mitigated) as quickly as possible.

Safety is associated with a set of specifications that physical installations must meet to reduce the risk of accidents. The topic of system monitoring and repeatability emerged in engineering during the 1960s, when important advances were made in the aerospace and nuclear industries, making these fields pioneers in systematizing and defining safety standards. Given the devastating consequences that failures may induce in these types of industries, they were classified as safety-critical systems. Today, there are standards for all types of complex systems, and they are generally standardized through international agreements. In this regard, it is essential that systems perform their assigned functions correctly and have the ability to detect (and later mitigate) in a timely manner when they cannot be carried out. Additionally, systems must be designed to withstand unforeseen conditions, culling actions whose consequences may be dangerous for installations, the environment, and society. This need has led to the concept of process and service unit monitoring, which is associated with the ability to continuously detect abnormal behavior.

System fault monitoring may be performed in diverse manners. At one end, humans can monitor the state of the installation via a control dashboard, e.g., operators in a power plant

or aircraft crew; at the other extreme, automatic systems can be designed where faults may be detected through redundant (physical or analytical) information. A middle ground between these options is to carry out a collaboration between operators and programmed functions in the automatic control system. Fault Detection and Isolation (FDI) analysis proposes a methodology that uses redundancy to identify faults in a process, so that once the fault is identified, the methodology suggests strategies to prevent this event from disrupting the proper (safe) functioning of the process.
In general terms, a fault is an undesired deviation of at least one characteristic property (feature) of the system from the acceptable, standard condition operation (Isermann, 2005a). It can manifest from an internal event that interrupts structural characteristics such as power supply, communication, or mechanical failures; or it can be triggered by component failure, such as a sensor of actuator fault. These faults can be triggered by changes in environmental conditions, inadequate control by the operator, or component malfunctioning. In any case, the fault is the underlying cause of changes in the system's structure or parameters, which can lead to degraded performance and even catastrophic outcomes. Therefore, it is crucial to design and implement methods that allow the detection of these signals so they can later be controlled.
The action that determines, in a binary manner, the presence of one or more faults, as well as the moment they occur, is known as fault *detection*. If the type of fault is specified and its location identified, then this action is termed fault *isolation*. On the other hand, when the magnitude and behavior over time are determined, this is called fault identification. Finally, when detection, isolation, and identification are all performed, it is considered that a fault diagnosis (FD) has been completed (Khan, 2010).

One approach to designing an FDI system is through hardware (physical) redundancy, which involves installing additional components alongside the main process. While this method provides high reliability and direct fault isolation, it also incurs additional costs and complexity. Alternatively, model-based FDI techniques utilize process models (analytic redundancy) to infer faults by comparing actual outputs with estimated outputs. These methods have proven efficient in detecting faults and have been successfully applied in numerous real-time scenarios. Due to their effectiveness and feasibility for online implementation, model-based FDI techniques have become powerful tools for addressing fault diagnosis in technical processes.

Regarding the model type for a specific dynamic system, observer-based fault detection and isolation (FDI) has attracted considerable interest over the past three decades. While fault detection for linear systems is well-established with numerous effective tools, there is an increasing focus on nonlinear fault detection techniques, as most systems exhibit nonlinear behavior. Although linear methods can be applied by linearizing systems around specific operating points, they lose effectiveness with significant deviations. Furthermore, some processes display hard nonlinearities that cannot be linearized, highlighting the need for specialized nonlinear fault detection methods.

Current application of methods for FDI analysis in pipelines, i.e. FDI analysis for estimating leaks, typically employs a combination of model-based methods, filtering techniques, acoustic monitoring, thermal imaging, data-driven approaches, and transient analysis. Each method has its strengths and limitations, and often a combination is used to enhance detection accuracy and reliability in various operational contexts. As technology evolves, these methods are becoming increasingly sophisticated, allowing for better leak management and mitigation strategies in pipeline systems. However, despite the combination of these methods, the potential for misinterpreting parametric uncertainties, disturbances, or sensor noise still remains at the forefront of research in this field. The interval model, expressed as interval observers, offers a solution by bounding false faults within a threshold. In the presence of actual leaks, the interval model can detect faults as they will fall outside this threshold, thereby reducing the likelihood of false fault detection.

This thesis explores the development of an interval observer model designed for fault detection in dynamic systems, particularly focusing on fluid dynamics in pipelines. The structure is organized into seven chapters, each contributing to the overarching goal of enhancing fault detection techniques through interval arithmetic and analytical modeling.

Chapter 2: Foundations of Analytical Concepts. This chapter establishes the foundational definitions and concepts related to interval arithmetic, positive systems, monotonicity, and fault detection and isolation (FDI) analysis.
Contributions:

- Clarifies essential terminologies necessary for understanding and developing the interval observer.
- Provides a theoretical basis for subsequent chapters focused on interval analytical models.

Chapter 3: Analytical Application Model. Presents a linearized model derived from a nonlinear representation of fluid dynamics in pipelines, particularly under leak conditions.
Contributions:

- Introduces two scenarios for FDI analysis:
  1. Treating leaks as exogenous inputs influencing system behavior, while incorporating parametric uncertainties and sensor noise.
  2. Integrating leak size as an additional state within the linearized dynamic system model.
- Enhances the understanding of how leaks affect system dynamics and monitoring.

Chapter 4: Interval Observer Design Theories. Design theories for interval observers.

Contributions:

- Presents the development of an interval observer that combines the dissipativity property with the H_∞ technique, aiming to ensure the stability of the estimation error system and to preserve the partial ordering between the actual state trajectories and their estimates, even in the presence of parametric uncertainties, disturbances, and sensor noise. This idea is used to integrate conditions of $\mathbb{D}$-stability.
- Introduces a novel interval fault detection design, using the interval observer scheme that provides adaptive thresholds to facilitate fault detection, enhancing the reliability of monitoring systems.

Chapter 5: Interval Observer under Positive Representation Describes the design of an interval observer using positive representations and Jordan transformations.

Contributions

- Ensures cooperative system behavior within the interval observer framework, effectively incorporating uncertainties and disturbances.
- Provides a robust method for enhancing system monitoring under uncertain conditions.
- Design of a bank of interval observers for augmented linearized system.

Chapter 6: Conclusions and Recommendations Summarizes the thesis findings and presents both general and specific conclusions.

Contributions

- Offers recommendations for future research, including new designs for unknown input interval observers and interval adaptive observers.
- Highlights potential pathways for further development of the proposed techniques to enhance fault detection in dynamic systems.

1.1 Objectives

Motivated by the previous discussion, this thesis focuses on developing an interval observer for Fault Detection and Isolation (FDI) analysis based on Arithmetic Theory. The effectiveness of the proposed method is tested on a leak detection application, where an interval observer that facilitates the detection, isolation, and reconstruction of leaks that may occur when fluid flows through a horizontal pipeline is designed.

To propose methods to detect and isolate the occurrence of faults (leaks) in a fluid-transporting duct based on the design of interval observers.

1.1.1 Specific Objectives

1. Study and analyze the mathematical models of dynamic systems that are usually described to represent a fluid circulating in a distribution network.

2. Design an analytical model based on interval arithmetic that describes the best fluid dynamics circulating in a distribution network.

3. Design a redundant analytical model through an interval state observer or an equivalent redundant interval analytical model that describes the best dynamics of the system representing the fluid.

4. Design robust interval residual generators, where interval thresholds are obtained that are highly sensitive to leaks (faults) in the duct but decoupled from the intervals of disturbances and uncertainties in the interval model of the fluid's dynamic system.

5. Design a fault diagnosis algorithm based on interval arithmetic to estimate the detection of faults (leaks) in the duct, using measurements of the fluid's kinematic and kinetic characteristics, such as flow rate, pressure, and velocity.

6. Verify, on an appropriate scale, the operation of the fault diagnosis algorithm based on interval arithmetic through computer simulation.

7. Compare, via computer simulation on an appropriate scale, the fault diagnosis algorithm for the duct described by the analytical model using interval arithmetic with a fault diagnosis algorithm for an analytical model described using conventional arithmetic to evaluate the advantages and disadvantages of the proposed interval FDI method.

1.2 Methodology proposed

The presented methods in this doctoral thesis are referred to the interval observers, which include theories of interval arithmetic, cooperative systems, and positive representations. Such methods are developed through the theories primarily proposed by Avilés and Moreno (2014), Raïssi et al. (2005), and Meslem et al. (2020). The interval observers are intended to enhance the Fault Detection and Isolation (FDI) method for improved analysis in fault (leak) detection and localization.
The proposed FDI analysis has been conducted using the following methodology:

1. Explore and evaluate the mathematical tools necessary for developing a reliable analytical model to represent physical systems that describe the flow of fluid through a horizontal pipeline.

2. Based on previous research Torres et al. (2014), it was found that these physical models are mathematically represented as a set of infinite partial differential equations. Since no analytical solution exists for this type of equation, it is necessary to use approximation methods. A reliable approach for solving these equations is the finite difference method, which is commonly used to discretize such models and derive a nonlinear system with a finite-dimensional independent variable. This approximated nonlinear model is then linearized using standard techniques widely referenced in the literature (Khalil, 2002). Once linearized, the model is represented as a dynamic system in the presence of parametric uncertainties, perturbations, and noise.

3. The first design of an interval observer is based on the positive representation and dissipativity conditions in order to estimate the state vector. Furthermore, a scheme of fault detection is proposed using a residual generator and adaptive thresholds. The method includes the design of the gains by means of Linear Matrix Inequalities. This interval observer is used to detect a leak in a pipeline when fluid is flowing through it.

4. In addition, a new interval observer is designed to preserve the partial ordering between the estimations and the state trajectories of the augmented plant based on cooperative systems. Moreover, it is added a fault detection and diagnosis scheme to detect, isolate, and reconstruct a leak. Furthermore, we incorporate a bank of observers to monitor the health of the pipeline model.

The proposed methodology demonstrated new results, by integrating the positive representation, dissipativity, and cooperativity, leading to the development of interval observers capable of accurate estimations. The interval observers designed in this thesis, have been applied to FDI analysis, which mitigates false fault detections caused by parametric uncertainties, disturbances, and sensor-induced noise. Moreover, it is sensitive to faults resulting from leaks in pipelines during fluid flow.
This thesis provides significant advancements in the field of fault detection through the development of innovative interval observer models. By addressing uncertainties and disturbances, it offers new solutions for monitoring dynamic systems, particularly in applications related to fluid dynamics in pipelines. The findings pave the way for future research and applications, enhancing both theoretical understanding and practical implementations of interval arithmetic in FDI analysis.

2 Preliminaries

This chapter is organized as follows: the first section reviews the state of the art related to the subject of this thesis, while the subsequent sections introduce key concepts such as interval arithmetic fundamentals, positive dynamic systems, monotonicity principles, and fault detection techniques. These sections also present important analytical elements supported by theorems, lemmas, and definitions. The aim is to establish the necessary theoretical foundations for understanding the framework behind the proposed analytical tools for a novel Fault Detection and Isolation (FDI) solution, with a focus on detecting leaks in horizontal pipelines during fluid flow.

2.1 FDI Methods for Leak Detection, Isolation, and Reconstruction in Pipelines

The development of Leak Detection, Isolation, and Reconstruction methods for pipelines has become increasingly important due to the need for ensuring the integrity of fluid distribution systems for water, oil, gas, and other materials; in other words, pipeline transport system are safety-critical and our social activity depends on their correct functioning. Effective leak detection is essential for minimizing economic losses, reducing environmental impact, and maintaining the safety of infrastructure (Verde et al., 2013). To address these challenges, several approaches have been explored within the framework of Fault Detection and Isolation (FDI). Below is an overview of the primary methods, including their advantages and disadvantages.

Model-Based Methods. FDI methods are based on mathematical models that use physical laws to describe the flow dynamics in pipelines. These models often rely on first principles equations (e.g. the continuity equation and the principle of energy conservation) to describe system variables (e.g. such as pressure and flow rate, among others). By comparing the model's estimated values to real measurements (i.e. estimation residual), anomalies that may indicate leaks can be detected. Model-based techniques present the following advantages:

- They provide high accuracy in leak detection when the model is well-calibrated and reliable data is available.

- These methods are capable of detecting small, gradual leaks, as minor deviations in the system's behavior can be identified.

Unfortunately, a proper implementation of model-based FDI techniques must take into account and mitigate the effects of the following disadvantages:

- The accuracy of detection depends heavily on the quality of the model and parameters of the pipeline, which can change over time (e.g., roughness, diameter).
- A dense network of sensors is required to achieve good coverage and ensure detection reliability.
- These methods are sensitive to measurement inaccuracies, especially in the presence of noise.

Key examples for the leak detection problem are given in Delgado-Aguiñaga et al. (2020) and Cugueró-Escofet et al. (2015), where models are based on the continuity equation to detect leaks in water distribution networks. Their study demonstrated that deviations in flow rate and pressure can accurately indicate the presence of leaks.

The *Mass and Energy Balance Method* is a traditional technique for detecting leaks by comparing the volume or energy entering a pipeline with the volume or energy exiting it. Any discrepancy between the two can signal the presence of a leak. It is easy to implement, requires few sensors, and has been extensively used in industry for many years. These techniques cannot precisely locate the leak; they can only detect its presence. Moreover, such methods may be ineffective in detecting small or distributed leaks. The work conducted by Karim et al. (2015), Hadroug et al. (2017) about gas pipelines showed that the mass balance method is effective for detecting large leaks but insufficient for smaller or slow-developing leaks.

Model-based FDI schemes typically rely on state-observers (Verde and Visairo, 2001; Besançon et al., 2013; Santos-Ruiz et al., 2018) where the analytical model is used to design an estimator that can determine the deviation of the estimated states from known and available measurements, i.e., create a residual. In the context of pipelines, state observers such as the Kalman filter or Luenberger observers are used to estimate critical variables like pressure and flow. When discrepancies arise between the estimated and actual measurements, they may indicate a leak. Using the *Unknown Input Observer* (UIO) approach presents the following advantages:

- Robust observers can reduce the system's sensitivity to noise and measurement disturbances.

- It is possible to isolate and locate leaks within specific areas of the network by analyzing the residuals generated by the observer.

Unfortunately, model based UIO requires detailed knowledge of the system, where dealing non-linear models or uncertain systems can be challenging. The success of detection is highly dependent on the quality of measurements and the precision of the model, hence noise highly affects detection and isolation properties.

The works developed by Gao et al. (2015), Besançon et al. (1996), Verde and Visairo (2001), implemented different types of estimators such as Luenberger and extended Kalman filters to monitor natural fluid distribution systems. Their real-time leak detection approach was effective, although it faced limitations in accurately locating leaks in systems with complex topologies.

In the last decade, *Data-Driven Methods* methods have seen an accelerated development due to the advancements in sensor technology and the availability of large datasets, and the introduction of new data-driven methods based on machine learning. These methods detect leaks by identifying abnormal patterns in historical operational data and do not require detailed physical models, making them applicable across various pipeline systems. Data-Driven (DD) FDI schemes can adapt to systems with changing operating conditions and are effective in identifying complex patterns that may be missed by traditional model-based methods. Unfortunately, DD FDI techniques require large amounts of training data and significant computational resources; methods often lack "interpretability", making it difficult to understand results in physical terms.

In Fares et al. (2023), Drogkoula et al. (2023), a neural network is designed to detect leaks in water distribution systems. While the method successfully detected leaks, its precision in locating the leaks was limited, and false alarms occurred frequently in the presence of noisy data.

The second part of this chapter provides the necessary foundations of Interval Arithmetic theory, which introduces the concept of lower and upper bounds as interval representations for numbers, algebraic expressions, matrices, and vectors. Additionally, this section covers concepts related to positive systems, monotonicity properties, and principles of FDI, establishing the foundational knowledge required for the proposed solution to detect leaks in fluid transport pipelines.

2.2 Fundamentals of Interval Arithmetic

This section presents the mathematical fundamentals through lemmas necessary for an appropriate analytical formulation (Moore et al., 2009; Jaulin and Walter, 1993).

Definition

Definition 2. *The interval representation of the scalar variable x is defined by a lower limit $\underline{x}$ and an upper limit $\overline{x}, as x^I = [\underline{x}, \overline{x}] \in \mathbb{IR}$* where $[\underline{x}, \overline{x}]$ are the minimum and maximum values of the numerical value of x represented in the bounded interval.

There also exists a special interval representation for a numerical or algebraic expression when given an interval representation $x^I = [\underline{x}, \overline{x}]$. If the values of $\underline{x}$ and $\overline{x}$ are equal, this interval representation is known as a degenerate interval Moore et al. (2009).

Definition 3. *Internal interval operation. The following algebraic operations exist within the bounds of the lower and upper limits of the interval. These operations are:*

1. *Midpoint or nominal value of an interval x^I. It is defined by:*

$$mid\,(x) = \frac{\underline{x} + \overline{x}}{2} \tag{2-1}$$

2. *The width of an interval x^I is defined by:*

$$w = \overline{x} - \underline{x} \tag{2-2}$$

3. *Absolute value of an interval x^I:is defined by:*

$$Magnitude = Max\,[\,|\,\underline{x}\,|, |\,\overline{x}\,|\,]$$

4. *Radius of an interval x^I is defined by:*

$$rad\,(x) = \frac{\overline{x} - \underline{x}}{2} \tag{2-3}$$

Definition 4. *Logical operations: The primary logical operations are as follows:*

1. *Intersection of two intervals x^I and y^I is defined by two cases:*
   a) *if either $\overline{y} < \underline{x}$ or $\overline{x} < \underline{y}$ then, $x^I \cap y^I = \emptyset$*
   b) *Otherwise, $x^I \cap y^I = \left[\max\left\{\underline{x}, \underline{y}\right\}, \min\left\{\overline{x}, \overline{y}\right\}\right]$*
2. *The union of two intervals x^I and y^I is also studied in two scenarios:*
   a) *if either $\overline{y} < \underline{x}$ or $\overline{x} < \underline{y}$ then, $x^I \cup y^I$ is not possible because the intervals are mutually exclusive*
   b) *Otherwise, $x^I \cup y^I = \left[\min\left\{\underline{x}, \underline{y}\right\}, \max\left\{\overline{x}, \overline{y}\right\}\right]$*

According to the above, the union operation between two intervals does not always exist. The subsequent logical operation encompasses the union operation (Moore et al., 2009).

3. *The interval hull operation is defined for given intervals x^I and y^I, as:*

$$x^I \underline{\cup} y^I = \left[\min\left\{\underline{x}, \underline{y}\right\}, \max\left\{\overline{x}, \overline{y}\right\}\right]$$

An additional property regarding the interval hull operation is as follows (Moore et al., 2009):

$$x^I \cup y^I \subseteq x^I \underline{\cup} y^I$$

Definition 5. *Order Relations for Intervals: It is a well-established fact that the real numbers, denoted by $\mathbb{R}$, are ordered by the relation $<$. This relation is known to be transitive if $a < b$ and $b < c$, then $a < c$ for any a, b, and $c \in \mathbb{R}$. A similar relation can be defined for intervals. For instance, the expression $x^I < y^I$ implies that $\overline{x} < \underline{y}$.*

Moreover, if within an interval x^I, where: $\underline{x} = \overline{x}$, this type of interval is defined as a degenerate interval. Hence, the interval contains a single real number x.

Furthermore, if an interval $x^I > 0$ implies that $\underline{x} > 0$ and $\overline{x} > 0$, similarly, if $x^I < 0$ implies that $\underline{x} < 0$ and $\overline{x} < 0$. Another transitive order relation for intervals is the set inclusion defined by

$$x^I \subseteq y^I$$

The statement holds true if and only if $\underline{y} \leq \underline{x}$ and $\overline{x} \leq \overline{y}$

Definition 6. *Interval vector: An interval vector is an n-dimensional array of intervals, where each component forms a closed and bounded subset defined as the Cartesian product of n intervals. These can be represented in vector form as a row vector:*

$$[\mathbf{x}] = ([x_1] \times [x_2] \times ... \times [x_n])$$

Interval vectors can also be represented in a compact form, such as:

$$[\mathbf{x}] = [\underline{\mathbf{x}}, \overline{\mathbf{x}}]$$

where the interval vector $\underline{x}$ is defined as the lower bound interval vector, and the interval vector $\overline{x}$ is defined as the upper bound interval vector.

$$\underline{\mathbf{x}} = \left(\underline{x_1}, \underline{x_2}, , , ., \underline{x_n}\right)$$

$$\overline{\mathbf{x}} = (\overline{x_1}, \overline{x_2}, ..., \overline{x_n})$$

The set of all interval vectors in $\mathbb{R}^n$ is denoted as $\mathbb{IR}^n$

$$\mathbb{IR}^n = \{([\mathbf{x_1}], ..., [\mathbf{x_n}] \mid [\mathbf{x_1}], ..., [\mathbf{x_n}] \in \mathbb{IR})\}$$

Definition 7. *An interval matrix $A^I \in \mathbb{IR}^{n\times n}$ is defined by having each or any of its components $a_{i,j}$ where $i = 1 : n$, $j = 1 : n$, represented as intervals $a^I_{i,j} = \left[\underline{a}_{i,j}, \overline{a}_{i,j}\right]$. In general, it is defined as follows:*

$$\mathbf{A^I} \in \left[\underline{\mathbf{A}}, \overline{\mathbf{A}}\right]$$

where:

$$\underline{A} = \begin{bmatrix} \underline{a}_{1,1} & \cdots & \underline{a}_{1,j} \\ \vdots & \ddots & \vdots \\ \underline{a}_{i,1} & \cdots & \underline{a}_{i,j} \end{bmatrix}, \overline{A} = \begin{bmatrix} \overline{a}_{1,1} & \cdots & \overline{a}_{1,j} \\ \vdots & \ddots & \vdots \\ \overline{a}_{i,1} & \cdots & \overline{a}_{i,j} \end{bmatrix}.$$

An alternative analytical expression for an interval matrix is by representing it as a combination of a central or nominal matrix and a radius matrix. The expressions for these equivalences are given below:

$$\begin{aligned} \mathbf{A_c} &= \frac{(\underline{\mathbf{A}}+\overline{\mathbf{A}})}{2}, \\ \Delta_\mathbf{r} &= \frac{(\overline{\mathbf{A}}-\underline{\mathbf{A}})}{2} \end{aligned}$$

Thus, the interval matrix can also be represented as:

$$\mathbf{A^I} = [\mathbf{A_c} - \boldsymbol{\Delta}_\mathbf{r}, \mathbf{A_c} + \boldsymbol{\Delta}_\mathbf{r}]$$

The radius matrix $\Delta_\mathbf{r}$ represents the component of the matrix that is analytically associated with the average perturbation within the interval matrix Deif (1990).

Definition 8. *Subset Property and Monotonic InclusionMoore (1987) : Consider an arbitrary interval mapping $g : M_1 \to M_2$, where M_1 and M_2 are two arbitrary interval sets. The union extension set $\overline{g} : S(M_1) \to S(M_2)$ exhibits the subset property of:*

$$X, Y \in S(M_1) \quad con \quad Y \subseteq X \iff \overline{g}(Y) \subseteq \overline{g}(X) \tag{2-4}$$

where $S(M_1)$ and $S(M_2)$ denote the families of all subsets of M_1 and M_2 respectively. As mentioned in definition 8, this subset property of $S(M_1)$ implies the condition of the union extension of the interval subset. Likewise, an interval function defined within an interval mapping is monotonically inclusive if all interval variables:

$$Y_i \subseteq X_i \quad i = 1, 2, \cdots, n$$

This implies that the finitely represented mapping between the sets of interval pairs, $(F(Y_1, Y_2, \ldots, Y_n))$ *and* $(F(X_1, X_2, \ldots, X_n))$ *, is related as follows:*

$$F\left(Y_1, Y_2, \cdots, Y_n\right) \subseteq F\left(X_1, X_2, \cdots, X_n\right) \tag{2-5}$$

Hence, it can be inferred that all functions $\overline{g}$ *are monotonically inclusive from:*

$$Y_1 \subseteq X_1 \quad y \quad Y_2 \subseteq X_2$$

and the subsequent algebraic properties of the interval function must be satisfied:

$$\begin{gathered} Y_1 + Y_2 \subseteq X_1 + X_2 \\ Y_1 - Y_2 \subseteq X_1 - X_2 \\ Y_1 \cdot Y_2 \subseteq X_1 \cdot X_2 \\ \frac{Y_1}{Y_2} \subseteq \frac{X_1}{X_2} \end{gathered} \tag{2-6}$$

Definition 9 (Inclusion function Sin (2006))**.** *Consider a function* `f` *defined on* $\mathbb{R}^n \to \mathbb{R}^m$*. The interval function* $[\mathtt{f}]$*, defined on* $\mathbb{IR}^n \to \mathbb{IR}^m$*, is an inclusion function for* `f` *if:*

$$\forall \quad [x] \quad \in \quad \mathbb{IR}^n \quad , \mathtt{f}\left([x]\right) \subset [\mathtt{f}]\left([x]\right)$$

The interval function: $[\mathtt{f}]\left([x]\right) \in \mathbb{IR}^m$*.*

As shown in Figure **2-1**, the red interval enclosure depicts the smallest image and therefore corresponds to the minimal inclusion function (Sin, 2006).

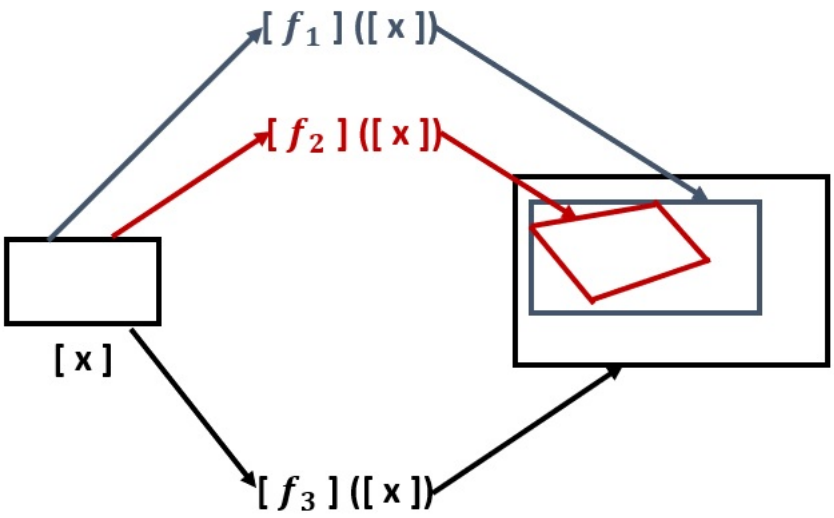

Figure 2-1: Graphical Representation of Inclusion Function.

Definition 10. *Function of Minimal Inclusion Sin (2006)*

Consider an interval inclusion function $[\mathtt{f}] : \mathbb{IR}^n \rightarrow \mathbb{IR}^m$. *It is termed as a minimal inclusion function if*

$$\forall \quad [x] \quad \in \quad \mathbb{R}^n, \quad [\mathtt{f}]\left([x]\right) = [\mathtt{f}\left([\mathtt{x}]\right)]$$

In order for a minimal inclusion function to exist, two conditions must be met:

1. *Extension: If there exists in the domain interval:* $[x] = [\underline{x}, \overline{x}] \mid \underline{x} = \overline{x}$, *then the value of the interval image must exist as well:* $[\mathtt{f}]\left([x]\right) = \mathtt{f}\left(\mathtt{x}\right)$.
2. *The second condition is related to monotonicity. In other words, if a specific subset is contained within the interval domain, then the image of this subset must also be included in a consistent manner.*

The aforementioned conditions lead to the introduction of the following two additional definitions.

Definition 11. *Consider a function* $\mathtt{f} : \mathbb{R}^n \rightarrow \mathbb{R}^m$. *The interval function* $[\mathtt{f}] : \mathbb{IR}^n \rightarrow \mathbb{IR}^m$ *is an interval extension if:*

$$\forall\, [x] \in \mathbb{IR}^n, [\mathtt{f}]\left([x]\right) = [\mathtt{f}\left([\mathtt{x}]\right)] \tag{2-7}$$

Definition 12. *An interval function* $\mathtt{f} : \mathbb{R}^n \rightarrow \mathbb{R}^m$ *exhibits monotonicity concerning inclusion if:*

$$\forall \quad [x], [y] \in \mathbb{IR}^n \mid [x] \subset [y] \quad , \quad [\mathtt{f}]\left([x]\right) \quad \subset \quad [\mathtt{f}]\left([y]\right) \tag{2-8}$$

The following lemma aims to provide the necessary analysis for defining the interval width concept based on the vector space concept.

Lemma 1. *Consider* X *and* Y *as sets of vectors represented within an interval vector space* $\mathbb{IR}^n$, *given by:*

$$X^I = \left[\underline{X}, \overline{X}\right] \wedge Y^I = \left[\underline{Y}, \overline{Y}\right]$$

The interval width for these two vectors is defined as the algebraic operation:

$$w^I = X^I - Y^I = \left[\ \underline{X} - \overline{Y} \quad , \quad \overline{X} - \underline{Y}\ \right]$$

Proof. The algebraic operator $\diamond \equiv -$ representing subtraction can be replaced by the operator $\diamond \equiv +$, as follows:

$$w^I = X^I - Y^I \equiv X^I + [-Y^I]$$

$$w^I = [\underline{X}, \overline{X}] + [-\overline{Y}, -\underline{Y}] = [\underline{X} - \overline{Y}, \overline{X} - \underline{Y}]$$

From the provided expression, it is stated that the interval vector Y^I is a subset of X^I.

$$\overline{Y} \succeq \underline{X} \quad \wedge \quad \underline{Y} \prec \overline{X} \wedge \overline{Y} \prec \overline{X}$$

□

2.3 Cooperative and Positive Systems

In dynamical systems, the property of cooperativity implies a partial ordering of the state and output trajectories, preserving a monotone structure, while the property of positivity ensures that these state and output trajectories remain within the non-negative set. Both properties are fundamental in the modeling and analysis of physical, biological, chemical, and socio-economic systems. In this subsection, we introduce key definitions and system classes associated with cooperativity and positivity, which constitute a subclass of monotone systems, as discussed in Angeli and Sontag (2003); Avilés and Moreno (2014). These concepts will be used in Chapters 4 and 5 for the design of interval observers and fault detection strategies.

Definition 13 (Angeli and Sontag (2003)). *$A \in \mathbb{R}^{n\times n}$ is a Metzler matrix if all its off-diagonal entries are nonnegative elements, i.e., $a_{i,j} \geq 0$ for all $i \neq j$.*

Definition 14 (Avilés and Moreno (2014)). *Consider the following linear system expressed as:*

$$\Sigma_L : \begin{cases} \dot{x}(t) = Ax(t) + Bu(t), \quad x(0) = x_0, \\ y(t) = Cx(t), \end{cases} \tag{2-9}$$

where $x(t) \in \mathbb{R}^n$ represents the state vector, $u \in \mathbb{R}^m$ denotes the input vector, and $y \in \mathbb{R}^q$ stands for the output vector. Σ_L is a cooperative system if, under a partial ordering over the initial states and inputs, namely: $x_{20} \succeq x_{10}$, $u_2(t) \succeq u_1(t)$, $\forall t \geq t_0$, then partial ordering remains consistent for the evolution of states $x(t)$ and trajectories $y(t)$ for all future times $t \geq t_0$, that is $x\left(t, t_0, x_{20}, u_2\left(t\right)\right) \succeq x\left(t, t_0, x_{10}, u_1\left(t\right)\right)$ and $y\left(t, t_0, x_{20}, u_2\left(t\right)\right) \succeq y\left(t, t_0, x_{10}, u_1\left(t\right)\right)$.

Based on the above, we present the following proposition:

Proposition 1 (Angeli and Sontag (2003)). *The system Σ_L is a cooperative linear system if and only if*

1. *A is a Metzler matrix ($a_{i,j} \geq 0, \ \forall i \neq j$),*
2. *$B \succeq 0 \quad (b_{i,j} \geq 0, \ \forall i, j)$,*
3. *$C \succeq 0 \ \ (c_{i,j} \geq 0, \ \forall i, j)$.*

We now address the definition and characterization of positive systems.

Definition 15 (Angeli and Sontag (2003)). *Σ_L is a positive linear system if for any $x_0 \succeq 0$ and any $u(t) \succeq 0$, then the trajectory of the state is non-negative $x(t,\, t_0,\, x_0,\, u) \succeq 0$.*

Proposition 2 (Angeli and Sontag (2003)). *If the Σ_L is a linear cooperative system, then it is positive. Conversely, if Σ_L is a positive system, then it is a cooperative system.*

Note that cooperativity shares similarities with the positivity property, particularly when the initial condition satisfies $x_0 \succeq 0$ and $u(t) \succeq 0$, under these conditions, the system yields non-negative trajectories for both the state and output vectors, i.e., $x(t) \succeq 0$, $y(t) \succeq 0$. This behavior highlights the necessary and sufficient conditions established in Proposition 1 for linear time-invariant (LTI) systems. The definition of a positive system implies that if all state trajectories originate from points in the non-negative orthant $\mathbb{R}^n_+$, they will remain in that orthant for all future time. This property characterizes $\mathbb{R}^n_+$ as a positively invariant set. Figure **2-2** illustrates this concept using three non-negative initial conditions, $x_0 \succeq 0$. If the trajectories begin outside the positive orthant, they will enter and remain within it for all future time (Lorenzo Farina, 2011).

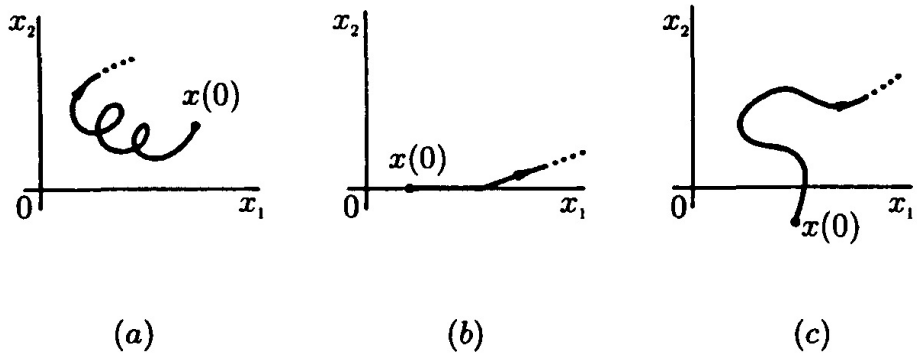

Figure 2-2: Behavior of the state trajectories of a positive system (Lorenzo Farina, 2011).

2.4 Dissipative systems

The dissipativity property, when applied to mathematical models of physical systems, formalizes the principle of energy conservation. In general terms, the amount of energy stored within the system at any given time is always less than or equal to the total energy supplied from the outside. This implies that the system is capable of storing and dissipating energy, but not of generating it (Brogliato et al., 2007; Avilés and Moreno, 2014).

Definition 16. *(Willems, 1972a,b) The linear system* Σ_L *in* (2-9) *is said to be dissipative if there exists an* internal storage function $V : \mathbb{R}^n \to \mathbb{R}$ *(continuous and positive semidefinite) and an* external supply rate function $w : \mathbb{R}^p \times \mathbb{R}^m \to \mathbb{R}$ *such that the* dissipative inequality *holds,*

$$V\left(x\left(t\right)\right) \leq V\left(x_0\right) + \int_0^t w\left(u\left(\tau\right), y\left(\tau\right)\right) d\tau, \qquad \forall \left(x_0, t\right) \in \mathbb{R}^n \times \mathbb{R}. \tag{2-10}$$

Passive systems represent a special class of dissipative systems characterized by an equal number of inputs and outputs $(m = p)$*, characterized through the specific supply rate function,*

$$w\left(u\left(t\right), y\left(t\right)\right) = y^T(t)u(t), \quad \forall \left(x,\, u\right) \in \mathbb{R}^n \times \mathbb{R}^m. \tag{2-11}$$

Moreover, it is worth noting that supply rate functions can be expressed as quadratic functions of the following form,

$$\begin{aligned} w(y,u) &= \begin{bmatrix} y \\ u \end{bmatrix}^T \begin{bmatrix} Q & S \\ S^T & R \end{bmatrix} \begin{bmatrix} y \\ u \end{bmatrix} \\ &= y^T Q y + 2y^T S u + u^T R u \end{aligned} \tag{2-12}$$

where $Q \in \mathbb{R}^{p\times p}, S \in \mathbb{R}^{p\times m}, R \in \mathbb{R}^{m\times m}$ with $Q = Q^\top$ and $R = R^\top$. On the other hand, it is possible to consider quadratic storage functions of the form

$$V(x) = x^T P x, \quad P = P^T > 0. \tag{2-13}$$

for the class of linear systems Σ_L. By applying the dissipative inequality with quadratic storage and supply functions, the following proposition is obtained.

Proposition 3 (Avilés and Moreno (2014))**.** *Σ_L is a dissipative system if there exists the matrix $P = P^\top > 0$ and a scalar $\epsilon > 0$ such that the following dissipative inequality holds*

$$\begin{bmatrix} A^\top P + PA + \epsilon P & PB \\ B^\top P & 0 \end{bmatrix} - \begin{bmatrix} C^\top Q C & C^\top S \\ SC & R \end{bmatrix} < 0 \tag{2-14}$$

Note that the condition in (2-14) can be represented as a Linear Matrix Inequality (LMI), which can be solved using various computational tools.

2.5 Interval observers

According to Avilés and Moreno (2018), an interval observer is formed by two observers that preserve the partial ordering from a partial ordering in the initialization and the inputs. In the following paragraph, we define the notion for this class of observers.

Definition 17. *Thus the dynamical systems*

$$\begin{aligned} \dot{\overline{\xi}}(t) &= \overline{\mathcal{G}}\left(t, \overline{\xi}(t), \overline{u}(t), \overline{v}(t)\right), \quad \overline{\xi}(0) = \overline{\xi}_0 \\ \hat{\overline{x}}(t) &= \overline{\mathcal{E}}\left(t, \overline{\xi}(t), \overline{u}(t), \overline{v}(t)\right) \end{aligned} \tag{2-15}$$

$$\begin{aligned} \dot{\underline{\xi}}(t) &= \underline{\mathcal{G}}\left(t, \underline{\xi}(t), \underline{u}(t), \underline{v}(t)\right), \quad \underline{\xi}(0) = \underline{\xi}_0 \\ \hat{\underline{x}}(t) &= \underline{\mathcal{E}}\left(t, \underline{\xi}(t), \underline{u}(t), \underline{v}(t)\right) \end{aligned} \tag{2-16}$$

where $\overline{\xi} : \mathbb{R}_+ \to \mathbb{R}^n$ and $\underline{\xi} : \mathbb{R}_+ \to \mathbb{R}^n$ represent the estimated states, and the initialisation is given by $\overline{\xi}_0 = \overline{g}(t_0, \overline{x}_0)$ and $\underline{\xi}_0 = \underline{g}(t_0, \underline{x}_0)$, constitute an interval observer if

1. *any solution $\left(\overline{x}(t), \underline{x}(t), \overline{\xi}(t), \underline{\xi}(t)\right)$ of (2-15-2-16) for all $t \in \mathbb{R}$ is such that*

$$\lim_{t\to\infty} |\, \hat{\overline{x}}(t) - \hat{\underline{x}}(t) \,| \to \beta \geq 0;$$

in addition

2. *for any vectors* $x_0, \overline{x}_0, \underline{x}_0 \in \mathbb{R}^n$ *and any input* $u(t)$*and disturbance* $v(t)$ *the solutions of* (2-15), (2-16) *satisfy for all* $t \geq t_0$ *the inequality*

$$\overline{\hat{x}}(t) \succeq x(t) \succeq \underline{\hat{x}}(t)$$

Remark 1. *It is possible to construct an interval observer using two observers: an upper and a lower, each preserving the partial ordering of initial conditions and exogenous inputs. This is the approach used in this thesis.*

In the following paragraphs, we present some important ideas associated to the interval observers.

Lemma 2 (Efimov et al. (2013))**.** *Consider three real vectors* $\underline{x}$,x *and* $\overline{x}$ *belonging to* $\mathbb{R}^n$ *such that* $\underline{x} \preceq x \preceq \overline{x}$*. Then, for any real matrix* $A \in \mathbb{R}^{m\times n}$ *and real vector* x *in the interval* $x \in [\underline{x}, \overline{x}]$*, one obtains*

$$A^+\underline{x} - A^-\overline{x} \preceq Ax \preceq A^+\overline{x} - A^-\underline{x}$$

Also, there are conditions such the matrix A has uncertainties $\Delta A \in \left[\Delta\underline{A},\, \Delta\overline{A}\right]$, where $\underline{A} = A - \Delta A$ and $\overline{A} + \Delta A$. In this case, we have the bounded set as: Khan et al. (2020)

$$\underline{A}^+\underline{x}^- - \overline{A}^+\underline{x}^- - \underline{A}^+x^+ + \overline{A}^-\overline{x}^- \preceq Ax \preceq \overline{A}^+\overline{x}^+ - \underline{A}^+\overline{x}^- - \overline{A}^-\underline{x}^+ + \underline{A}^-\underline{x}^-$$

For this case, the uncertainty ΔA can be evaluated in advance using the methods described in Shary (2018) and Cruz et al. (2023). This is essential because the dynamic system with uncertainties must be analyzed to ensure that the conditions for observability and controllability are met.

2.6 FDI environment

In an industrial context, safety is associated with a set of requirements that any physical installation or work environment must meet to mitigate the risk of accidents. Fault Detection and Isolation (FDI) began to develop as a distinct engineering discipline in the 1960s. Isermann (2005a); Verde et al. (2013). The aerospace and nuclear industries were pioneers in systematizing and defining safety standards due to the consequences of disasters in these types of activities. Currently, there are standards for all types of complex system, generally standardized through regulations in international agreements. In this perspective, it is essential that each system executes its assigned functions correctly and has the ability to communicate in advance when these cannot be performed correctly. In addition, each system must be designed to withstand unforeseen conditions and factors of human error, preventing actions whose consequences could be potentially dangerous to facilities, the environment,

and social surroundings. These facts motivated the creation of analysis tools consolidated under the concept of monitoring processes and service units, which is related to the ability to infer undesired performance continuously.
This inference capability can be feasible through various means. One way is to have human resources assigned to monitor the status of the installation, such as operators in a power plant or the crew of an aircraft. The other way, of extreme nature, is evidenced by the option to automatically monitor systems. A turning point in these options is to have cooperative actions between operators and functions programmed in the automatic control system. FDI analysis is responsible for establishing the design of a methodology whose objective is to identify the scenario of each of the faults that will be involved in a process, so that once the fault is identified, the FDI methodology will propose strategies for the detection, isolation, and reconstruction of each fault, with the purpose of alerting and/or preventing malfunctioning in the process under study.

2.6.1 Methods used for fault detection and diagnosis

The methods used for fault detection and diagnosis are classified in various ways. Some propose models of the system to be evaluated, while others are based on approximation, and still others rely on the process history (Isermann, 2005a,b).

The methods that use system models or their approximations are usually classified into two subgroups:

- Quantitative model-based methods.
- Qualitative model-based methods.

Methods based on processes similarly depend on pre-existing knowledge of the system in both normal and faulty states. This implies that anomalies are anticipated. Much like methods utilizing system models, they are categorized into two subgroups, namely:

- Quantitative methods based on process history.
- Qualitative methods based on process history.

Figure **2-3** presents the general structure for an FDI analysis.

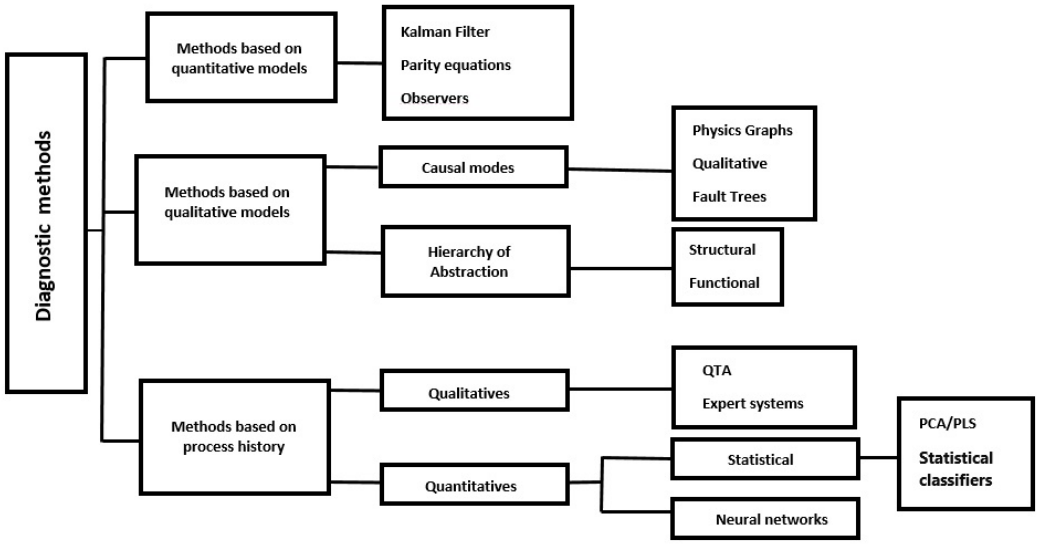

Figure 2-3: Methods for evaluating Fault Detection and Diagnosis,Carrillo et al. (2012)

Methods based on quantitative models of the system

The model originates from a mathematical representation of the system. Its effectiveness and efficiency hinge on how closely it approximates the actual plant. All variables within the model must be correlated with those of the real process to gauge the compatibility between process and model performance. Figure **2-3** illustrates various methods employed to derive models in this category. Observers for dynamic systems, parity equations, Kalman filters, and parametric estimation methods. In these approaches, the plant model incorporates real variables, and the computation of outputs or state variables is executed. Under specific circumstances, comparing real variables with those derived from the model yields quantitative differences known as *residual generators*. When the plant operates correctly, the residual ideally equals zero. The structure of the residual generator determines variations in plant behavior under fault conditions. Additionally, similarities may arise between plant performance and models designed for isolated and specific fault scenarios.

Methods relying on qualitative models of the system or its approximation

These methods rely on an understanding of the process, enabling the recognition of behavioral patterns that deviate from the norm. They are grounded in quantitative knowledge forms.
These methodologies can be categorized into two groups:

- **Causal models** employ cause-and-effect reasoning techniques and tools (abductive, inductive, and deductive reasoning) to describe the system's behavior. Among these, fault trees and graph theory are commonly used reasoning tools, functioning akin to logical operators such as *and* and *or*, thereby generating numerous hypotheses for potential faults. Consequently, decision-making is tailored to each of these hypotheses.

- **Abstraction hierarchy models** break down the system into functional units using input and output data information. This enables the identification of, for instance, the unit malfunctioning in the plant.

Methods based on process history

These methods require a large amount of historical process data and a systematic methodology for extracting process data.
These methods are classified into two groups: qualitative methods and quantitative methods.

- Qualitative methods primarily involve Qualitative Trend Analysis (QTA) and Expert Systems. The Qualitative Trend Analysis (QTA) method utilizes data from sensors monitoring the system to build databases. These databases create trends of variables when the plant is operating correctly, and if these trends deviate from a mean value, a fault alarm is generated.
  Expert systems consist of a database for fault events, containing a set of rules to construct a probabilistic expert system that detects: the fault, the reasons for the fault, and a feasible solution to correct it.

- Quantitative methods based on process history are statistical context methods. To identify and interpret trends and find thresholds close to the mean value that indicate faults, they require analysis time, so continuous calibrations for the system under study are initially necessary. An excellent analysis method for this type of approach is Principal Component Analysis (PCA), where the statistical analysis method is multivariable, offering an alternative for detecting, isolating faults, and transforming multivariate data into a lower-dimensional space. This space retains the most relevant information about the priority fault to identify in the process, significantly simplifying surveillance of the system.
  Another alternative method is based on neural network algorithms (RNA). Neural networks are defined as computing algorithms that base their efficiency on adjusting indicators through weights that weigh the inputs of each neuron (basic calculation element) to calculate the output that should be delivered to other neurons and achieve a common calculation objective throughout the network. The strategy of adjusting these weighting weights constitutes the learning of the system, and the topology (interconnection between neurons) will be the determining factor to evaluate functionality and efficacy. Once training is completed, the weights are established (learning has ended),

and the RNA is ready to function as a system that responds to input stimuli. The fields of application are diverse, such as classification, modeling, function approximation, pattern recognition, etc. There are multiple RNA topologies and various learning strategies.
In fault detection analysis, neural networks perform well in approximating nonlinear functions. Under well-defined conditions, neural networks can replace analytical models when the dynamics of these systems are highly nonlinear and linear approximation is difficult to achieve, such as in flexible chemical process plants, nuclear plants, and aircraft flight control systems.

Classification of Failures according to their Structure

Typically, a failure occurs due to a defect that deviates from the normal operation of a system. This deviation is typically detected through system control signals or measurements. The presence of a failure is associated with the following characteristics:

Failure by Impact

Associated with the effect that the failure will have on the operation of the system. Therefore, two expressions are defined to characterize a failure.

- If the failure, despite occurring, can be corrected, and the system returns to normal performance, this type of failure is known as a fault.
- When the occurrence of the failure results in a total or irreversible collapse in the operation or performance of the system, this type of failure is referred to as a failure.

Failure by Localization

This is associated with the location of the failure, which will be within the system's operation. Figure **2-4** depicts the scheme representing this characteristic of failure and how it is articulated within the system.

- Actuator Failures: Actuators are considered the operational part of the system, responsible for executing the input signals $u(t)$. Therefore, when there are failures in the actuators, these signals are added to the control signals, contributing to the set of issues related to the elements that act on the process. Consequently, this is evidenced by an incompatibility between actuator control and the response at its output $y(t)$. An actuator failure can result in either total loss or partial loss. In the case of total loss, the actuator completely loses its ability to control the system, such as a gate that becomes stuck in its initial position. In a partial loss scenario, the actuator operates in

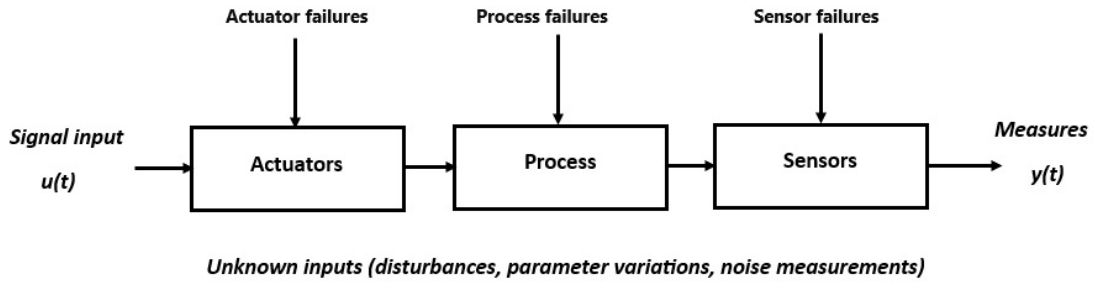

Figure 2-4: Failure by Localization.

a degraded manner, meaning it works nominally but its control action on the system is only partially effective. This phenomenon is typically characterized by a significant loss of energy.

- Process Failures: These directly impact the system itself and involve degradation of system components due to variations in internal parameters. These deficiencies result from modifications or degradation of the system structure compared to the system used to build the model.

- Sensor Failures: Sensors convert a physical quantity into a measurable quantity by an instrument. Sensors serve as the output interface of the system with the external environment. Defects or failures originating from sensors are characterized by discrepancies between the actual value of the physical quantity and the measured value being displayed. Sensor failure measurements are added to the system outputs and represent the set of issues related to capturing information about the system's state. Similar to actuators, sensors can experience either total failure or partial failure. In the case of total sensor failure, it results in the absolute measurement signal from the sensor not being possible. For partial sensor failure, it may be represented by saturation, calibration error, tolerance defect, or the presence of noise.

Temporal Effects Failure

A Temporal-Effects failure is any fault whose signature lies in the time domain. Figure **2-5** illustrates the time behavior of the occurrence of the failure that the three types of trends within the system may exhibit.

Internal System Fault

The study focuses on faults that originate within the dynamic system and evaluates how their characteristics affect overall performance, as revealed by the system's transfer function. Based on this analysis, such faults can be classified into two categories:

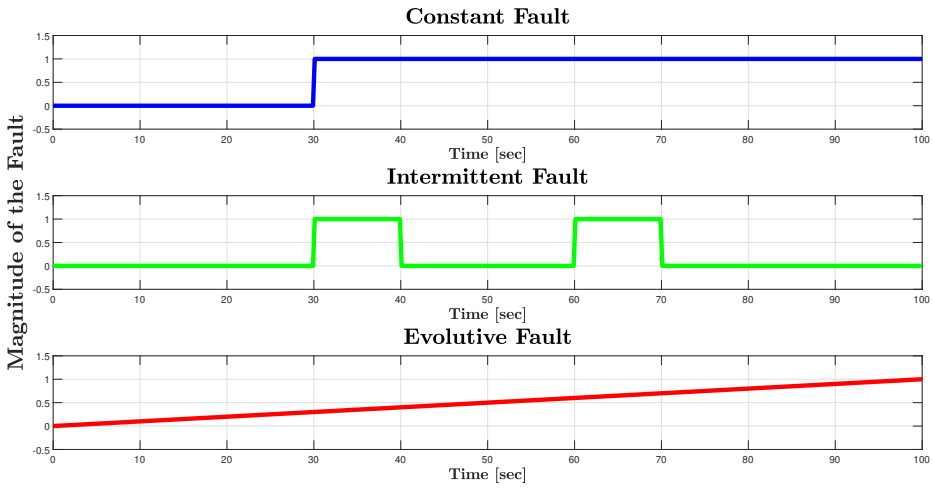

Figure 2-5: Temporal Effects Failure

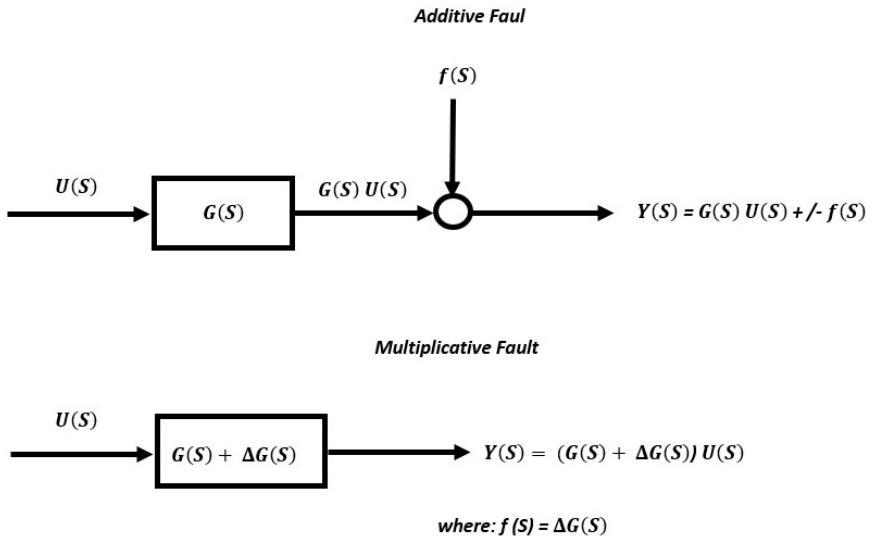

Figure 2-6: Internal System Fault

- Additive Fault: Covers output deviations that arise independently of the nominal inputs, for example, sensor or actuator offsets and external disturbances.

- Multiplicative fault: This category covers output variations that depend on both the magnitude of the fault and the input signals of the system, for example, sensor gain errors, component degradation, or power loss. Figures **2-6** show symbolic representations of additive and multiplicative faults.

2.6.2 Generating residuals using analytical models.

Designing the residual generator aims to maximize its sensitivity to the fault of interest while isolating it from all other inputs of the process, disturbances. The sensitivity condition in terms of the output $y(t)$ can be interpreted in various ways. It can be stated that the dynamic effects of faults should be captured through measurable variables. In other words, defining equivalences regarding the fact that the frequency components of faults should excite the dynamics of the process and these conditions should be evident in measurement readings.
Faults are analyzed as signals and the system is viewed as a filter, implying that the operating frequencies of faults cannot be filtered. It is important to note that aspects related to the operating frequencies of other inputs in the system should not affect the residue.
Considering analytical models to design residue generation algorithms offers the advantage of formulating procedures with a wide range of fault scenarios, supported by robust tools grounded in the study of system dynamics.

Analytical models are used to generate residuals under the following conditions:

- There is a superficial understanding of the impact of faults on the output. This condition is reflected in the limited historical data, which does not allow for fault diagnosis under a frequency or statistical analysis scheme.
- A weak indicator on differentiating effects and minimal evidence to categorize and distinguish between the existence of a fault and a normal condition. Multiple and varied categories with respect to fault effects that cannot be grouped into a minimal set of signal characteristics that are quantified.

An inconvenience when using analytical models to generate residues is formulating models with a high degree of precision and reliability. It is necessary to project the evolution of the model over time, with adequate identification of the type of faults that need to be diagnosed. Achieving this condition in real-world applications is not always 100 % possible; however, it should be very close to real conditions.

Analytical design methods for obtaining residue generators are classified into three groups:

1. Parity equations-based methods.
2. State observer-based methods.
3. Model parameter-based methods.

The methods outlined above will now be described.

1. Methods based on parity equations The method of generating residues from the parity equation is a particular case of a method called redundant relation generation Verde et al. (2013). This method applies to the input-output representation of the system through the transfer matrix, as well as to a model represented in state space. The concept of parity equation method originated in the pioneering work of Chow and Willsky (1984) considering models of dynamic systems in state spaces. The idea involves comparing the measured output with an estimation derived from the model, either in an input-output representation (IO) or in state space representation.

   - Input-output (IO) model. This concept of input-output representation was primarily disseminated by Gertler (1997, 1998) and can be conducted indifferently concerning continuous or discrete-time representation. Consider the linear time-invariant system described by the equation

   $$Y(p) = G(p,\theta_0)\,U(p) + G_f(p,\theta_0)\,F(p) + G_{\overline{f}}(p,\theta_0)\,\overline{F}(p) \tag{2-17}$$

   where p is the Laplace operator in continuous-time (S) or in the Z transform in discrete-time, depending on whether the system is continuous or discrete. $G(p,\theta_0) = C(pI - A)^{-1}B + D$ is the nominal transfer matrix relating the input to the output, $G_f(p,\theta_0) = C(pI - A)^{-1}F_1 + F_2$ is the nominal transfer matrix from the faults of interest F_1 and F_2 concerning the output, and $G_{\overline{f}}(p,\theta_0) = C(pI - A)^{-1}E_1 + E_2$ is the nominal transfer matrix associated with non-interest faults E_1 and E_2 and/or disturbance signals at the output.

   Given the parameter vector θ_0, the error between the measured output and the model-based estimation is:

   $$\begin{aligned} R(p) &= Y(p) - G(p,\theta_0)\,U(p) \\ &= G_f(p,\theta_0)\,F(p) + G_{\overline{f}}(p,\theta_0)\,\overline{F}(p), \end{aligned} \tag{2-18}$$

   where $R(p)$ is the primitive residue, and equation 2-18 is referred to as the parity equation, defining the robust structure of the model with measurements. The schematic representation corresponds to Figure **2-7**.

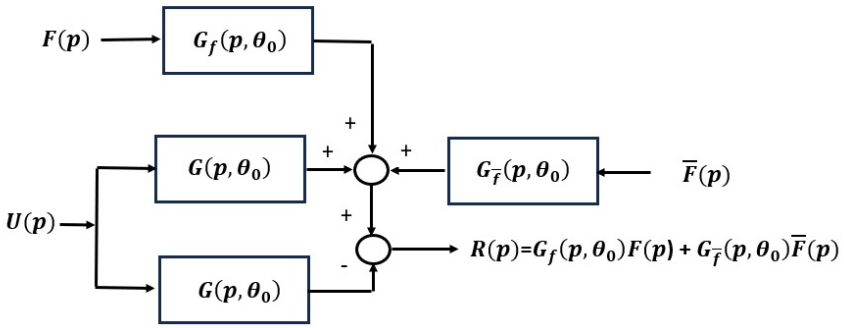

Figure 2-7: Parity equation with the transfert function,Verde et al. (2013).

where $\overline{F}(p)$ are associated to the disturbances.
From the primitive parity equation $R(p)$, it is possible to derive relationships with complementary properties. This is evident when generating specific residues by addressing the detection problem individually concerning particular faults present in the process, sensors, or actuators. In addition, other types of faults $\overline{f}$ must be considered, for which the residue should be insensitive. To achieve these objectives, a decoupling matrix $W(p)$ is introduced. Thus, the design of the parity space is expressed as:

$$\begin{aligned} R_w(p) &= W(p)\left(Y(p) - G(p)U(p)\right) \\ &= W(p)\left(G_f(p)f(p) + G_{\overline{f}}(p)\overline{f}(p)\right) \end{aligned} \tag{2-19}$$

where:

$$W(p)G_{\overline{f}}(p) = 0 \quad and \quad W(p)G_f(p) \neq 0 \tag{2-20}$$

The use of the decoupling matrix $W(p)$, dependent on the Laplace operator S or the Z transform, entails a non-trivial design and implementation. Therefore, it is suggested to apply this capability if it is not feasible to obtain constant decoupling matrices that fulfill the desired design parameters. If the decoupling matrix $W(p)$ is constant, the design is straightforward and translates into a transformation of the residue space.
It is important to clarify that equation (2-19) is used to adjust the tuning of the filter $W(p)$, and once tuned, the diagnostic system is implemented through digital filters, as described in equation (2-20).

- State Model. The generation of residues is obtained from the state representation model of the reference dynamic system defined as:

$$\begin{aligned} \dot{x}(t) &= Ax(t) + Bu(t) + Vv(t) + Ff_F(t) \\ y &= Cx(t) + N\eta(t) + Mf_M(t) \end{aligned} \tag{2-21}$$

where $x(t) \in \mathbb{R}^n$ is the state vector, $u(t) \in \mathbb{R}^p$ is the input vectors, $y(t) \in \mathbb{R}^r$ is the output vectors, $v(t) \in \mathbb{R}^{p_v}$ is the disturbance vector, $f_F(t) \in \mathbb{R}^{p_F}$ is the vector of additive faults associated with the inputs, $f_M(t) \in \mathbb{R}^{p_M}$ is the vector of additive faults associated with the outputs, $\eta(t) \in \mathbb{R}^{p_E}$ they are the noise vectors. The total fault vector is: $f(t) = \begin{bmatrix} f_F(t) & f_M(t) \end{bmatrix}^\top$ and the matrices A, B, V, F, C, N, and M have known dimensions. The parity model analysis method is obtained by deriving the output $y(t)$ according to the order of derivatives $r \leq n$, as shown in Figure **2-8**. For more details, refer to Isermann (2005a).

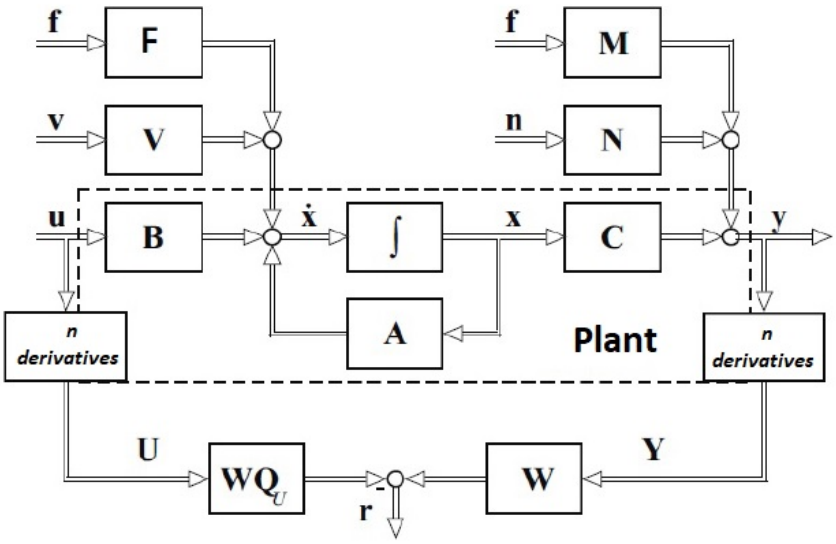

Figure 2-8: Parity Space based on Models (Isermann, 2005a).

2. Generation of residues using state observers. State observers are analytical methods that estimate the states of a system based on measurements of output and input signals. The observer sends estimated information regarding the value of each state, allowing for an approximate value relative to the real value for each state. Observers are also known as virtual sensors; they serve the same function as a physical sensor. There are linear and nonlinear approaches to state estimation. In the case of linear systems, the observer commonly used is of the Luenberger type. This structure offers a satisfactory solution to the problem of state variable estimation.
   For nonlinear models, a linear approximation for designing state observers involves performing local linearization methods of the mathematical model of the process to be estimated and then designing the linear observer based on this linearization. However, to overcome limitations arising from the application of methods for designing linear observers, it is conventionally required to design nonlinear observers that are effective enough to directly capture the nonlinearities of the process. Nonetheless, using interval observers can provide adequately estimation to conceive novel and efficient estimation

techniques, rather than resorting to nonlinear observers, as they require necessary conditions for their design. Figure **2-9** illustrates in a general manner the fundamental structure of a Luenberger-type observer.

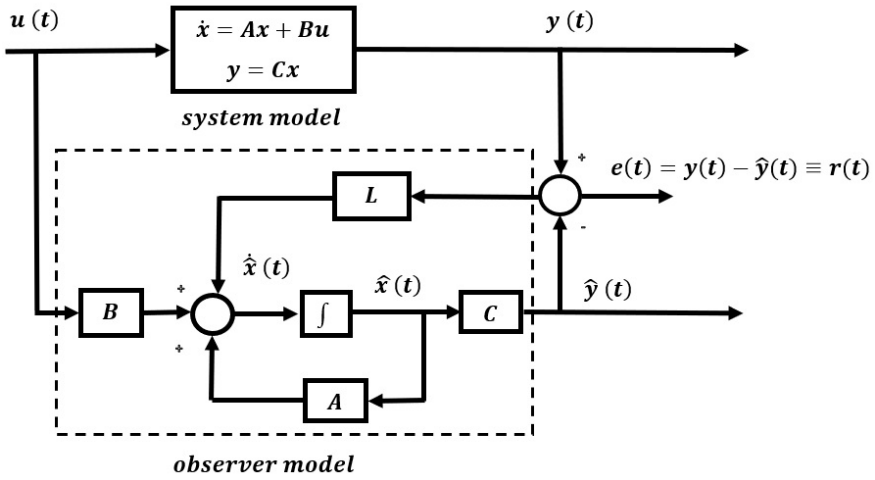

Figure 2-9: Basic framework of a Luenberger-type observer.

In the dashed frame, the observer's analytical scheme is consolidated, where the observation error, denoted by $e(t)$, corresponds to the residue $r(t)$ during Failure Detection and Isolation (FDI) analysis. Under normal conditions, when no failure occurs, $r(t) \rightarrow 0$. In the presence of disturbances but with absence of faults, the residual performance $r(t) = y_m(t) - \hat{y}(t)$ remains in the vicinity of zero. However, in the presence of failures, the residue $r(t)$ does not equal zero: $r(t) \neq 0$. Therefore, the residual resulting from a fault is larger than that disturbances, that is $r_f(t) > r(t)$. Based on the aforementioned information, there are more efficient state estimation observers, such as Unknown Input Observers (UIOs) and adaptive observers, among others. Furthermore, recent techniques such as interval observers, as demonstrated in this doctoral thesis, have shown promising results in detection. Interval observers establish a threshold where residue variations $\Delta r(t)$, $\Delta r(t) \rightarrow 0$ remain within the threshold, while variations of interest for detecting failures lie outside the threshold. This significant advantage sets them apart from other techniques.

3. Fault indicators parameters. A failure can be detectable, depending on the information available about the process and the specific failure. Assume that the sequence of data consisting of exogenous signals and endogenous signals of a process, which is known:

$$\mathcal{U} = \{u(0), u(1), \ldots, u(k)\} \tag{2-22}$$

$$\mathcal{Y} = \{y(0), y(1), \ldots, y(k)\} \tag{2-23}$$

and the set of faults:

$$\mathcal{F} = \{f_1, f_2, \ldots, f_f\} \tag{2-24}$$

It is necessary that the fault $f_i \in \mathcal{F}$ to be detectable requires to occur within time windows of the sequences $\mathcal{U}$ and $\mathcal{Y}$, or equivalently, it must induce a deviation from the normal behavior of the process sequences. This condition implies that the fault induces a deviation in at least one variable or parameter from its normal condition.

4. Identification and Parameter Estimation Methods. They are used to solve fault diagnosis problems when faults are associated with model parameters, represented in the state matrix A for LTI systems. This means that faults are not represented as additional signals in the process components, but as alterations in the values of the process parameters as shown in Figure **2-10**.

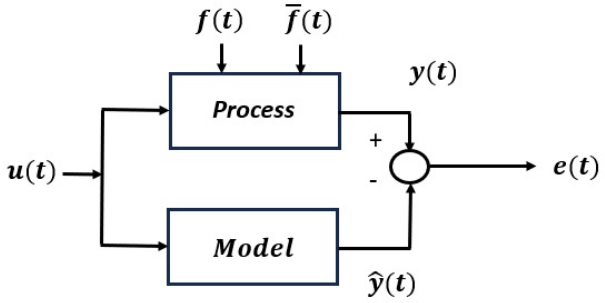

Figure 2-10: Fault Detection based on Parametric Methods, source (Verde et al. (2013))

3 Modeling the Dynamics of Flow in Pipelines

In this chapter, we introduce the fluid model in a pipeline described by the momentum and continuity partial differential equations. By using the Finite-Difference Discretization method in the infinite-dimensional representation, we obtain a discretized nonlinear model described by partial differential equations for the pipeline system model. Finally, we present the space-state linearized model for the single leak case, for which will be designed interval observer-based fault detection schemes, in the following chapters, in order to detect the occurrence of the leaks.

3.1 Infinite Dimensional System Model of the Fluid

In general, the classical fluid model in a horizontal pipeline is based on the Water Hammer (WH) equations, which govern the internal behavior of transient fluid flows by means of the mass and momentum conservation balances (Chaudhry, 2014; Roberson et al., 1998). By assuming negligible convective velocity changes, incompressible fluid flows, and slightly deformable duct wall, the HW equations can be expressed by a pair of nonlinear hyperbolic Partial Differential Equations (PDE) (Delgado-Aguiñaga et al., 2016):

- Momentum equation,

$$\frac{\partial Q(z,t)}{\partial t} + gA_T \frac{\partial H(z,t)}{\partial z} + \mu Q(z,t)\Big|Q(z,t)\Big| = 0, \tag{3-1}$$

- Continuity equation,

$$\frac{\partial H(z,t)}{\partial t} + \frac{b^2}{gA_T}\frac{\partial Q(z,t)}{\partial z} = 0, \tag{3-2}$$

where $Q(z,t)$ represents the fluid flow rate [m^3/s], $H(z,t)$ is the hydraulic pressure head [m], $z \in (0,\, L)$ is the length coordinate along the pipeline $[m]$, where L is the Equivalent Straight Length (Delgado-Aguiñaga et al., 2016), and t is the time coordinate [s]. Moreover, g denotes the gravity acceleration [m/s^2], A_T is the pipe cross-section area [m^2], b is the pressure wave speed in the fluid [m/s]. Finally, $\mu = \tau/2DA_T$, where τ stands for the friction coefficient and D denotes the inner diameter [m]. The boundary conditions for the PDE model in (3-1) and (3-2) are given by the pressure head extremes of the pipe, $H(0,t) = H_{in}(t)$ and

$H(L,t) = H_{out}(t)$, which are also considered as inputs, while the fluid flows represent the output conditions, $Q(0,t) = Q_{in}(t)$ and $Q(L,t) = Q_{out}(t)$.

It is possible to express the fluid mathematical model in (3-1) and (3-2) into the state-space representation using the Finite-Difference discretization (Verde, 2001), that approximates the pipe into discrete spatial partitions, which is written as follows,

$$\begin{aligned} \frac{\partial H(z_i,t)}{\partial z} &\approx \frac{H_{i+1} - H_i}{\Delta z_i}, \qquad \forall\, i = 1,\ldots,n \\ \frac{\partial Q(z_{i-1},t)}{\partial z} &\approx \frac{Q_i - Q_{i-1}}{\Delta z_{i-1}}, \qquad \forall\, i = 2,\ldots,n \end{aligned} \tag{3-3}$$

where sub-index i represents the discretized variable in (3-1) and (3-2) at partition i, H_i and Q_i stand for the pressure and rate flow at space abscissa z_i, $H(z_i,t)$ and $Q(z_i,t)$, and $\Delta z_i = z_{i+1} - z_i$. The variables at each section i and the boundary condition for each section are given by

$$Q_{i+1} = \lambda\sqrt{H_{i+1}}\ , \quad \forall\, i = 1,...,n-1, \tag{3-4}$$

where $\lambda = C_d A_l \sqrt{2g}$, with C_d is the discharge coefficient, and A_l is the cross-section area at that point. Then, the PDE model is now approximated by a finite-dimensional model that depends on number of partitions, given as follows (Verde, 2001; Chaudhry, 2014):

$$\begin{aligned} \dot{Q}_i &= \frac{a_1}{\Delta z_i}\left(H_i - H_{i+1}\right) - \mu Q_i\left|Q_i\right|,\ i = 1,\ldots,n \\ \dot{H}_{i+1} &= \frac{a_2}{\Delta z_i}\left(Q_i - Q_{i+1}\right),\ i = 2,\ldots,n. \end{aligned} \tag{3-5}$$

where the parameters are given by

$$a_1 = gA_T, \qquad a_2 = \frac{b^2}{gA_T} \qquad \mu = \frac{\tau}{2DA_T},$$

where τ can be modeled as follows (Delgado-Aguiñaga et al., 2016),

$$\tau(Q_i) = \frac{0.25}{\left[\log_{10}\left(\dfrac{\epsilon}{3.7\,D} + \dfrac{5.74}{Re(Q_1)^{0.9}}\right)\right]^2},$$

with ϵ is the pipe roughness [m] and $Re(Q_i)$ is the Reynolds number given by $Re(Q_i) = Q_i D/\varrho A_T$, where ϱ is the kinematic viscosity of water [m^2/s] and Q_i is the flow rate in the i^{th} section.

In the context of applying the finite difference method to fluid transport, the procedure involves dividing the pipeline length L into n sections, where n represents the total number of sections into which the pipeline is divided. For each section, the distance is defined as z_n.

It is possible to establish n sections, for which it is necessary to divide the pipeline length into $n+1$ sections (see Figure **3-1**).

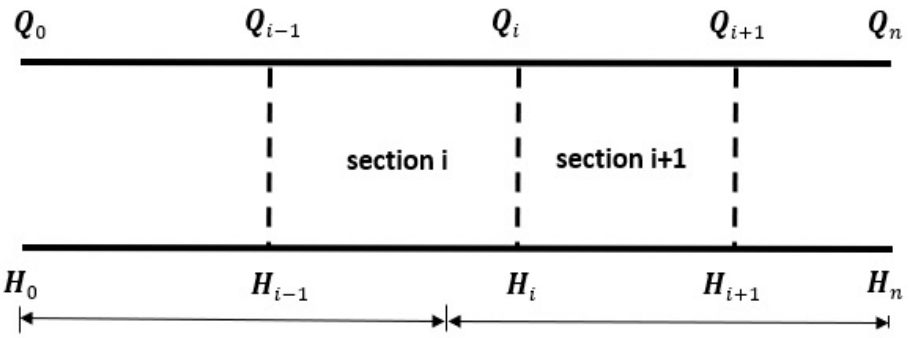

Figure 3-1: Finite-dimensional pipeline model divided the length into n sections.

Solutions of resulting pipeline equations in (3-5), given by Figure **3-1**, are broadly complex. Considering the finite difference discretization method, we divide the pipeline into n sections while time is a continuous variable, reducing the initial difficulty. Then, the fluid dynamics are described by the flow rate in each section and the pressures at each section end. In this way, we can obtain a more convenient way of using observer-based fault detection structures.

In particular, taking into account two partitions (see Figure **3-2**), pipeline variables Q_i and Q_{i+1}, as well as H_{i+1}, H_{i+2}, and Q_{i+2}, are quantities required for calculating through direct or indirect measurements. The upstream pressure head $H_1 = H_{in}$ and downstream pressure head $H_{i+1} = H_{out}$ determine the input vector $u(t)$, while the values of inlet flow rate $Q_i = Q_{in}$ and outlet flow rate $Q_{i+2} = Q_{out}$ correspond to the output vector $y(t)$.

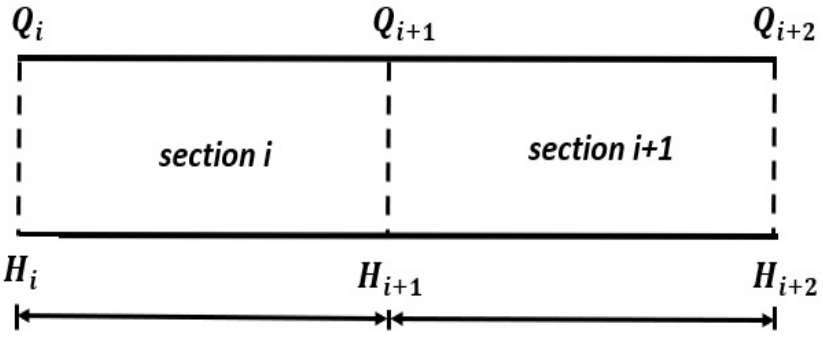

Figure 3-2: Finite-dimensional model of the fluid considering two partitions.

3.2 Leakage Model in a Pipeline

In this work, we consider the leakage model in a pipeline from the discretized set, $\{z\} = \{0,\, z_l,\, L\}$, where z_l represents the position of a leak. It is shown clearly in Figure **3-3**, This is achieved by partitioning the pipeline into $n = 2$ sections.

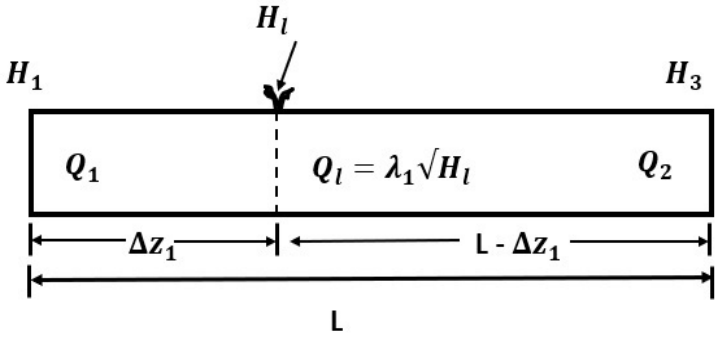

Figure 3-3: Model of Pipeline approximated by two partitions, considering with three-points for the discretization $\{0,\, z_l,\, L\}$.

From Figure **3-3**, we can see that Q_l stands for the leakage flow rate that is produced at the pipeline position z_l, and can be modeled by the following expression (Navarro-Díaz et al., 2021),

$$Q_l = \lambda_1 \sqrt{H_l} \tag{3-6}$$

where $\lambda_1 = C_d\sqrt{2g}\, A_l$ is a positive constant defined by the discharge coefficient C_d, the gravitational acceleration g, and the leak's cross-sectional area A_l, while $H_l = H_2$ denotes the pressure head at the leak location. Hence, in the single-leak scenario, the system is approximated by the following nonlinear differential equations:

$$\Sigma_{\text{NL}} : \begin{cases} \dot{Q}_1 = \dfrac{a_1}{\Delta z_1}\,(H_1 - H_2) - \mu_1\, Q_1\big|Q_1\big|, \\ \dot{H}_2 = \dfrac{a_2}{\Delta z_1}\left(Q_1 - Q_2 - \lambda_1\sqrt{\big|H_2\big|}\right), \\ \dot{Q}_2 = \dfrac{a_1}{L - \Delta z_1}\,(H_2 - H_3) - \mu_2\, Q_2\big|Q_2\big| \end{cases} \tag{3-7}$$

where $H_1 = H_{in}$, $H_3 = H_{out}$, $Q_1 = Q_{in}$, $Q_2 = Q_{out}$, and Δz_1 represents the distance between upstream point and the leak position.

Remark 2. *The analytical model of the fluid takes into account the input signals associated with the measurements of the upstream pressure head $H_{in}(t)$ and the downstream pressure head $H_{out}(t)$, with sensors positioned at the entrance and exit points of the pipeline. Similarly, the measurements necessary for evaluation are associated with the inlet flow rate $Q_{in}(t)$ and*

the outlet flow rate $Q_{out}(t)$, respectively, as they allow the assessment of the presence or absence of one or multiple leaks in the pipeline due to the physical law that defines the continuity equation in the permanent regimen as: $\rho_{in}V_{in}A_{in} = \rho - outV_{out}A_{out}$ where for the analysis of the pipeline the cross-sectional area A_{in} and the cross-sectional area A_{out} are equal and the fluid density $\rho_{in} = \rho_{out}$ for the case of an incompressible fluid. Based on the information provided above, the absence of a leak is determined taking into account the continuity equation, where the measured values of the inlet flow rate Q_{in} and outlet flow rate Q_{out} are nearly equal, that is, $\lim_{t\to\infty} |Q_{out}(t) - Q_{in}(t)| \approx 0$. In contrast, if the measured values of Q_{in} and Q_{out} differ, $\lim_{t\to\infty} |Q_{out}(t) - Q_{in}(t)| \neq 0$, it indicates the presence of a leak.

3.2.1 Nonlinear Pipeline Model

Taking into account the state vector as $\zeta = [Q_1,\, H_2,\, Q_2]^T$, the input vector as $\nu = [H_1,\, H_3]^T$, and the measurement vector as $h = [Q_1,\, Q_2]^T$, the approximate model Σ_{NL} in (3-7) can be transformed into the state-space representation, expressed in the form

$$\Gamma_{\text{NLF}} : \begin{cases} \dot{\zeta}(t) = f(\zeta) + G\,\nu(t) + f_a(t), \quad \zeta(0) = \zeta_0, \\ \eta(t) = h(\zeta) + f_s(t), \end{cases} \tag{3-8}$$

where $\zeta(t) \in \mathbb{R}^n$ stands for the *state vector*, $\nu(t) \in \mathbb{R}^m$ is the *control input vector*, and $\eta(t) \in \mathbb{R}^n$ is the *output vector*. Moreover, we consider the additive term $f_a(t) \in \mathbb{R}^n$, which stands for faults in the pipeline dynamics in Γ_{NL} such as leaks, and $f_s(t) \in \mathbb{R}^p$ are the faults in the sensors. The nonlinear function $f(\cdot) : \mathbb{R}^n \to \mathbb{R}^n$ is defined as follows

$$f(\zeta) = \begin{bmatrix} -\dfrac{a_1}{\Delta z_1}\zeta_2 - \mu_1\,\zeta_1\big|\zeta_1\big| \\ \dfrac{a_2}{\Delta z_1}\left(\zeta_1 - \zeta_3 - \lambda_1\sqrt{\big|\zeta_2\big|}\right) \\ \dfrac{a_1}{L - \Delta z_1}\zeta_2 - \mu_2\,\zeta_3\big|\zeta_3\big| \end{bmatrix}.$$

Additionally, we have the matrix

$$G = \begin{bmatrix} \dfrac{a_1}{\Delta z_1} & 0 \\ 0 & 0 \\ 0 & \dfrac{-a_1}{L - \Delta z_1} \end{bmatrix},$$

and the nonlinear function given as $h(\zeta) = \begin{bmatrix} \zeta_1,\ \zeta_3 \end{bmatrix}^T$.

Remark 3. *It is important to mention that the nonlinear model in* Γ_{NLF} *in* (3-8) *considers the term related to the faults in the pipeline dynamics, denoted by* $f_a(t)$*, which can physically represent breakdowns, leaks, blockages, additional/fluctuating flows as well as variations of pressure heads in the pipeline. Moreover, it is regarded that faults are present in the measurements, which are given by* $f_s(t)$*. These terms represent a typical behavior that occurs in physical systems of the pipeline.*

3.2.2 Linearized Pipeline Model

By assuming an unidirectional flow, the term $Q_i\left|Q_i\right| = Q_i^2$ with $i = 1, 2$. In particular, the nonlinear system dynamics in (3-8) are linearized around an equilibrium point given as $(\zeta_{10}, \zeta_{20}, \zeta_{30}) = (Q_{10}^*, H_2^*, Q_{20}^*)$ and $(\nu_{10}, \nu_{20}) = (H_{10}^*, H_{30}^*)$. Hence, the linearized model can be written by,

$$\Upsilon_{\text{LF}} : \begin{cases} \dot{x}(t) = Ax(t) + Bu(t) + f_a(t), \quad x(t_0) = x_0, \\ y(t) = Cx(t) + f_s(t)\,, \end{cases} \tag{3-9}$$

where $x(t) = \zeta(t) - \zeta^*$ is the *state*, $u(t) = \nu(t) - \nu^*$ is the *control input*, and $y(t)$ is the *output* of the system Υ_{L}. In addition, we consider $f_a(t)$ to represent the term of faults, and $f_s(t)$ to be the fault signal of the sensors. These latter terms $f_a(t) = 0$ and $f_s(t) = 0$ are given in the nominal case. $A \in \mathbb{R}^{3\times3}$ and $B \in \mathbb{R}^{3\times2}$ are defined as the Jacobian matrices of $f(\zeta) + G\nu$ with respect to ζ and ν, respectively. Besides, $C \in \mathbb{R}^{2\times3}$ is the measurement Jacobian matrix of $h(\zeta)$ with respect to ζ. Such Jacobian matrices are expressed as

$$A = \begin{bmatrix} -2\mu_1\zeta_{10} & -\dfrac{a_1}{\Delta z_1} & 0 \\ \dfrac{a_2}{\Delta z_1} & -\dfrac{a_2\lambda_1}{2\Delta z_1\sqrt{\zeta_{20}}} & -\dfrac{a_2}{\Delta z_1} \\ 0 & \dfrac{a_1}{L-\Delta z_1} & -2\mu_2\zeta_{30} \end{bmatrix},$$

$$B = \begin{bmatrix} \dfrac{a_1}{\Delta z_1} & 0 \\ 0 & 0 \\ 0 & -\dfrac{a_1}{L-\Delta z_1} \end{bmatrix}, \quad C = \begin{bmatrix} 1 & 0 & 0 \\ 0 & 0 & 1 \end{bmatrix}.$$

Remark 4. *It is important to note that the dynamics of the pipeline nonlinear model* Γ_{NL} *in* (3-8) *is linearized with respect to an equilibrium point* $(\zeta_{10}, \zeta_{20}, \zeta_{30}) = (Q_{10}^*, H_2^*, Q_{20}^*)$ *that assumes that the inlet and outlet flow rate are equal. If it is considered that these flows enter and exit are relatively small volumes of water in relation to the volume of the pipeline, the variation that they will produce in the pipeline will be equally small, which implies that, under these conditions, the linearized model* Υ_{LF} *in* (3-9) *adequately represents the dynamic behavior of the nonlinear pipeline system model* Γ_{NLF} *in* (3-8).

3.3 Numerical Simulations

In this section, we show numerical simulations for observing the behavior in the pipeline system model Γ_{NLF} in the presence of a leak.

The values of the parameters, for the pipeline model with a leak Γ_{NLF} in (3-8), are listed in Table 3-1.

Table 3-1: Numeric values of the parameters.

Parameter	**Numeric value**	**Units**
L	200	m
D	0.1044	m
A_T	0.0086	m^2
g	9.81	m/s^2
b	721.653	m/s
μ_1	0.0027	m^{-3}
μ_2	0.0027	m^{-3}

Here, L denotes the pipeline length; D the pipeline diameter; A_T the cross-sectional area; g the acceleration due to gravity; b the fluid velocity; and μ_1, μ_2 are coefficients related to the fluid's physical properties.

We have run the pipeline system in Γ_{NLF} in (3-8), considering two scenarios. The first considers the nominal case during the first 50 seconds, that is, there is no presence of leaks. Subsequently, a leak occurs in the pipeline from the 50th second. For this simulation, the inputs of the pipe, given by pressure heads in the beginning and end of the pipeline, have been set *constant* with values $H_1 = H_{in} = 18$ m and $H_3 = H_{out} = 6$ m. The initial conditions for the pipeline were $Q_{10} = 0.018495\ \frac{\text{m}^3}{\text{s}}$, $H_{20} = 9$ m, and $Q_{20} = 0.018495\ \frac{\text{m}^3}{\text{s}}$.

The pressure heads at the inlet and outlet of the pipeline, which represent the input vector $u = [H_{in},\ H_{out}]^\top$ of the nonlinear pipeline system in Γ_{NLF} in (3-8). Additionally, Figures **3-4** and **3-5** present the behavior of the real states of the pipeline model. In particular, Figure **3-4** illustrates the evolution of the inflow and outflow, $Q_1 = Q_{in}$ and $Q_2 = Q_{out}$, while Figure **3-5** describes the evolution of the pressure head at $H_2 = H_l$. It is easy to see that a leak occurs at time 50 seconds since the flow rate and pressure head change at the leak point (head) and end of the pipeline.

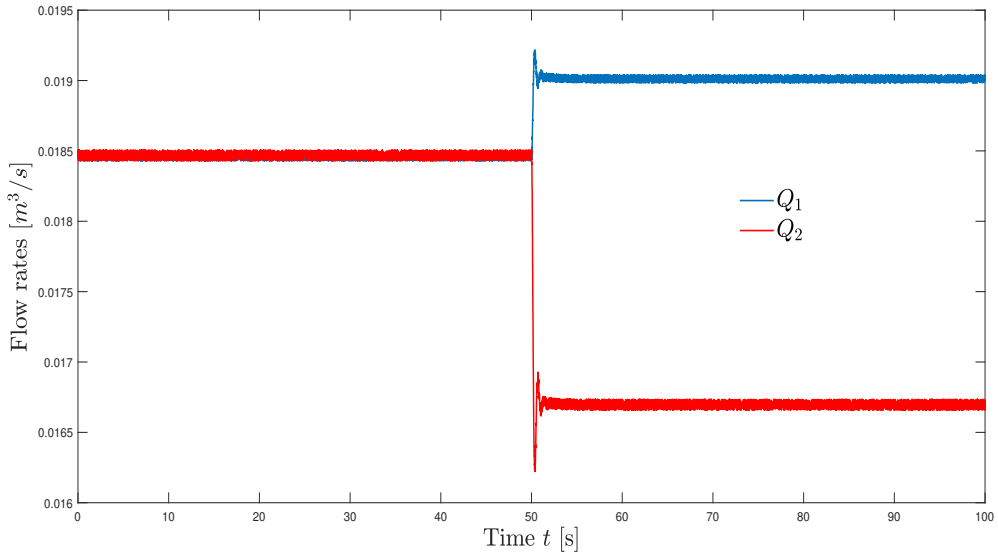

Figure 3-4: Inlet flow rate Q_1 and and Outlet flow rate Q_2.

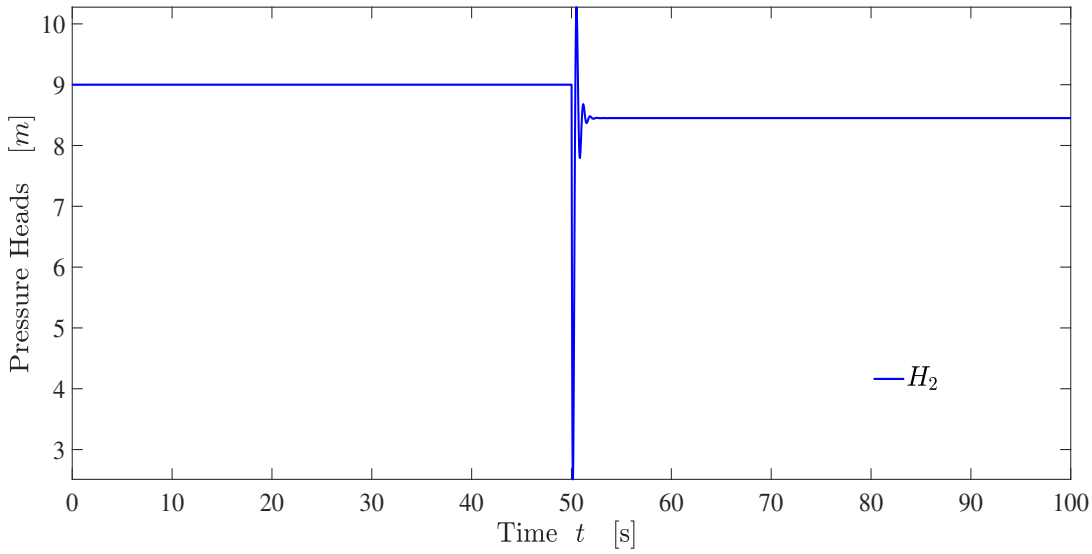

Figure 3-5: Pressure head at the pipeline.

The expressions derived for the matrix A indicate that the position offset Δz of the leak can affect the stability criteria of the model. Treating the leak as a state variable can consequently influence the observability or detectability conditions. Therefore, to evaluate the effect on the stability behavior of the system when altering the eigenvalues based on the value of Δz, a simulation was performed to calculate the eigenvalues of the matrix A

as the leak position Δz varied. Figure **3-6** presents the dynamics of the eigenvalues for the linearized pipeline model:

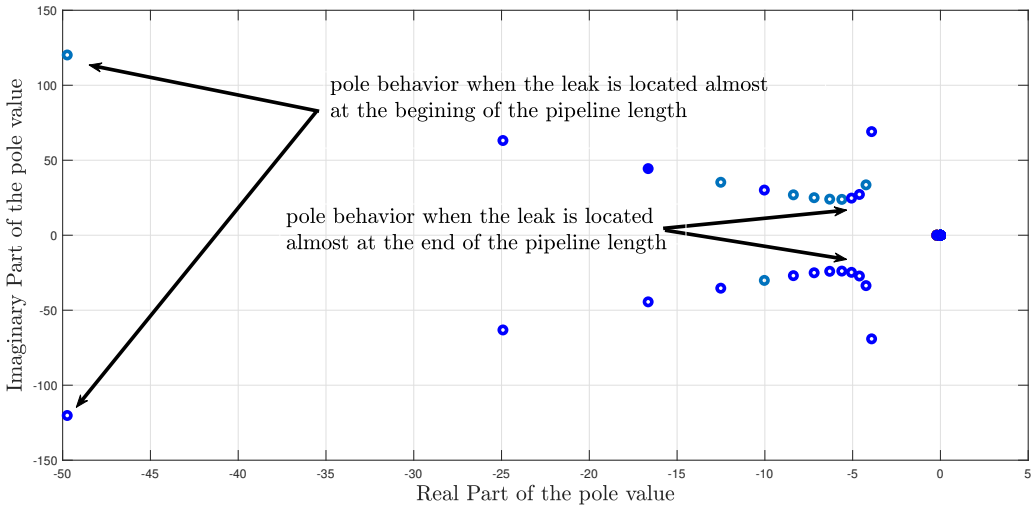

Figure 3-6: Behavior of eigenvalues with respect to the leak position along the pipeline

As shown in Figure **3-6**, when the leak occurs near the beginning of the pipeline, the eigenvalues indicate stability with larger magnitudes in their complex conjugates. However, as the leak position moves toward the end of the pipeline, the eigenvalues tend to introduce oscillatory behavior in the system. These characteristics are crucial because, for designing any state observer, it is essential to verify whether the dynamic system satisfies the conditions of observability or detectability.

3.4 Experimental Data

In this section, we present the experimental data of a pipeline with a leak, utilizing information provided by the Hydraulics Laboratory of the National Technological Institute of Mexico (TecNM) in Tuxtla Gutiérrez of the TURIX-Dynamics Diagnosis and Control Group. The prototype of the pipeline test system, and the model diagram of the pipeline, are shown in Figure **3-7**. The pipe is made with a 2-inch inner diameter PVC pipe. Moreover, the pipeline water is transported by a 5 HP centrifugal pump. Additionally, the prototype includes two pressure head sensors placed at the beginning and end of the pipeline. Finally, in a similar way, flow rate measurements are obtained from sensors located both at the inlet and outlet of the prototype Santos-Ruiz et al. (2018); Delgado-Aguiñaga et al. (2022).
As previously noted, the Turix Group supplied the data, and the laboratory tests were performed in the laboratory of the National Technological Institute of Mexico.

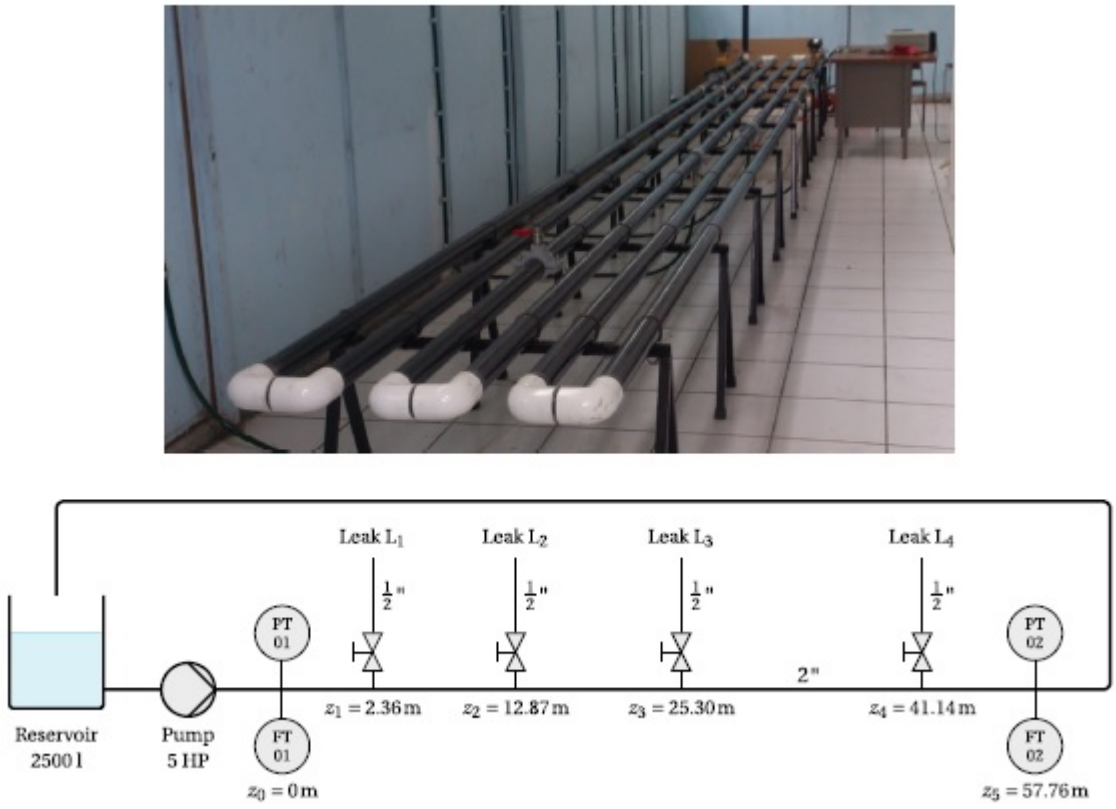

Figure 3-7: Pipeline prototype installed at the Tecnológico Nacional, IT-Tuxtla Gutiérrez Chiapas Santos-Ruiz et al. (2018); Delgado-Aguiñaga et al. (2022).

According to Santos-Ruiz et al. (2018), the parameters of the pipeline prototype, used to simulate a leak, are presented in the following table **3-2**.

Table 3-2: Parameters of the pilot pipeline.

Parameter	Value
Pipeline diameter	4.86 cm
Pipeline length	112.22 m
Tested leak position Δz	39.99 m
Fluid kinematic viscosity, ν	8.03×10^{-7} $\frac{m^2}{s}$
Fluid density, ρ	996.59 $\frac{kg}{m^3}$
Gravity acceleration, g	9.79 $\frac{m}{s^2}$
Pressure wave speed, b	1250 $\frac{m}{s}$

The following experimental data were collected from the installation of the pipeline prototype, emulating a leak by means of a flow valve positioned in the pipeline. Figure **3-8** presents the pressure heads in the beginning and end of the pipeline, which are set as pipe inputs by the constant values $H_1 = H_{in} = 9.8$ m, $H_3 = H_{out} = 2.7$ m. It is easy to see a light drop in both pressures when the leak appears.

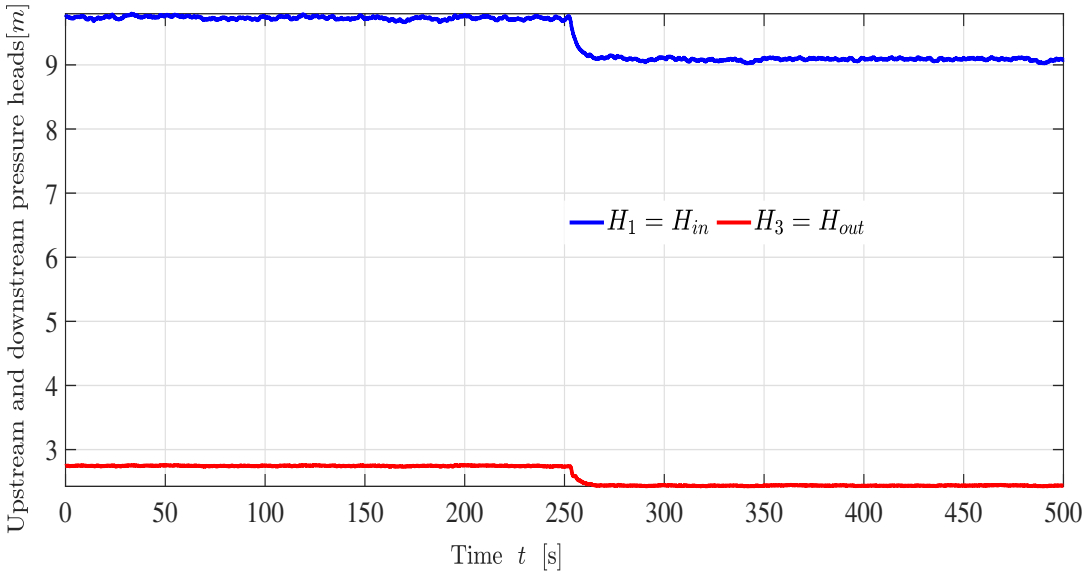

Figure 3-8: Pressure head at inlet and outlet of the pipeline test system.

Figures **3-9** and **3-10** depict the behavior of the real states of the pipeline test prototype. Particularly, the flow rates $Q_1 = Q_{in,real}$ and $Q_2 = Q_{out,real}$ are show in Figure **3-9**, while the pressure head at leak point $H_2 = H_l$ is presented in Figure **3-10**. It is clear to see that the effect of a leak at time $t = 250$ s is apparent for all real states of the pipeline plant. Such behaviors are similar to the numerical simulations presented in the previous section.

In the following chapters, we will present some FDI methods, based on the design of interval observers, in order to detect, isolate, and locate the occurrence of leaks from numerical simulations and/or experimental data of the pipeline systems.

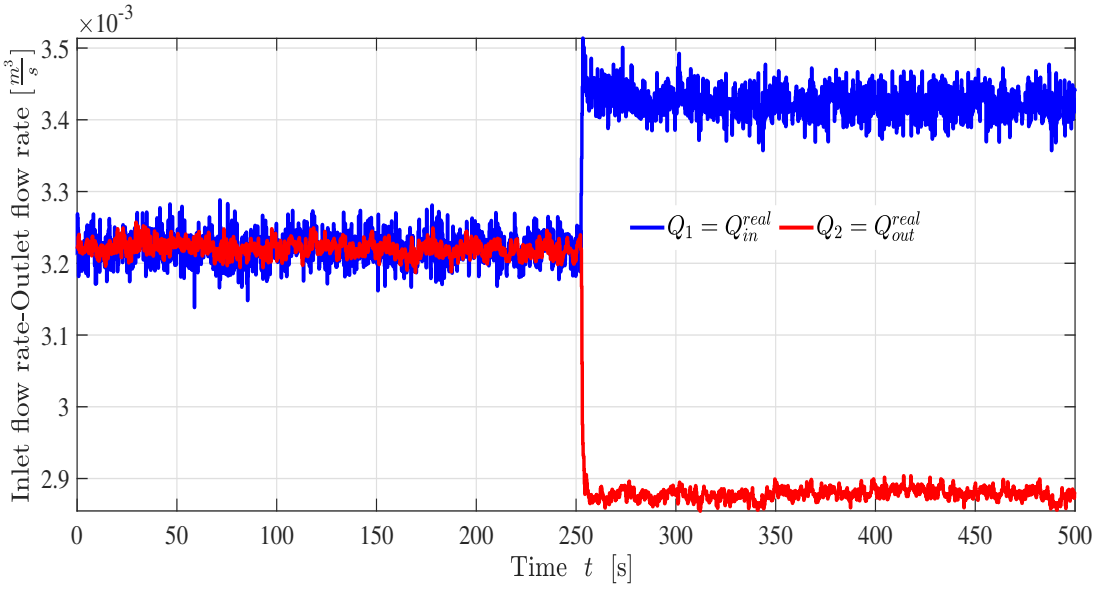

Figure 3-9: Flow rates at beginning and end of the pipeline test system.

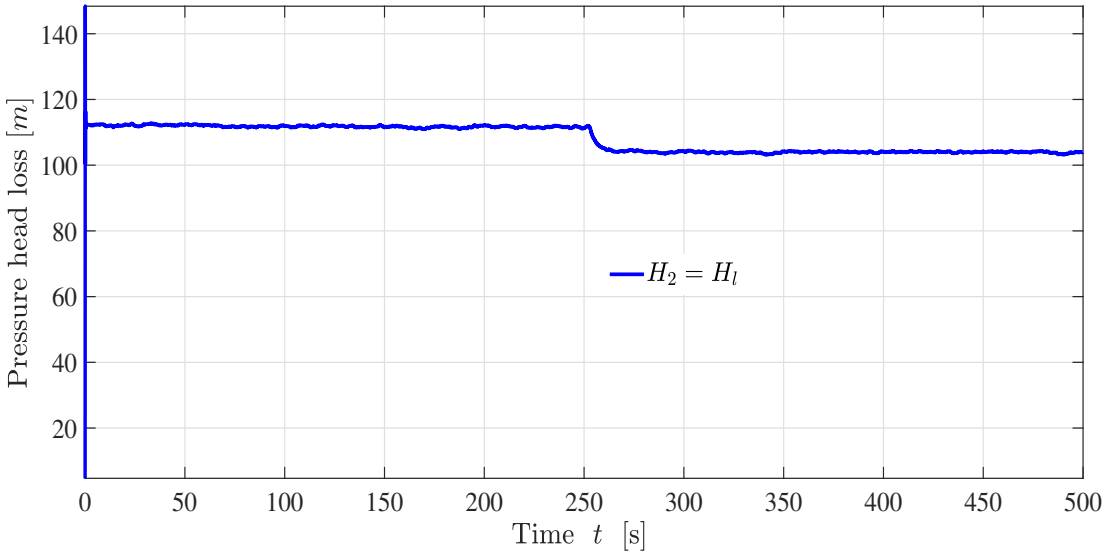

Figure 3-10: Pressure head at the point $H_2 = H_l$ of the pipeline test prototype.

4 Robust Scheme of Fault Detection based on an Interval Observer

In this chapter, we present a robust scheme to detect faults, based on an interval observer, for a class of continuous-time linear systems in the presence or absence of disturbances or parametric uncertainties. Such interval observer is based on combining a Luenberger observer and an interval predictor. The design can be represented as a feasibility problem of Linear Matrix Inequalities (LMIs). The design method is applied to the fluid model with leaks to validate its effectiveness in the occurrence of faults.

4.1 Interval Observer Design for Disturbed and Uncertain Systems

Consider the following continuous-time system, subjected to disturbances and/or variations of parameters, given by the next equations,

$$\Upsilon_{\mathrm{L}} : \begin{cases} \dot{x}(t) = Ax(t) + B_u u(t) + B_w w(t), \quad x(t_0) = x_0, \\ y(t) = Cx(t)\,, \end{cases} \tag{4-1}$$

where $(x(t), y(t), u(t)) \in \mathbb{R}^n \times \mathbb{R}^p \times \mathbb{R}^m$ are the state, the output, and the input vectors, respectively. In addition, $w(t) \in \mathbb{R}^l$ stands for the term of disturbances and/or parametric uncertainties. $A \in \mathbb{R}^{n\times n}$, $B_u \in \mathbb{R}^{n\times m}$, $C \in \mathbb{R}^{q\times n}$, $B_w \in \mathbb{R}^{n\times l}$, are constant matrices with appropriate dimensions.

We assume that the perturbed system Υ_{L} satisfies the following suppositions.

Assumption 1. *The pair* $(A,\, C)$ *is detectable.*

Assumption 2. *Suppose that the upper and lower bounds* $(\underline{x}_0, \overline{x}_0)$*, which are known, for the initial condition fulfill the inequality by intervals*

$$\overline{x}_0\,(t) \succeq x_0\,(t) \succeq \underline{x}_0\,(t) \tag{4-2}$$

Note that the inequality (4-2) *is equivalently written as* $x_0 \in [\underline{x}_0, \overline{x}_0]$

Assumption 3. *The disturbances and/or parametric uncertainties are also bounded by intervals described by,*

$$\overline{w}(t) \succeq w(t) \succeq \underline{w}(t), \qquad \forall t \geq 0, \tag{4-3}$$

where $\overline{w}(t)$ and $\underline{w}(t)$ are known Lipschitz functions defined from a domain $\mathcal{D}_w$.

Remark 5. *It is important to notice that the parametric uncertainties of the system matrices in Υ_{L}, can be also expressed as $A + \Delta A$ and $B_u + \Delta B_u$, where such uncertain terms (ΔA, ΔB_u) are bounded by intervals as*

$$\Delta\overline{A} \succeq \Delta A \succeq \Delta\underline{A} \quad \textit{and} \tag{4-4}$$

$$\Delta\overline{B}_u \succeq \Delta B_u \succeq \Delta\underline{B}_u \tag{4-5}$$

where ($\Delta\overline{A}$, $\Delta\overline{B}_u$) and ($\Delta\underline{A}$, $\Delta\underline{B}_u$) are upper and lower known bounds of (ΔA, ΔB_u), respectively. These terms are included in the Assumption 3 in the expression in (4-3) *with* $w := \{\Delta A x, \Delta B u\}$.

Now, we present the structure of the interval observer, reported in Meslem et al. (2020), for the family of linear systems Υ_{L} in (4-1) to estimate and bound the state vector, through the upper and lower estimations. Here, our design unifies and generalizes the convergence property of the novel interval observer, based on dissipativity and (or) $\mathbb{D}$-stability, considering the special case of H_∞. This approach ensures that the estimation error remains confined within a bounded region.

Let the Luenberger-type state observer for continuous-time linear systems Υ_{L} in (4-1), described as follows

$$\Upsilon_{\mathrm{O}_1} : \begin{cases} \dot{\hat{x}}(t) = A\hat{x}(t) + B_u u(t) + L(y(t) - \widehat{y}(t)), \quad \hat{x}(t_0) = \hat{x}_0, \\ \widehat{y}(t) = C\hat{x}(t), \end{cases} \tag{4-6}$$

where $\xi(t)$ stands for the estimated state vector of $x(t)$. Besides, the matrix L has to be selected to guarantee the convergence property of the state observer. We add the next interval predictor to the Luenberger observer equations, described as follows,

$$\Upsilon_{O_2} : \begin{cases} \dot{\overline{\sigma}}(t) = \overline{\Phi}(t, t_0)\left(\overline{B}_w\overline{w} - \underline{B}_w\underline{w}\right) - \underline{\Phi}(t, t_0)\left(\overline{B}_w\underline{w} - \underline{B}_w\overline{w}\right) \\ \dot{\underline{\sigma}}(t) = \overline{\Phi}(t, t_0)\left(\overline{B}\underline{w} - \underline{B}\overline{w}\right) - \underline{\Phi}(t, t_0)\left(\overline{B}_w\overline{w} - \underline{B}_w\underline{w}\right) \end{cases} \tag{4-7}$$

$$\Upsilon_{O_3} : \begin{cases} \overline{\hat{x}}(t) = \hat{x}(t) + \overline{\sigma}(t) + \overline{\Phi}(t, t_0)\,\overline{e}(t_0) - \underline{\Phi}(t, t_0)\,\underline{e}(t, t_0) \\ \underline{\hat{x}}(t) = \hat{x}(t) + \underline{\sigma}(t) + \overline{\Phi}(t, t_0)\,\underline{e}(t, t_0) - \underline{\Phi}(t, t_0)\,\overline{e}(t_0) \end{cases} \tag{4-8}$$

where $\overline{\hat{x}}(t)$ and $\underline{\hat{x}}(t)$ represent the upper and lower (bounds) estimations of the real trajectory of the state $x(t)$. The estimation error is defined as $e(t) := (x(t) - \hat{x}(t)) \in [\underline{e},\ \overline{e}]$. The quantities $\overline{\sigma}(t)$, $\underline{\sigma}(t)$, $\overline{\Phi}(t)$, and $\underline{\Phi}(t)$ will be introduced momentarily.

The estimation error dynamics can be written as follows,

$$\Upsilon_{\mathrm{E}}: \begin{cases} \dot{e}(t) = A_L e(t) + B_w w(t),\, e\,(t_0) = e_0, \\ y_e(t) = I_n e(t), \end{cases} \tag{4-9}$$

where $w\,(t)$ is the term of the (bounded) unknown signals. The matrix A_L is given by $A_L = A - LC$ and I_n is the identity matrix of dimensions $n \times n$. We can analyze the evolution of the estimation error using its solution of the system Υ_{E}, given by

$$e(t) = \Phi\,(t,\, t_0)\, e(t_0) \,+\, \sigma\,(t)\,, \tag{4-10}$$

where

$$\sigma\,(t) = \int_{t_0}^{t} \Phi\,(t,\, \tau)\, B_w w(\tau)\, d\tau, \tag{4-11}$$

with

$$\Phi\,(t,\, t_0) = \exp\left(A_L(t - t_0)\right), \tag{4-12}$$

The function $\Phi(t)$ is known as the state transition matrix of the system Υ_{E} in (4-9).

Remark 6. *Notice that the equations in Υ_{O_3} in* (4-8)*, can be rewritten as*

$$\begin{aligned} \overline{e}\,(t) &= \overline{\sigma}\,(t) + \overline{\Phi}\,(t, t_0)\,\overline{e}\,(t_0) - \underline{\Phi}\,(t, t_0)\,\underline{e}\,(t_0) \\ \underline{e}\,(t) &= \underline{\sigma}\,(t) + \overline{\Phi}\,(t, t_0)\,\underline{e}\,(t_0) - \underline{\Phi}\,(t, t_0)\,\overline{e}\,(t_0) \end{aligned}$$

Convergence Condition

In the following paragraphs, we analyze the convergence property of the interval observer, composed from (Υ_{O_1}, Υ_{O_2}, Υ_{O_3}), for the disturbed/uncertain linear system in Υ_{L}. In particular, we guarantee the stability of the observer Υ_{O_1}, applying the $\mathcal{H}_\infty$ approach in the estimation error system Υ_{E}.

Remark 7. *Note that the influence of the disturbance input w to the error output is determined by the expression,*

$$e(s) = G_{we}(s)\, w(s), \tag{4-13}$$

where the transfer function from $w\,(t)$ to $e\,(t)$, under the initial condition $e_0 = 0$, is given as

$$G_{we}\,(s) \;=\; (sI_n - A_L)^{-1}\, B_w. \tag{4-14}$$

From (4-13)*, we can consider the $\mathcal{H}_\infty$ performance in order to minimize the influence of the disturbance $w(t)$ on the estimation error signal $e(t)$ in Υ_{E}, through using the expression*

$$||G(s)||_\infty := ||\left(sI_n - A_L\right)^{-1} B_w||_\infty \leq \gamma, \qquad \gamma > 0 \tag{4-15}$$

where γ is the upper bound of the $\mathcal{H}_\infty$-norm, that is,

$$||e(t)||^2 \leq \gamma^2 ||w(t)||^2, \tag{4-16}$$

for $w(t) \neq 0$. Note that the previous inequalities can be rewritten by the $\mathcal{H}_\infty$-approach on the transfer function

$$||G(s)||_\infty = \max_{w \neq 0} \frac{||e(t)||}{||w(t)||} \leq \gamma. \tag{4-17}$$

Such inequalities in (4-15)-(4-17) *are validated if all its eigenvalues of A_L must be in the left half of the s-plane. In the $\mathcal{H}_\infty$ approaches, there are some ways to guarantee equivalently the asymptotic stability of Υ_E. One of them is the so-called Bounded-Real Lemma (BRL).*

In this chapter, we propose the use of dissipative theory, combining the notion $\mathcal{H}_\infty$ to guarantee the convergence property of the observer. Let the dissipative inequality,

$$\dot{V}\left(e(t)\right) - \omega\left(e(t), w(t)\right) < -\epsilon V\left(e(t)\right) \tag{4-18}$$

where, $V(e)$ is the storage function, and $\omega(e, w)$ stands for the supply rate for Υ_{E}. In particular, we consider quadratic supply rates, described as,

$$\omega\left(y, u\right) = \begin{bmatrix} e \\ w \end{bmatrix}^T \begin{bmatrix} Q & S \\ S^T & R \end{bmatrix} \begin{bmatrix} e \\ w \end{bmatrix} \tag{4-19}$$

with $Q \in \mathbb{R}^{n \times n}$, $S \in \mathbb{R}^{n \times l}$, $R \in \mathbb{R}^{l \times l}$ and Q, R are symmetric. From the cost functional,

$$\mathcal{F}(e, w) \triangleq \int_0^t e^\top(\tau)\, e(\tau) d\tau - \gamma^2 \int_0^t w^\top(\tau)\, w(\tau) d\tau, \tag{4-20}$$

we have the supply function matrices that are $(Q,\, S,\, R) = (-I_n, 0, \gamma^2 I_l)$.

The following proposition establishes the conditions to ensure exponential stability in the system Υ_E, using the dissipative method.

Proposition 4. *Consider the linear system Υ_L, subjected to the bounded disturbances/uncertainties as in the Assumption 3. If there exists the matrices $P = P^\top > 0$, L and the scalars ϵ and γ such that*

$$\begin{bmatrix} A_L^\top P + P A_L + I_n + \epsilon P & P B_w \\ B_w^\top P & -\gamma^2 I_m \end{bmatrix} < 0 \tag{4-21}$$

is fulfilled, then Υ_{O_1} is a convergent observer.

Proof. We propose the *storage function*, given by a positive-definite quadratic form,

$$V(e) = e^T P e, \quad P = P^T > 0. \tag{4-22}$$

Considering the dissipative inequality in (4-18), the difference of the time derivative of $V(e)$ along the solutions of Υ_{E} minus the supply rate,

$$\begin{aligned}\dot{V}(e) - \omega(\cdot) &= \begin{bmatrix} e \\ w \end{bmatrix}^\top \begin{bmatrix} A_L^\top P + P A_L & P B_w \\ B_w^\top P & 0 \end{bmatrix} \begin{bmatrix} e \\ w \end{bmatrix} - \begin{bmatrix} e \\ w \end{bmatrix}^\top \begin{bmatrix} -I_n & 0 \\ 0 & \gamma^2 I_m \end{bmatrix} \begin{bmatrix} e \\ w \end{bmatrix} \\ &< -\epsilon\, e^\top P e\,.\end{aligned}$$

Therefore, we have $\dot{V}(e) < -\epsilon V(e)$. This completes the proof. □

Remark 8. *The matrix inequality in* (4-21) *is generally a nonlinear matrix inequality in the parameters* (P, L, γ)*, being hard to solve. There are many cases to reduce the matrix inequality complexity to a Linear Matrix Inequality (LMI), or even a Bilinear Inequality Matrix (BMI) problem. We present some simplifications:*

1. *The inequality matrix in* (4-21) *can become a BMI in* (P, L, ϵ) *when* γ *is fixed.*
2. *We can replace the term* ϵP*, which is bilinear, by* ϵI*, which does not modify the feasibility of the matrix inequality in* (4-21)*.*
3. *In the term* $P A_L = PA - PLC$*, which is bilinear, we use a change of variable* $\overline{L} \triangleq PL$ *to rewrite it as* $PA_L = PA + \overline{L}C$*. Then, this latter expression is linear in* $(P, \overline{L})$*. The gain* L *is obtained by* $L = P^{-1}\overline{L}$*. Therefore, the matrix inequality in* (4-21) *is an LMI in* $(P, \overline{L})$ *fixing* γ*.*

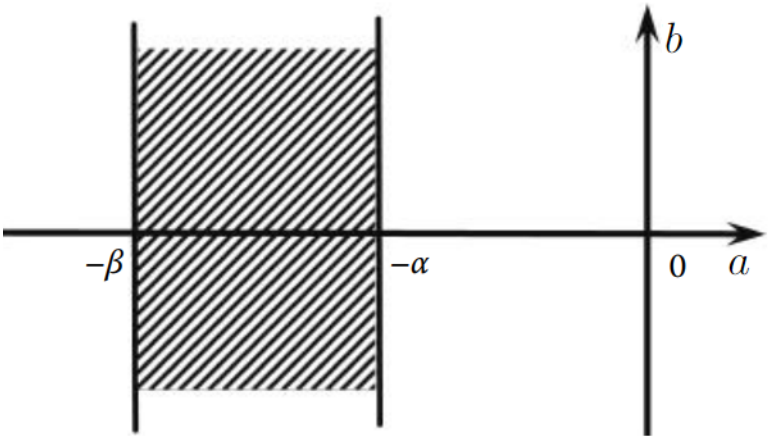

Figure 4-1: Strip region $\mathbb{D}_{\alpha,\beta}$.

We can integrate the $\mathbb{D}-$ stability approach to guarantee the convergence property of the observer Υ_{O_1}. In such an approach, we accelerate the observer dynamics by considering

the location of the eigenvalues inside stability regions. In particular, we take the $\mathbb{D}-$region defined by the following segments, which is depicted in Figure **4-1**.

$$\mathbb{D}_{\alpha,\beta} = \{a + jb \,|\, -\beta < a < -\alpha\}. \tag{4-23}$$

The following proposition combines the dissipativity conditions of the Proposition 4 and the $\mathbb{D}_{\alpha,\beta}$-stability approach.

Proposition 5. *Consider the linear system Υ_L, subjected to bounded disturbances/uncertainties as in the assumption 3. If there exists the matrices $P = P^T > 0$, L and the scalars $\epsilon > 0$ and $\gamma > 0$ such that*

$$\begin{bmatrix} A_L^\top P + PA_L + 2\alpha P + I_n + \epsilon P & PB_w \\ B_w^\top P & -\gamma^2 I_m \end{bmatrix} \leq 0 \tag{4-24}$$

$$\begin{bmatrix} -A_L^\top P - PA_L - 2\beta P + I_n + \epsilon P & PB_w \\ B_w^\top P & -\gamma^2 I_m \end{bmatrix} \leq 0 \tag{4-25}$$

is fulfilled, then Υ_{O_1} is a convergent observer.

Proof. We consider that $(A_L + \alpha I_n)$ is Hurwitz. From the *storage function*,

$$V(e) = e^T P e, \quad P = P^T > 0, \tag{4-26}$$

then the dissipative inequality in (4-18) is expressed as

$$\begin{aligned} \dot{V}(e) - \omega(\cdot) = & \begin{bmatrix} e \\ w \end{bmatrix}^\top \begin{bmatrix} (A_L + \alpha I_n)^\top P + (PA_L + \alpha I_n) & PB_w \\ B_w^\top P & 0 \end{bmatrix} \begin{bmatrix} e \\ w \end{bmatrix} \\ & - \begin{bmatrix} e \\ w \end{bmatrix}^\top \begin{bmatrix} -I_n & 0 \\ 0 & \gamma^2 I_m \end{bmatrix} \begin{bmatrix} e \\ w \end{bmatrix} \\ & \leq -\epsilon\, e^\top P e\,. \end{aligned}$$

Hence, we obtain the following inequality matrix

$$\begin{bmatrix} A_L^\top P + PA_L + 2\alpha P + \epsilon\, e^\top P e & PB_w \\ B_w^\top P & 0 \end{bmatrix} - \begin{bmatrix} -I_n & 0 \\ 0 & \gamma^2 I_m \end{bmatrix} \leq 0$$

which is expressed in the matrix inequality in (4-24). Similarly, we consider $-(A_L + \beta I)$ is Hurwitz from using the same storage function in (4-26), then we have

$$\begin{bmatrix} -(A_L + \beta I_n)^\top P - P(A_L + \beta I_n) + \epsilon\, e^\top P e & PB_w \\ B_w^\top P & 0 \end{bmatrix} - \begin{bmatrix} -I_n & 0 \\ 0 & \gamma^2 I_m \end{bmatrix} \leq 0.$$

The latter is equivalent to the matrix inequality in (4-25). Therefore, A_L is a $\mathbb{D}_{\alpha,\beta}-$stable matrix. □

Partial-Ordering Condition

The next proposition considers conditions to preserve the bounding of the estimation error in the system Υ_E.

Proposition 6. *[Meslem et al. (2020)] The state-space representation* $(\Upsilon_{\mathrm{O}_2}, \Upsilon_{\mathrm{O}_3})$ *in* (4-7)-(4-8) *provides a tight outer approximation of the reachable set of system* Υ_{E} *in* (4-9)*. That is, for any* $\mathcal{E}_0 \subset \mathbb{R}^n$*, there are lower and upper bounds* $\left[\underline{e}_(t_0), \overline{e}_(t_0)\right]$ *such that the following inequalities are satisfied:*

$$\overline{e}_(t_0), \succeq e(t_0) \succeq \underline{e}(t_0), \quad \forall e(t_0) \in \mathcal{E}_0 \tag{4-27}$$

Then, the solutions of $(\Upsilon_{\mathrm{O}_2}, \Upsilon_{\mathrm{O}_3})$ *fulfill, for all* $e(t)$*, the following inequalities*

$$\overline{e}(t) \succeq e(t) \succeq \underline{e}(t). \tag{4-28}$$

Moreover, if the matrix A_L *is Hurwitz, then the practical stability is achieved for* Υ_{O_2} *satisfying the following inequality*

$$\lim_{t\to\infty} (\overline{e}(t) - \underline{e}(t)) \preceq c, \tag{4-29}$$

for all initial condition $e(t_0) \in \mathcal{E}_0$*, where* c *is a positive real vector.*

It is now possible to blend the conditions of the Proposition 6 and method $\mathcal{H}_\infty$ to design the interval observer, which is composed of $(\Upsilon_{\mathrm{O}_1}, \Upsilon_{\mathrm{O}_2}, \Upsilon_{\mathrm{O}_3})$, for the disturbed/uncertain linear system in Υ_{L}.

Proposition 7. *Consider the Assumptions 2 and 3. If there exists the matrices* $P = P^\top > 0$*,* L *and the scalars* ϵ *and* γ *such that the conditions of the Propositions 4 and 6 hold. Then* $(\Upsilon_{\mathrm{O}_1}, \Upsilon_{\mathrm{O}_2}, \Upsilon_{\mathrm{O}_3})$ *is an interval observer for the linear system in* Υ_{L}*.*

Proof. The convergence condition is derived from Proposition 4. The partial ordering condition follows from Proposition 6, by noting that this case requires the interval predictor combined with the Luenberger-type observer. □

Notice that if the Assumptions 2 and 3 hold, that is, the initial conditions and the perturbations of the plant are bounded, then an *interval observer* is given by $(\Upsilon_{O_1}, \Upsilon_{O_2}, \Upsilon_{O_3})$ for the uncertain/disturbed plant Υ_L, satisfying the next conditions:

$$\overline{\hat{x}}_0 \succeq \overline{x}_0 \succeq x_0 \succeq \underline{x} \succeq \underline{\hat{x}}_0 \implies \hat{\overline{x}}(t) \succeq x(t) \succeq \hat{\underline{x}}(t). \tag{4-30}$$

This latter inequality describes the typical behavior of the interval observers. The following algorithm presents a code to implement an interval observer

4.1.1 Pseudocode for the Proposed Interval Observer

Below, we provide pseudocode for the interval observer described in this section.

Algorithm 1 Interval Observer from Luenberger Observer and Predictor Estimator

Require: System matrices A, B, C, D, B_w; bounded disturbances $\overline{w}(t), \underline{w}(t)$
Ensure: Interval state estimates $\hat{\overline{x}}(t)$ and $\hat{\underline{x}}(t)$
1: **Read** $A, B, C, D, B_w, \overline{w}(t), \underline{w}(t)$
2: **Verify** observability (or detectability) of the pair (A, C)
3: **Solve** the LMI conditions in (4-21) or (4-24)-(4-25) to obtain the observer gain L
4: **Construct** the Luenberger observer Υ_{O_1} 4-6
5: **Build** the interval predictor Υ_{O_2} 4-7
6: **Form** the interval observer Υ_{O_3} 4-8
7: **return** $\hat{\overline{x}}(t)$, $\hat{\underline{x}}(t)$

4.2 Fault Detection Based On the Interval Observer

Consider the class of systems as follows

$$\Upsilon_{\mathrm{F}}: \begin{cases} \dot{x}(t) = Ax(t) + B_u u(t) + B_w w(t) + F_a\, f_l(t), \quad x(t_0) = x_0, \\ y(t) = Cx(t) + C_\eta \eta(t) + F_b\, f_s(t)\,, \end{cases} \tag{4-31}$$

where $x(t) \in \mathbb{R}^n$ is the state vector, $u(t) \in \mathbb{R}^m$ is the control input vector, $y(t) \in \mathbb{R}^p$ is the output vector, $f(t)$ denotes leak fault, $w(t)$ is the unknown disturbance and parametric uncertain, and $\eta(t)$ is the noise vector. The matrices A, B_u, B_w, F_a, F_b, C, and C_η are constant matrices with appropriate dimensions. The fault distribution matrices are indicated by F_a and F_b. In particular, $f_l(t)$ represents the term of leaks, and $f_s(t)$ stands for sensor faults. The magnitude and time occurrence of the faults are considered unknown. We consider the next assumption.

Assumption 4. *Suppose that the measurement matrix can be subjected to parametric uncertainties, expressed by $C + \Delta C$, which is bounded by the inequality,*

$$C_1 := C + \Delta\overline{C} \succeq C + \Delta C \succeq C - \Delta\underline{C} =: C_2, \tag{4-32}$$

where C_1 and C_2 are known bounds. Finally, we also consider that the noise signal $\eta(t)$ is bounded by intervals as follows

$$\overline{\eta}\,(t) \;\succeq\; \eta\,(t) \;\succeq\; \underline{\eta}\,(t)\,, \qquad \forall t \geq 0. \tag{4-33}$$

Using the interval observer, composed of $(\Upsilon_{O_1}, \Upsilon_{O_2}, \Upsilon_{O_3})$, for the plant Υ_{L} affected by the occurrence of faults, the estimation error dynamics is now given as

$$\Upsilon_{\mathrm{FE}}: \begin{cases} \dot{e}(t) = A_L e(t) + Dv(t) + Ef_u(t),\ e(t_0) = e_0, \\ y_e(t) = I_n e(t), \end{cases} \tag{4-34}$$

where $v(t) = [w(t) \ \ \eta(t)]^\top$ is the bounded unknown vector of the noise and uncertainty , and $f_u(t) = [f_l(t) \ \ f_s(t)]^\top$ stands for the fault signals. The augmented matrices are

$$D = [B_w \quad -LC_\eta]$$

and

$$E = [F_a \quad -LF_b].$$

Moreover, we define the new variable

$$\begin{aligned} r(t) &= y(t) - \widehat{y}(t) \\ &= Ce + C_\eta \eta(t) + F_b f_s(t), \end{aligned} \tag{4-35}$$

which denotes the residual signal given by the difference of the measured and estimated output. Furthermore, the following expressions

$$\begin{aligned} \overline{r}(t) &= y(t) - \hat{\overline{y}}(t) \\ &= C\overline{e}(t) + C_\eta \overline{\eta}(t) \end{aligned} \tag{4-36}$$

$$\begin{aligned} \underline{r}(t) &= y(t) - \underline{\hat{y}}(t) \\ &= C\underline{e}(t) + C_\eta \underline{\eta}(t), \end{aligned} \tag{4-37}$$

where $\overline{r}(t)$ and $\underline{r}(t)$ are the upper and lower (bounds) adaptive thresholds of the residual.

Definition 18. *The fault detection scheme is defined by the comparison between the residual signal $r(t)$ and the adaptive thresholds $(\underline{r}(t),\ \overline{r}(t))$ in order to detect the occurrence of faults on the plant Υ_{F}. If the $r(t)$ exceeds the interval generated by the adaptive threshold $[\underline{r}(t),\ \overline{r}(t)]$, then faults can be detected. Otherwise, the residual inside the interval $[\underline{r}(t),\ \overline{r}(t)]$.*

The following theorem states the conditions of the fault detection scheme based on the interval observer's estimations.

Theorem 1. *Consider the plant Υ_{F}, subject to noise, parametric uncertainties and/or disturbances, which satisfies the assumptions 1, 2, 3, and 4. Moreover, suppose that there exist the matrices $P = P^\top \succ 0$, L and the positive scalar γ such that the condition* (4-21) *hold. The fault detection scheme guarantees the occurrence of a fault in the plant Υ_{F} by means of the following set*

$$\begin{aligned} &r(t) \in [\underline{r}(t),\ \overline{r}(t)], \quad \textit{if} \quad f_u(t) = 0, \\ &r(t) \notin [\underline{r}(t), \overline{r}(t)], \quad \textit{if} \quad f_u(t) \neq 0, \end{aligned} \tag{4-38}$$

Proof. If $f_u(t) = 0$, that is, $f_l(t) = 0$ and $f_s(t) = 0$, this leads to $\overline{r}(t) \succeq r(t)$ and $r(t) \succeq \underline{r}(t)$, which implies that $\overline{\hat{y}}(t) \succeq y(t)$ and $y(t) \succeq \underline{\hat{y}}(t)$ due to the property of increasing monotone functions. Then $r(t) \in [\underline{r}(t),\ \overline{r}(t)]$. This idea is not preserving when there exists the occurrence of a fault $f_l(t) \neq 0$ or $f_s(t) \neq 0$, resulting $\overline{r}(t) \preceq r(t)$ or $r(t) \preceq \underline{r}(t)$, which implies that $\overline{\hat{y}}(t) \preceq y(t)$ or $y(t) \preceq \underline{\hat{y}}(t)$ losing the partial ordering of the increasing monotone functions, leading $r(t) \notin [\underline{r}(t),\ \overline{r}(t)]$. □

Remark 9. *Note that the residual values will be inside the set $r(t) \in [\underline{r}(t),\ \overline{r}(t)]$ when the plant is fault-free, which is equivalently written as $y(t) \in [\underline{\hat{y}}(t),\ \overline{\hat{y}}(t)]$. In particular, when there is no presence of parametric uncertainties, disturbances, or noise, then $y(t) = \overline{\hat{y}}(t) = \underline{\hat{y}}(t)$. If there is an occurrence of faults $f_u(t) \neq 0$, then the output will be outside the set, $y(t) \notin [\underline{\hat{y}}(t),\ \overline{\hat{y}}(t)]$.*

4.3 Numerical simulations

In this section, we verify the effectiveness of the above method for detecting the presence of faults in the pipeline system presented in the previous chapter.

We become the linearized pipeline model to the class of uncertain and perturbed systems in Υ_{F} in (4-31), which is also subject to faults, with states $x = [Q_1,\ H_2,\ Q_2]$. Hence, the matrices of Υ_{F} as

$$A = 1 \times 10^4 \begin{bmatrix} 0.000055 & -0.000000056 & 0 \\ 4.104794 & 0 & -4.104794 \\ 0 & 0.00000016 & -0.0000550 \end{bmatrix}, B = \begin{bmatrix} 0.0005638 & 0 \\ 0 & 0 \\ 0 & -0.001691 \end{bmatrix}$$

$$F_a = \begin{bmatrix} 0 \\ 1 \\ 0 \end{bmatrix}, \quad F_b = \begin{bmatrix} 1 \\ 0 \end{bmatrix}, C = \begin{bmatrix} 1 & 0 & 0 \\ 0 & 0 & 1 \end{bmatrix}, C_\eta = \begin{bmatrix} 1 \\ 0 \end{bmatrix}, B_w = \mathbf{0}_{3\times 1}.$$

The designed parameters are

$$L = 1 \times 10^4 \begin{bmatrix} 0.00088 & -0.000447 \\ 2.58239 & 0.708037 \\ -0.00042 & 0.0021035 \end{bmatrix}, \text{ and } \gamma = 1.12.$$

such that the conditions of the Proposition 7 are fulfilled.

We consider three scenarios for the interval observer-based fault detection design:

1. There are no uncertainties in the pipeline model, but noise exists in the measurement sensor for Q_1.

2. There exists the occurrence of a leak.

3. We consider an intermittent sensor fault in Q_1.

In the first test, we consider the case without a leak but there is the presence of noise, which is bounded by the set $\eta(t) \in [\underline{\eta}, \overline{\eta}]$, where $\overline{\eta} = 5.9987 \times 10^{-5}$ and $\underline{\eta} = 4.2156 \times 10^{-9}$. In addition, the initial conditions for the plant are $Q_{10} = 0.01842\,\frac{\mathrm{m}^3}{\mathrm{s}}$, $H_{20} = 9\,\mathrm{m}$, and $Q_{20} = 0.01842\,\frac{\mathrm{m}^3}{\mathrm{s}}$. The inputs are $H_1 = H_{in} = 18$ m and $H_3 = H_{out} = 6$ m. Furthermore, the initial conditions for the interval observer are $\overline{x}_0 = [0.020, 18.5, 0.020]$ and $\underline{x}_0 = [0.0006, 7.5, 0.0006]$, which satisfies the assumption 2. Figures **4-2**- **4-4** illustrate the behavior of the pipeline model and the interval observer, without the faults, but the presences of bounded noise.

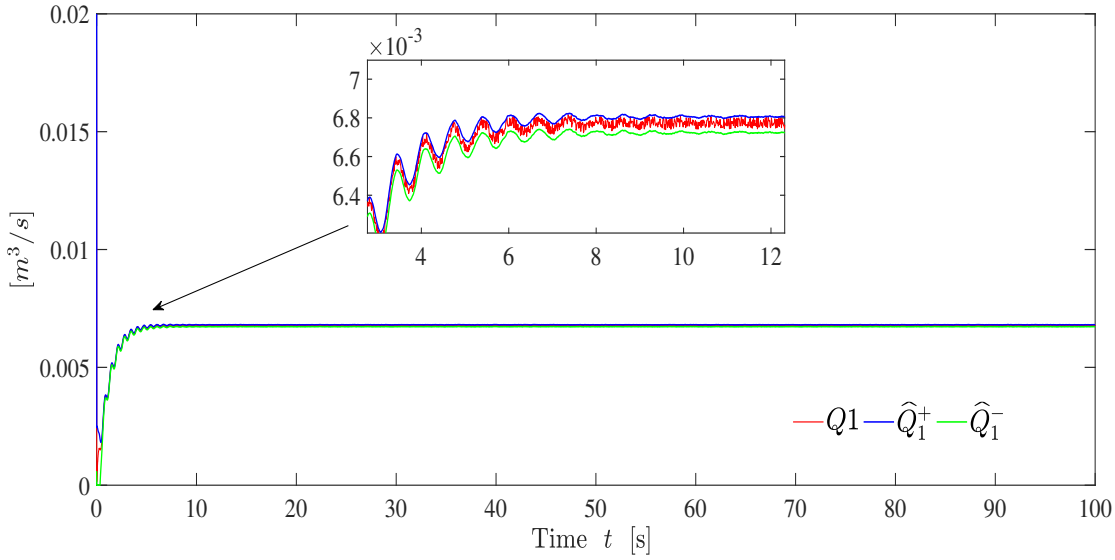

Figure 4-2: Behavior Q_1 and their upper and lower estimations of the interval observer $\widehat{\overline{Q}}_1 = \hat{Q}_1^+, \widehat{\underline{Q}}_1 = \hat{Q}_1^-$.

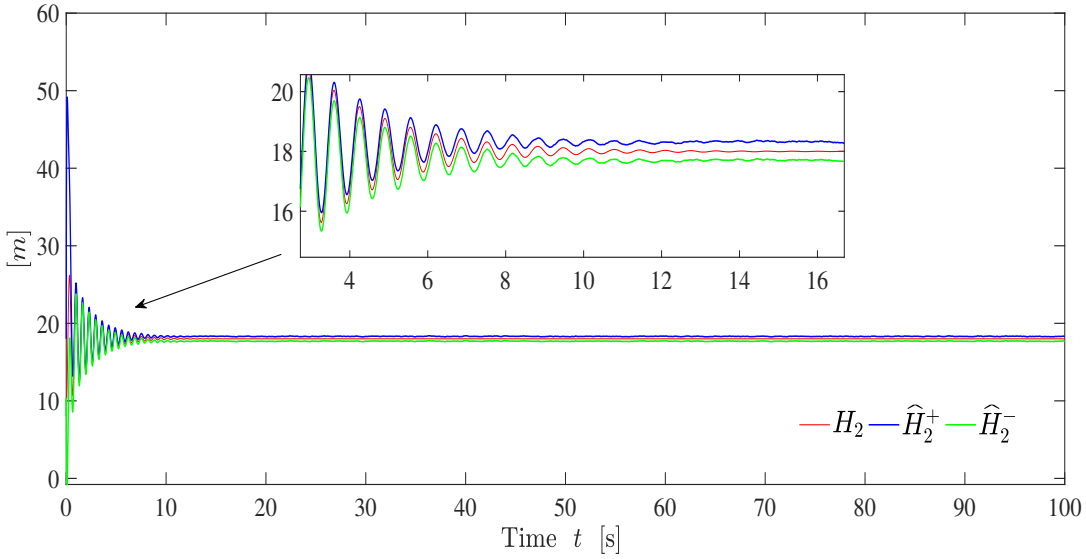

Figure 4-3: Behavior H_2 and their upper and lower estimations of the interval observer $\hat{\overline{H}}_2 = \hat{H}_2^+, \hat{\underline{H}}_2 = \hat{H}_2^-$.

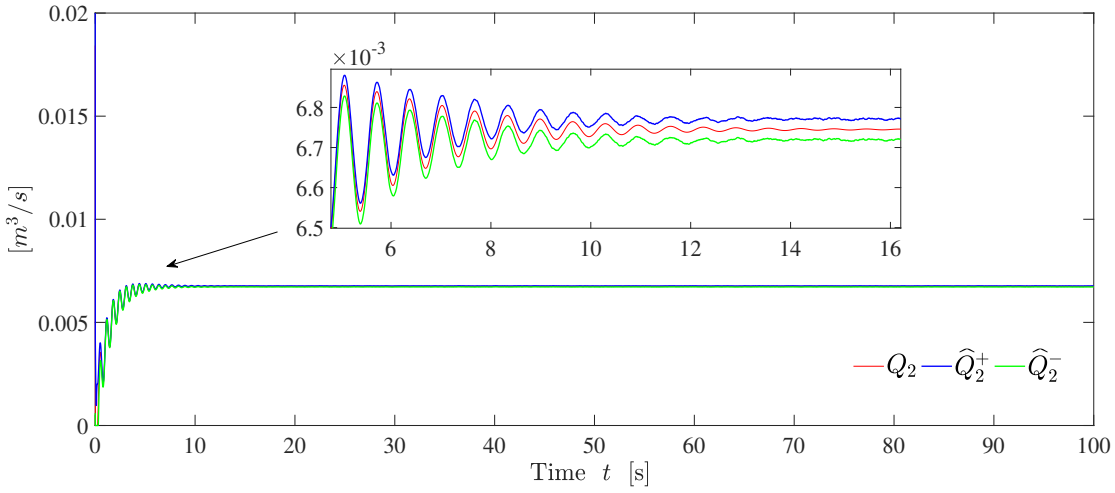

Figure 4-4: Behavior Q_2 and their upper and lower estimations of the interval observer.$\hat{\overline{Q}}_2 = \hat{Q}_2^+, \hat{\underline{Q}}_2 = \hat{Q}_2^-$.

In the second test we investigate the occurrence of a leak. The leak is introduced as an unknown input of magnitude λ_l defined in (3-6); therefore, the leak signal is modelled as $f(t) = \lambda_l \mathcal{H}(t - t_l)$, where $\mathcal{H}(t - t_l)$ is the Heaviside step function activated at the leak-occurrence time t_l. Measurement noise is added, and the initial conditions and bounds are the same as in the first test. Figures **4-5**, **4-7** show the responses of the pipeline model and the interval observer during the leak event, demonstrating that the proposed method successfully identifies the fault. Detection is corroborated in Figures **4-8** and **4-9**, where the residual leaves the admissible interval, i.e. $r(t) \notin \left[\underline{r}(t), \overline{r}(t)\right]$.

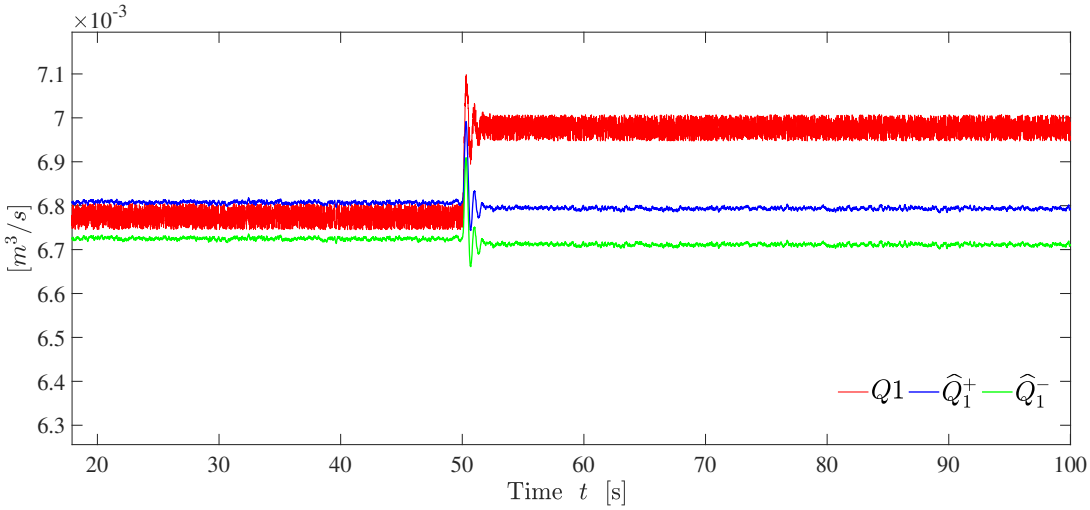

Figure 4-5: Behavior Q_1, with the occurrence of a leak and presence of noise, and their upper and lower estimations of the interval observer.$\overline{\hat{Q}}_1 = \hat{Q}_1^+$,$\underline{\hat{Q}}_1 = \hat{Q}_1^-$.

In the third test, we consider the occurrence of an intermittent sensor fault and a leak, as well as there is the presence of noise. Besides, we set the same initialization and bounding as in the first case. Figure **4-10** shows the behavior of the flow Q_1 and their estimations of the interval observer. Similarly, it can be depicted in the residual in Figure **4-11**.

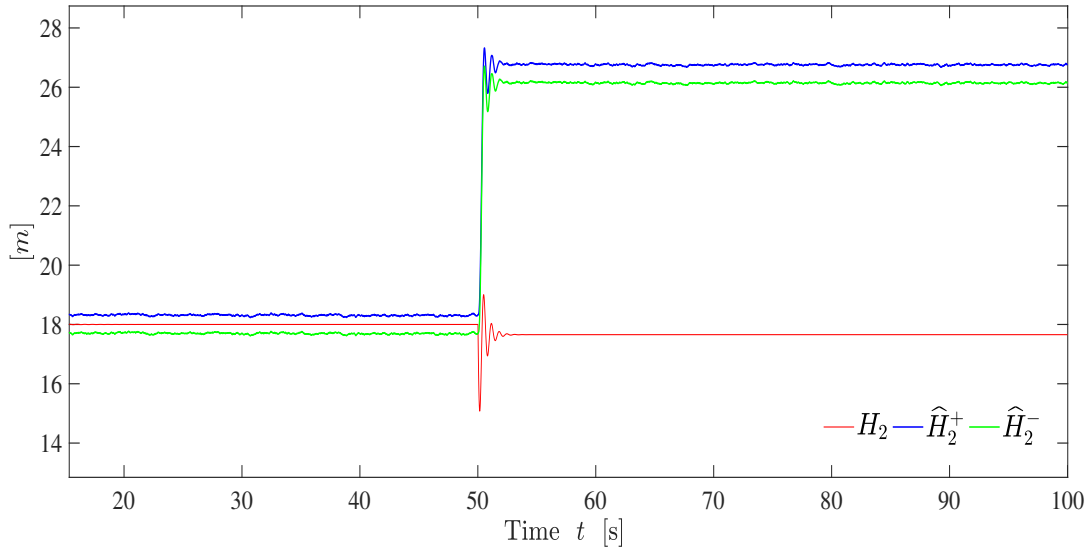

Figure 4-6: Behavior H_2, with the occurrence of a leak, and their upper and lower estimations of the interval observer.$\widehat{\overline{H}}_2 = \hat{H}_2^+$,$\underline{\hat{H}}_2 = \hat{H}_2^-$.

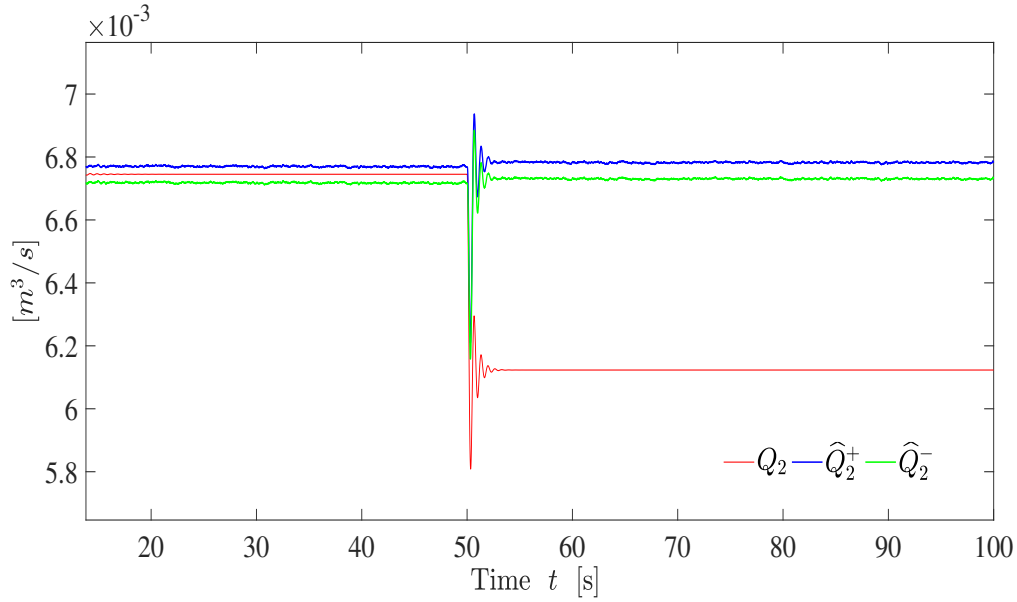

Figure 4-7: Behavior Q_2, with the occurrence of a leak, and their upper and lower estimations of the interval observer.$\widehat{\overline{Q}}_2 = \hat{Q}_2^+$,$\underline{\hat{Q}}_2 = \hat{Q}_2^-$.

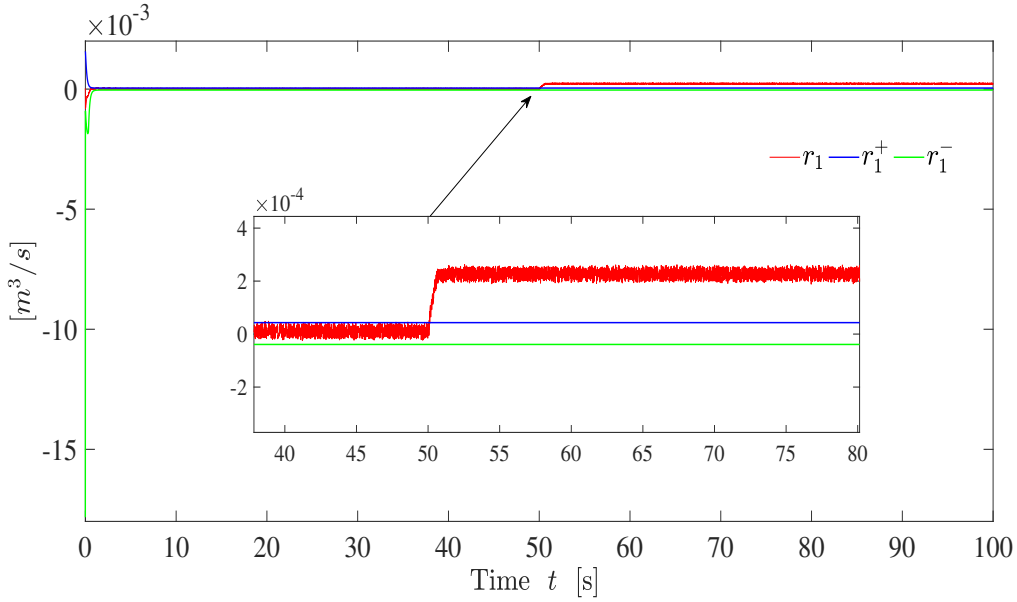

Figure 4-8: Behavior of residual $r_1(t)$, which guarantees the occurrence of a leak at that time.$\overline{r}_1 = r_1^+$, $\underline{r}_1 = r_1^-$.

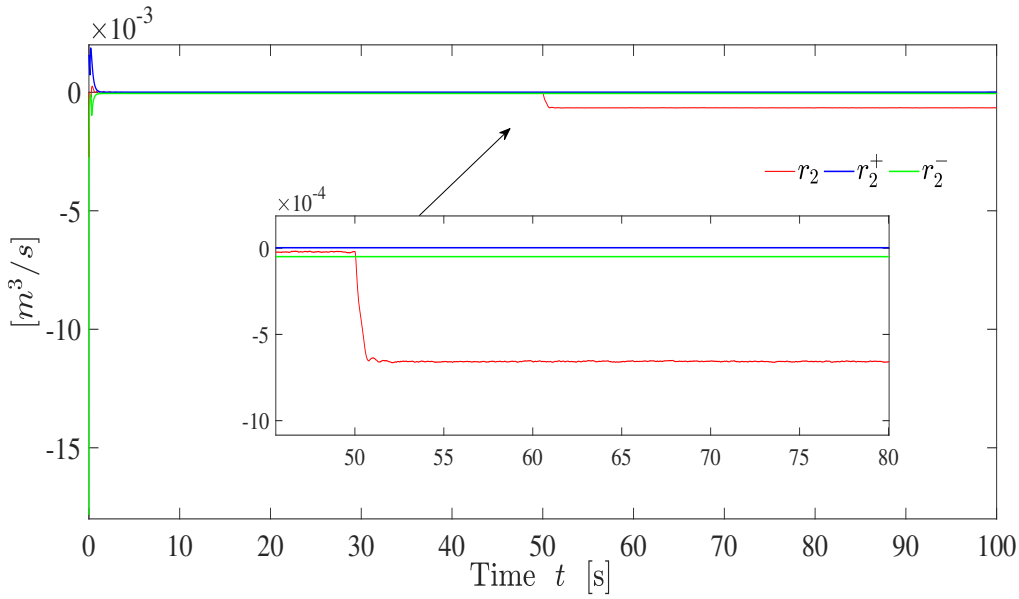

Figure 4-9: Behavior of residual $r_2(t)$, which guarantees the occurrence of a leak at that time.$\overline{r}_2 = r_2^+$,$\underline{r}_2 = Q_2^-$.

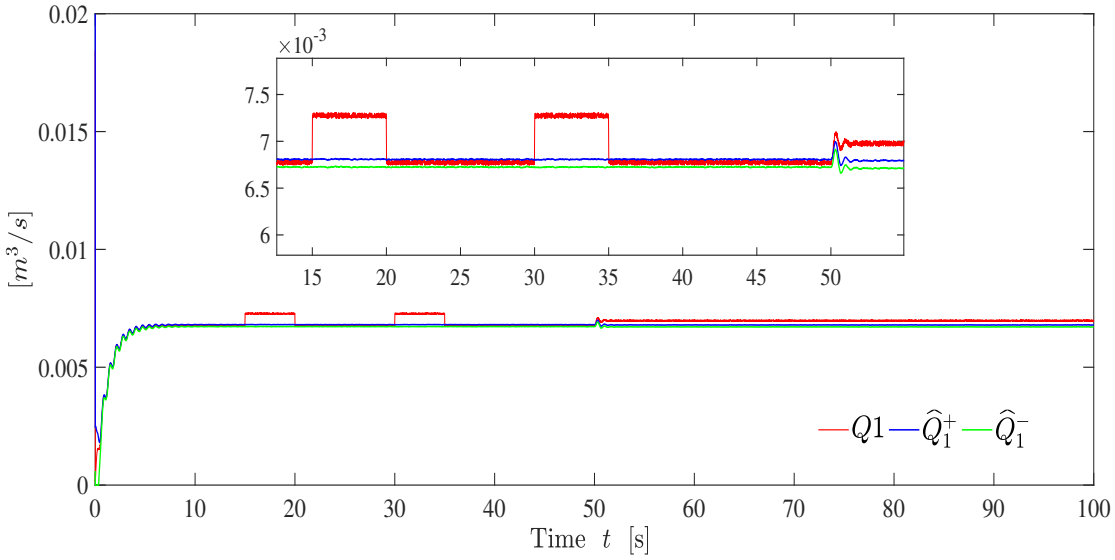

Figure 4-10: Behavior Q_1, with the occurrence of an intermittent sensor fault and a leak, and their upper and lower estimations of the interval observer.$\overline{\widehat{Q}}_1 = \hat{Q}_1^+$,$\underline{\hat{Q}}_1 = \hat{Q}_1^-$.

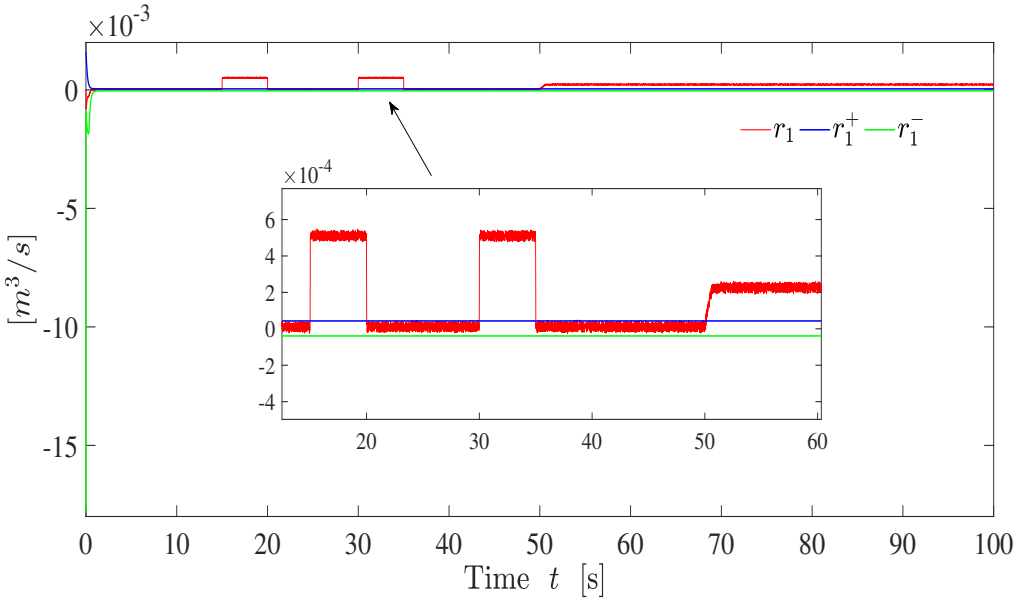

Figure 4-11: The behavior of the residual $r_1(t)$, confirms that a leak occurs at those times.$\overline{r}_1 = r_1^+$,$\underline{r}_1 = r_1^-$.

5 Interval observer-based FDI methods

This chapter delivers formal guarantees for fault detection and isolation in a class of perturbed linear systems. The proposed framework extends interval-observer designs—functionally similar to state observers by (i) treating the fault signal as an unknown input and (ii) embedding the fault condition as two static augmenting states expressed in a positive representation. We then deploy this methodology to fluid-transport pipelines, enabling reliable detection, localization, and magnitude reconstruction of single or multiple leaks along the conduit.

5.1 Interval Observer design using the Positive Representation method

The positive representation method, as discussed above, is based on the transformation of a linear system into a cooperative system, enabling the use of positive system techniques for designing an interval observer. This theoretical framework is focused on designing an observer that ensures that the estimated interval system provides valid and accurate bounds for the system states.

Consider the continuous-time linear system represented as:

$$\Upsilon_{\mathrm{S}}: \begin{cases} \dot{x}(t) = Ax(t) + Bu(t) + Ed(t) + Ff(t),\ x\left(t_0\right) = x_0, \\ y_e(t) = Cx(t) + \eta(t), \end{cases} \tag{5-1}$$

Where $x \in \mathbb{R}^n$ is the state vector, $u \in \mathbb{R}^m$ is the control vector, $d \in \mathbb{R}^{n_d}$ is the disturbance vector, $f \in \mathbb{R}^{n_f}$ is the fault vector and $y \in \mathbb{R}^p$ is the measured output vector. Matrices $A \in \mathbb{R}^{n\times n}, B \in \mathbb{R}^{n\times m}, E \in \mathbb{R}^{n\times n_d}, F \in \mathbb{R}^{n\times n_f}, C \in \mathbb{R}^{p\times n}$ are known matrices describing the system dynamics. The signal $\eta \in \mathbb{R}^{n_p}$ is the measurement noise and $x(0)$ is the vector of initial conditions

The goal of the observer design is to estimate the state $x(t)$ of the system in the presence of disturbances and noise, providing upper and lower bounds for the state.

To apply the positive representation method, the original or transformed system must be cooperative. If the system does not naturally meet this property, it is transformed in the following ways:

- **Decomposition of** A: The matrix A can be decomposed into a cooperative part and a non-cooperative part. When the A matrix in its original coordinates is necessary to do a linear transformation, usually Jordan Transformation Cacace et al. (2015) is used to ensure the dynamics matrix of the transformed system is cooperative.

In the following sections, we will present how to derive an interval observer using positive representation.

5.2 Interval Observers from Internally Positive Realization

We consider two variants of the plant:

1. **Unknown–input scenario.** The fault acts as an *unknown input* that directly perturbs the system dynamics.
2. **Augmented–state scenario.** The fault is represented as an *additional state*, enlarging the state vector to capture the fault's dynamics explicitly.

Building on the positive–representation framework of Cacace et al. (2015), we design an *interval observer* that:

- treats the fault signal $f(t)$ as an extra disturbance,
- employs a Lyapunov-based synthesis to guarantee fault sensitivity, and
- preserves strong robustness against all other bounded disturbances.

The system introduced below complies with these specifications and serves as the basis for the subsequent derivations.

5.2.1 Design

Consider the system $\Upsilon_{d,\eta,f}$ defined in (5-1)

$$\Upsilon_{d,\eta,f} = \begin{cases} \dot{x}(t) &= Ax(t) + Bu(t) + Ed(t) + Ff(t) \\ y(t) &= Cx(t) + \eta(t) \\ x(0) &= x_0 \end{cases} \tag{5-2}$$

with $x(t) \in \mathbb{R}^n$,$u(t) \in \mathbb{R}^m$, $y(t) \in \mathbb{R}^p$,$d(t) \in \mathbb{R}^{n_d}$,$f(t) \in \mathbb{R}^{n_f}$,$\eta(t) \in \mathbb{R}^p$ and the matrices A, B, C, E, F have known dimensions. Assume that there are known bounds for the input disturbances $d(t)$, represented as an interval vector

$$d(t)^I = \left[\underline{d}(t),\ \ \overline{d}(t)\right].$$

The fault vector $f(t)$ is assumed to be unknown; the measurement noise $\eta(t)$ is bounded and is represented by an interval vector.

$$\eta(t)^I = \left[\underline{\eta}(t), \quad \overline{\eta}(t)\right].$$

The initial conditions are also bounded, with the interval vector of initial conditions represented as

$$x_0^I = \left[\underline{x}_0, \quad \overline{x}_0\right],$$

where $\underline{x}_0$ and $\overline{x}_0$ denote the lower and upper bounds, respectively.

The dynamic interval system is described by:

$$\dot{Z}(t) = F(Z(t), u(t), y(t), d(t), f(t), \eta(t)) \tag{5-3}$$

with initial conditions

$$Z(0) = G(\underline{x_0}, \overline{x_0}),$$

and outputs:

$$\left[\underline{x}(t), \quad \overline{x}(t)\right] = \left[T_1(t, Z), \quad T_2(t, Z)\right].$$

The system is defined as an interval observer if the following conditions hold:

1. The dynamic system (5-3) is Input-State Stable (ISS) (see Sontag (2007)).
2. For any interval vector of initial conditions $x(0)^I$, the solutions $x(t)$ and $Z(t)$ of (5-2) and (5-3), respectively, satisfy the inequalities

$$\underline{x}(t) \preceq x(t) \preceq \overline{x}(t), \quad \forall t \geq 0.$$

3. If the normed spaces of $\|\overline{d}(t) - \underline{d}(t)\|$, and $\|\overline{\eta}(t) - \underline{\eta}(t)\|$ are uniformly bounded, and $f(t) \in \mathcal{L}_2$, then $\|\overline{x}(t) - \underline{x}(t)\|$ is also uniformly bounded. Moreover, if

$$\overline{d}(t) = \underline{d}(t), \ \overline{\eta}(t) = \underline{\eta}(t),$$

for all $t \geq 0$, it can be concluded that

$$\|\overline{x}(t) - \underline{x}(t)\| \to 0.$$

Before we describe the IPR of the interval observer, first we must consider the conditions for a well-posed positive Luenberger observer for the system described in (5-1).

Given an internally positive system (5-2), the following Luenberger observer is used:

$$\Upsilon_{\mathcal{O}} = \left\{ \begin{array}{rcl} \dot{\hat{x}}\left(t\right) & = & A\hat{x}\left(t\right) + Bu\left(t\right) + L\left(y\left(t\right) - C\hat{x}\left(t\right)\right) \\ \hat{x}\left(0\right) & = & \hat{x}_0 \end{array} \right. \tag{5-4}$$

The dynamic estimation error $\dot{e}(t)$ between the dynamic system in (5-2) and the Luenberger observer given in (5-4) is

$$\dot{e}(t) = A_L e(t) + Ed(t) + Ff(t) - L\eta(t) \tag{5-5}$$

where $A_L = A - LC$, being L the observer matrix such that asymptotic stability of the estimation error $e(t) \to 0$ when $d(t) = f(t) = \eta(t) = 0$ and when $d(t)$, $\eta(t)$ and $f(t)$ are uniformly bounded, then $e(t)$ will also be ultimately bounded.

Proposition 8. *Consider the systems Υ_S that satisfies the previous assumptions (without occurrence of faults). If there exists the matrices $P = P^\top > 0$, $H = H^T > 0$ and L such that*

$$P(A - LC) + (A - LC)^T P + H < 0,$$

$A_L \overset{M}{\succeq} 0$ (Metzler) and $E \succeq 0$, then $\Upsilon_{\mathcal{O}}$ is an Interval Observer for $\Upsilon_{\mathcal{S}}$.

Proof. The stability of the estimation error can be demonstrated by considering the quadratic Lyapunov candidate function, $V(e(t)) = e(t)^T P e(t)$, where $P = P^T > 0$ is a positive definite matrix. The time derivative of this Lyapunov quadratic function is:

$$\dot{V}(e(t)) = \frac{d}{dt}(e(t)^T P e(t)) = e(t)^T P\dot{e}(t) + \dot{e}(t)^T P e(t) \tag{5-6}$$

To achieve asymptotic stability of the estimation error for the case where $d(t) = \eta(t) = f(t) = 0$, the matrix $(A - LC)$ must be Hurwitz, i.e. a Lyapunov equation is guaranteed for some positive H, that is

$$P(A - LC) + (A - LC)^T P + H < 0$$

By solving this LMI, it is possible to find a suitable observer gain L that satisfies this condition, ensuring that the unperturbed estimation error converges to zero when $d(t) = f(t) = \eta(t) = 0$.

To ensure partial ordering, the property of cooperativity is applied. Consequently, A_L is required to be Metzler.

If disturbances, noise are bounded and the failures $f(t) \to 0$, boundedness of the estimation error can be guaranteed. To demonstrate this, the Lyapunov derivative in equation (5-6) can be rewritten as:

$$V\left(\dot{e}\left(t\right)\right) = -e^T\left(t\right) He\left(t\right) + e^T\left(t\right) P\mathcal{B}w\left(t\right) + w^T\left(t\right)\mathcal{B}^T Pe\left(t\right)$$

where $\mathcal{B} = [E \;\; F \;\; L]$ and $w = [d^T \;\; f^T \;\; \eta^T]^T$. It can be easily shown that there exists an attractive set, which depends on the bounds imposed on w, such that $\|e(t)\| \leq c$ for a long enough time t. □

Previously, we have demonstrated the ultimate boundedness for all bounded external inputs. Now we separate the disturbances and noise from the faults, since part of our goal is to distinguish them apart. The second part of this proof will examine the behavior of the stability of the system when the fault $f(t)$ is analyzed separately and assesses its impact on the estimation error.

Remark 10. *The following theorem builds on the work of Cacace et al. (2015), extending it to incorporate separate fault signals $f(t)$, disturbances $d(t)$, and noise $\eta(t)$ into a dynamic system, thereby establishing a positive-representation framework for a state observer.*

Theorem 2. *Consider the system $\Upsilon_{d(t),f(t),\eta(t)}$ described in (5-2) with $L \in \mathbb{R}^{n\times q}$ with $A_L = A - LC$, such that L is selected to ensure that the positive representation of $A_L \equiv [A_L]$ is Hurwitz. Define the (positive representation) observer system*

$$\Upsilon_{\mathcal{O}} = \begin{cases} \dot{\hat{Z}}(t) &= [A_L] Z(t) + \tilde{B}\pi(u(t)) + \tilde{L}\pi(y(t)) \\ Z(0) &= \pi(\hat{x}_0) \in \mathbb{R}^{2n}_{+} \\ \hat{x}(t) &= \Delta_n Z(t) \end{cases} \tag{5-7}$$

where $\tilde{B}$ and $\tilde{L}$ are the positive representations of B and L respectively, and $\pi(\cdot)$ is the positive representation of the signal.
The matrix $[A_L]$ is defined as

$$[A_L] = \begin{bmatrix} d^{A_L} + \left(A_L - d^{A_L}\right)^{+} & \left(A_L - d^{A_L}\right)^{-} \\ \left(A_L - d^{A_L}\right)^{-} & d^{A_L} + \left(A_L - d^{A_L}\right)^{+} \end{bmatrix}$$

In addition, the following properties hold $\forall\ t \geq 0$:

- $Z(t) \succeq 0$
- *if $d(t) = f(t) = \eta(t) = 0$, then $\hat{x}(t)$ exponentially converges to $x(t)$. Furthermore if $Z(0) = \pi(x(0))$, then $\hat{x}(t) = x(t)$*
- *if $x(t), d(t), \eta(t)$ are uniformly bounded and $f(t) \to 0$, the positive representation $Z(t)$ is uniformly bounded.*

Proof. The positive representation $Z(t)$ follows from the assumption that $[A_L]$ is Metzler, and $\tilde{B}, \tilde{L}$ are non-negative, the input vector $\pi(u(t))$ is positive and the initial conditions are positive representation $Z(0) \succeq 0$. The affirmation $\hat{x}(t) \to x(t)$ exponentially when $d(t) = \eta(t) = 0$ and $f(t) \to 0$ concludes from the fact that (5-4) defines the Luenberger observer $\Sigma_{\mathcal{O}}$ is internally positive realization. To prove this: Given $\dot{\hat{x}}(t) = \Delta_n \dot{Z}(t)$

$$\begin{aligned} \dot{\hat{x}}(t) &= \Delta_n \dot{Z}(t) \\ &= \Delta_n [A_L] Z(t) + \Delta_n \tilde{B}\pi(u(t)) + \Delta_n \tilde{L}\pi(y(t)) \\ &= A_L \Delta_n Z(t) + Bu(t) + Ly(t) \\ &= A_L \hat{x}(t) + Bu(t) + Ly(t) \end{aligned} \tag{5-8}$$

Concluding that (5-8) is the Luenberger observer defined in (5-4). Since $[A_L]$ is Hurwitz, the bounded condition of $x(t)$, and therefore $\pi(y(t))$, and of $d(t), \eta(t)$, $f(t) \to 0$ also concludes that $Z(t)$ is bounded. □

A set of state observers constructed using IPR under Theorem 2 is designed as an interval observer. The following Lemma establishes the properties of the interval observer, ensuring that the estimation trajectories remain bounded between the lower limit $\underline{\hat{x}}$ and the upper limit $\overline{\hat{x}}$.

Lemma 3. *Cacace et al. (2015) Given the state vector $x(t) \in \mathbb{R}^n$ and its positive representation $X(t) \in \mathbb{R}^{2n}_+$. Given $x(t) = \Delta_n X(t)$ and considering the lower and upper bounds as the following positive vector respectively:*

$$\underline{X}(t) = \begin{bmatrix} \underline{X}_1^T(t) & \underline{X}_2^T(t) \end{bmatrix}^T \in \mathbb{R}^{2n}_+ \qquad \overline{X}(t) = \begin{bmatrix} \overline{X_1}^T(t) & \overline{X_2}^T(t) \end{bmatrix}^T \in \mathbb{R}^{2n}_+$$

$\forall\ t \geq 0$, *with*

$$X(t) \subseteq \begin{bmatrix} \underline{X}(t) & \overline{X}(t) \end{bmatrix} \equiv \underline{X}(t) \leq X(t) \leq \overline{X}(t)$$

then

$$\underline{X}_1(t) - \overline{X_2}(t) \preceq x(t) \preceq \overline{X_1}(t) - \underline{X}_2(t) \tag{5-9}$$

The interval observer consists of two subsystems, as described in Theorem 2. It is convenient to represent the disturbance $d(t)$, fault $f(t)$, and noise $\eta(t)$ as:

Proposition 9. *Given an known fault signal $f(t) \to 0$ the following consolidated vector is proposed*

$$\gamma(t) = Ed(t) + Ff(t) - L\eta(t)$$

From the gain of the observer L, an interval-bound representation of the equivalent disturbance, $\gamma^I(t) = \begin{bmatrix} \underline{\gamma}(t) & \overline{\gamma}(t) \end{bmatrix}$, can be derived. This interval represents the bounded effects caused by the disturbance $d(t)$ and the measurement noise $\eta(t)$ with a fault signal unknown $f(t) \to 0$.

Theorem 3. *For the system $\Upsilon_{d(t),f(t),\eta(t)}$ given in (5-2), with $L \in \mathbb{R}^{n\times q}$, where $[A_L]$ is Hurwitz and Metzler, and with $w(t)$ being bounded, the following dynamic system holds:*

$$\begin{aligned} \dot{\underline{\hat{Z}}}(t) &= [A_L]\,\underline{Z}(t) + \tilde{B}\Phi(u(t)) + \tilde{L}\Phi(y(t)) + \Phi_{\underline{\gamma}(t)}\left(\underline{\gamma}(t)\right) \\ \dot{\overline{\hat{Z}}}(t) &= [A_L]\,\overline{Z}(t) + \tilde{B}\Phi(u(t)) + \tilde{L}\Phi(y(t)) + \Phi_{\underline{\gamma}(t)}(\overline{\gamma}(t)) \\ \underline{Z}(0) &= \Phi_{\underline{x}(0)}(\underline{x}(0)), \overline{Z}(0) = \Phi_{\underline{x}(0)}(\overline{x}(0)) \end{aligned} \tag{5-10}$$

Here,

$$\Phi_{\underline{\gamma}(t)}\left(\underline{\gamma}(t)\right) \quad \textit{and} \quad \Phi_{\overline{\gamma}(t)}\left(\overline{\gamma}(t)\right)$$

denote the positive representations of the interval vector $\gamma^I(t)$, which captures disturbances and noise under the assumption $f(t) \to 0$. Likewise,

$$\Phi\Big(u(t)\Big) \quad \textit{and} \quad \Phi\Big(y(t)\Big)$$

are the positive-representation functions of the input and output signals, respectively, and the functions $\Phi_{\underline{x}(0)}\Big(\underline{x}(0)\Big)$ and $\Phi_{\overline{x}(0)}\Big(\overline{x}(0)\Big)$ denote the positive representations of the initial-condition interval vector. The equivalence of this system in the original coordinates is

$$\begin{aligned} \underline{x}\,(t) &= \begin{bmatrix} \mathbb{I}_n & \mathbb{O}_{n\times n} \end{bmatrix} \underline{Z}\,(t) - \begin{bmatrix} \mathbb{O}_{n\times n} & \mathbb{I}_n \end{bmatrix} \overline{Z}\,(t) \\ \overline{x}\,(t) &= \begin{bmatrix} \mathbb{I}_n & \mathbb{O}_{n\times n} \end{bmatrix} \overline{Z}\,(t) - \begin{bmatrix} \mathbb{O}_{n\times n} & \mathbb{I}_n \end{bmatrix} \underline{Z}\,(t) \end{aligned} \tag{5-11}$$

It is an interval observer for $\Sigma_{d(t),f(t),\eta(t)}$ for $\underline{x}\,(t) \preceq x\,(t) \preceq \overline{x}\,(t)$.

Proof. According with the interval observer exposed in (5-10), its configuration proposes two positive subsystems because $\underline{Z}(t), \overline{Z}(t) \in \mathbb{R}^{2n}_+$, and therefore the state of the interval observer is given as $Z(t) = \begin{bmatrix} \underline{Z}\,(t) & \overline{Z}\,(t) \end{bmatrix}^T \in \mathbb{R}^{4n}_+$. And it is known that $[A_L]$ is Hurwitz and Metzler, then (5-9) is Input State Stable (ISS), and therefore the positive state $Z(t)$ is uniformly bounded if the input $u(t)$, $y(t)$, and $\Gamma(t)$ are uniformly bounded. For proving that $\underline{x}(t) \preceq x(t) \preceq \overline{x}(t)$ the following procedure shows that:

$$\dot{\chi}(t) = [A_L]\chi(t) + \tilde{B}\pi(u(t)) + \tilde{L}\pi(y(t)) + \phi(\Gamma(t))$$

where $\chi(0) = \phi_{\underline{x}(0)} \in \mathbb{R}^{2n}_+$ represents an Internally Positive Realization (IPR) of the system $\Sigma_{d(t),f(t),\eta(t)}$, with the original coordinates related by $x(t) = \Delta_n\chi(t)$, the next step is to demonstrate that the inequality $\underline{Z}(t) \preceq \chi(t) \preceq \overline{Z}(t)$ holds for all $t \geq 0$. This condition arises from the fact that the trajectories satisfy the monotonicity property, given the initial condition bounds $\underline{Z}(0) \preceq \chi(0) \preceq \overline{Z}(0)$, and the expression $\phi(\underline{\Gamma}(t))_{\underline{\Gamma}(t)} \preceq \phi(\Gamma(t))_{\underline{\Gamma}(t)} \preceq \phi(\overline{\Gamma}(t))_{\underline{\Gamma}(t)}$.

This inequality leads to the conclusion that if $\phi(\underline{\Gamma}(t)) = \phi(\overline{\Gamma}(t))$ for all $t \geq 0$, the two subsystems will converge, yielding coincident estimates. Moreover, the Hurwitz property of $[A_L]$ ensures that $\| \overline{Z}(t) - \underline{Z}(t) \| \to 0$, and consequently, $\| \overline{x}(t) - \underline{x}(t) \| \to 0$ as well. In addition it is necessary to prove that if $\| \overline{\Gamma}(t) - \underline{\Gamma}(t) \|$ is bounded also $\| \overline{x}(t) - \underline{x}(t) \|$ is bounded. If the diference $\Xi = \overline{x}(t) - \underline{x}(t)$ is expressed as the positive transformation equivalence: $\Xi = \begin{bmatrix} \mathbb{I}_n & \mathbb{I}_n \end{bmatrix} \begin{pmatrix} \underline{Z}\,(t) & \overline{Z}\,(t) \end{pmatrix}$ From this:

$$\begin{aligned} \dot{\chi}\,(t) &= \begin{bmatrix} \mathbb{I}_n & \mathbb{I}_n \end{bmatrix} [A_L] \begin{pmatrix} \underline{Z}\,(t) & \overline{Z}\,(t) \end{pmatrix} \\ &\quad + \overline{\Gamma}\,(t) - \underline{\Gamma}\,(t) \\ &= \Big(d^{A_L} + \mid A_L - d^{A_L} \mid\Big)\,\chi\,(t) + \overline{\Gamma}\,(t) - \underline{\Gamma}\,(t) \end{aligned} \tag{5-12}$$

with $[A_L]$ being both a Hurwitz and Metzler matrix simultaneously.
The matrix $d_{A_L} + |A_L - d_{A_L}|$ is Hurwitz, because the eigenvalues $\lambda(d_{A_L} + |A_L - d_{A_L}|)$ are a subset of $\lambda(A_L)$. Consequently, the fact that $\| \overline{\Gamma}(t) - \underline{\Gamma}(t) \|$ is uniformly bounded implies that $\| \overline{x}(t) - \underline{x}(t) \|$ is also uniformly bounded. □

5.2.2 The interval observer defined by a coordinate transformation

. This situation occurs when the matrix in its positive representation, $[A_L]$, with the chosen gain L, does not result in a Hurwitz matrix. To address this issue, a method proposed by Cacace et al. (2015), based on the Real Jordan Form, can be applied. This method transforms the matrix $A_L \in \mathbb{R}_-^{n\times n}$ into its positive representation $[A_L] \in \mathbb{R}_+^{2n\times 2n}$, ensuring that it is both Hurwitz and Metzler simultaneously.

Remark 11. *Typically, the observable canonical form is used to design state observers. However, when aiming for a positive system representation, one cannot simply place the eigenvalues in the observable canonical form and expect the resulting matrix to be both Hurwitz and Metzler. The A-matrix of the canonical observable representation is not Metzler and as a result, it is necessary to apply a linear change of basis to the closed-loop matrix A_L, transforming it into a Hurwitz and Metzler form before performing the positive system representation. In other words, using the observable canonical form alone is insufficient; one must first use a suitable linear transformation to obtain a matrix that is simultaneously Hurwitz and Metzler prior to the positive representation.*

The following procedure outlines this method:

- Find L by assigning to $A - LC$ a set of eigenvalues in a region $\mathcal{S}$, defined as:

$$\mathcal{S} \subset \mathbb{C}_- \mid \mathcal{S} = \{z \in \mathbb{C} : \Re(z) + |\Im(z)| < 0\}$$

  if the matrix $A-LC$ is in Real Jordan Form, its positive representation $[A_L]$ is Metzler and Hurwitz if and only if its spectrum $\sigma(A_L) \subset \mathcal{S}$. This transformation guarantees that the Jordan matrix, which contains only real eigenvalues, satisfies the observer stability condition Cacace et al. (2015).

- find the simmilarity transformation for converting A_L to its real Jordan Form J_L.

- Finally, design the interval observer for the transformed system and translate the resulting interval back to the original coordinates.

Proposition 10. *Given the system: $\Upsilon_{d(t),f(t),\eta(t)}$ exposed in (5-2), where $L \in \mathbb{R}^{n\times q}$ such that the eigenvalues $\sigma(A_L) \subset \mathcal{S}$ a bound equivalent to the total disturbance state $\gamma(t)$: $\underline{\gamma}(t) \preceq \gamma(t) \preceq \overline{\gamma}(t)$ and a nonsingular matrix $T \in \mathbb{R}^{n\times n}$ the real Jordan Form will : $J_L = T^{-1}A_LT$, With the transformed functions for the total disturbances, $\Psi_{T,\underline{\gamma}(t)}\Big(\underline{\gamma}(t)\Big)$ and $\Psi_{T,\overline{\gamma}(t)}\Big(\overline{\gamma}(t)\Big)$, which are the interval functions described earlier, the system becomes:*

$$\begin{aligned}\dot{\underline{Z}}(t) &= [J_L]\,\underline{Z}(t) + \tilde{B}_T\pi(u(t)) + \tilde{L}_T\pi(y(t)) + \Psi_{T,\underline{\gamma}(t)}\Big(\underline{\gamma}(t)\Big)\\ \dot{\overline{Z}}(t) &= [J_L]\,\overline{Z}(t) + \tilde{B}_T\pi(u(t)) + \tilde{L}_T\pi(y(t)) + \Psi_{T,\underline{\gamma}(t)}(\overline{\gamma}(t))\end{aligned} \tag{5-13}$$

with:

$$\underline{Z}(0) = \Psi_{T,\underline{x}(0)}(\underline{x}(0)) \quad , \quad \overline{Z}(0) = \Psi_{T,\underline{x}(0)}(\overline{x}(0))$$

and with the interval estimate states in original coordinates:

$$\begin{array}{l} \underline{x}\left(t\right) = \left[\begin{array}{cc} \mathbb{I}_n & \mathbb{O}_n \end{array}\right] \tilde{T}\underline{Z}\left(t\right) - \left[\begin{array}{cc} \mathbb{O}_n & \mathbb{I}_n \end{array}\right] \tilde{T}\overline{Z}\left(t\right) \\ \overline{x}\left(t\right) = \left[\begin{array}{cc} \mathbb{I}_n & \mathbb{O}_n \end{array}\right] \tilde{T}\overline{Z}\left(t\right) - \left[\begin{array}{cc} \mathbb{O}_n & \mathbb{I}_n \end{array}\right] \tilde{T}\underline{Z}\left(t\right) \end{array} \tag{5-14}$$

where: $[J_L]$ *is Metzler and Hurwitz, and* $\tilde{B}_T, \tilde{L}_T$ *are the positive representation of* $B_T = T^{-1}B$ *and* $L_T = T^{-1}L$ *respectively.*

Proof. The interval observer described in equations (5-14) is Input-to-State Stable (ISS) Sontag (2007), since the Hurwitz properties of $T^{-1}A_LT$ are preserved in the positive representation, ensuring $\sigma(T^{-1}A_LT) \subset \mathcal{S}$. Furthermore, to guarantee the inclusion property of the observer in the interval on bounded trajectories, it is essential to verify the positive nominal condition of the estimated state $\hat{X}(t)$, ensuring that $\underline{\hat{X}}(t) \preceq \hat{X}(t) \preceq \overline{\hat{X}}(t)$, where $X(t) \in \mathbb{R}^{2n}$.

$$\dot{\hat{X}}\left(t\right) = \left[J_L\right]\hat{X}\left(t\right) + \tilde{B_T}\left(t\right)\pi\left(u\left(t\right)\right) + \tilde{L_T}\left(t\right)\pi\left(y\left(t\right)\right) + \Psi_{T,\underline{\gamma}(t)}\left(\gamma\left(t\right)\right)$$

with $\hat{X}\left(0\right) = \Psi_{T,\underline{x}(0)}\left(x\left(0\right)\right)$, $\forall\ \underline{x}\left(0\right) \preceq x\left(0\right) \preceq \overline{x}\left(0\right)$, such that the transformation in original coordinates is $x\left(t\right) = T\Delta_n X\left(t\right)$. Additionally, the cooperative properties of the trajectories are preserved because the positive transformation of the matrix T guarantees the following equivalence:

$$\begin{array}{rcl} & & \underline{\hat{X}}(t) \preceq \hat{X}(t) \\ \preceq \overline{\hat{X}}(t) & \iff & \tilde{T}\,\underline{\hat{X}}(t) \preceq \tilde{T}\,\hat{X}(t) \preceq \tilde{T}\,\overline{\hat{X}}(t) \end{array}$$

□

5.2.3 Designing the Observer Gain

The design of the observer gain L plays a crucial role in ensuring that the estimated state bounds converge accurately to the actual state of the system. The general structure of a Luenberger observer for the system described in (5-4) is given by:

$$\dot{\hat{x}}(t) = A\hat{x}(t) + Bu(t) + L(y(t) - \hat{y}(t))$$

Where $\hat{x}(t)$ is the estimated state, $\hat{y}(t) = C\hat{x}(t)$ is the estimated output, and L is the observer gain to be designed.

To ensure that the estimation error remains bounded, the error dynamics $e(t) = x(t) - \hat{x}(t)$ must be stabilized:

$$\dot{e}(t) = (A - LC)e(t) + Ed(t) + Ff(t) - L\eta(t)$$

Where $d(t)$, $f(t)$ and $\eta(t)$ represent disturbances and faults, respectively. The goal of designing the gain L is for the matrix $A-LC$ to be Hurwitz, meaning that all its eigenvalues have negative real parts, ensuring the stability of the estimation error.

The gain L is designed under the following conditions:

- **Stability**: $A - LC$ must be Hurwitz. This can be achieved by solving a Lyapunov equation or formulating an optimization problem.
- **Cooperativity**: It is essential that the resulting system preserves the cooperativity property, ensuring that the observer maintains the order relationships between the upper and lower state bounds.
- **Optimization**: In some cases, the design of L can be formulated as an optimization problem, minimizing the size of the estimation intervals under stability constraints.

Through the use of Liapunov functions the idea is to verify that the interval observer ensures the stability of the estimations. According with the exposed above the purpose is to define the Lyapunov function that describes the estimation error for assuring the convergence error to zero between the bounded estimations about the real state, taking into account the disturbances $d(t)$ and measurement noise $\eta(t)$. Note that at this point the system, will be assumed to be fault-free, i.e. $f(t) \to 0$,but not $f(t) = 0$. Assuming a quadratic Liapunov function $V(e(t)) = e^T(t) Pe(t)$,By expanding the equation (from (5-6)) we obtain:

$$\begin{array}{c} V(\dot{e}(t)) = e^T(t) PAe(t) - e^T(t) PLCe(t) \\ +e^T(t) A^T Pe(t) - e^T(t) C^T L^T C^T Pe(t) \\ +e^T(t) PEd(t) + e^T(t) PFf(t) \\ -e^T(t) PL\eta(t) + d^T(t) E^T Pe(t) \\ +f^T(t) F^T Pe(t) - \eta^T(t) L^T Pe(t) \end{array} \tag{5-15}$$

where $Q = PL$. According with (5-15) , in this Liapunov Quadratic Function the expressions, P is a symmetric matrix $P = P^T$ and positive definite $P \succ 0$ with $L = P^{-1}Q$, and the expressions $e(t)^T PEd(t)$, $d(t)^T E^T Pe(t)$, $e(t)^T PFf(t)$, $f(t)^T F^T Pe(t)$, $e^T(t)Q\eta^T(t)$ and $\eta^T(t)Q^T e(t)$ must be minimized for assuring the stability conditions therefore it is necessary to define a Cost function for obtaining this purpose.

Proposition 11. *Define an appropriate minimization problem in the following way:*

$$\min J \leq \theta^2 d^T(t) d(t) + \tau^2 \eta^T(t) \eta(t) \tag{5-16}$$

such that θ and τ are scalar values where $0 < \theta < 1$ and $0 < \tau < 1$. being

$$J = V(\dot{e}(t)) + r^T r(t) \quad \leq \quad 0$$

The goal is to determine the values of P and L that minimize the effect of $d(t)$ and $\eta(t)$ on the residual, i.e. the smallest possible values for θ and τ that solve the constraints.

If the minimization problem is solved for some positive definite P, the following are true:

1. **Stability**: The observer error system is stable, meaning that $e(t) \to 0$ as $t \to \infty$.

2. **Optimality** The matrix gain L is such that it minimizes the effects of both $d(t)$ and $\eta(t)$, i.e. θ and τ are small.

In the cost function J, the term $r(t)$ represents the residual signal, defined as:

$$r(t) = y(t) - \hat{y}(t) = Cx(t) + \eta(t) - C\hat{x}(t) = Ce(t) + \eta(t).$$

Furthermore, noise corrupts the measurements, therefore affecting the residual. Using the $\mathcal{S}$-procedure, the constraints can be rewritten as a single constraint. First note that

$$r^T(t)\, r(t) = e^T(t)\, C^T C e(t) + e^T(t)\, C^T \eta(t) + \eta^T(t)\, Ce(t) + \eta^T(t)\, \eta(t) \tag{5-17}$$

Now note that the minimization problem is solved if the inequality J has a solution for some P for small enough θ, τ, where

$$\begin{aligned} J \;&= V\big(\dot{e}(t)\big) \;+\; r^T(t)\, r(t) \;-\; \theta^2\, d^T(t)\, d(t) \;+\; \tau^2\, \eta^T(t)\, \eta(t) \;\leq\; 0 \\ &= e^T(t)\, P\, A\, e(t) \;-\; e^T(t)\, P\, L\, C\, e(t) \\ &\quad +\; e^T(t)\, A^T\, P\, e(t) \;-\; e^T(t)\, C^T\, L^T\, C^T\, P\, e(t) \\ &\quad +\; e^T(t)\, P\, E\, d(t) \;+\; e^T(t)\, P\, F\, f(t) \\ &\quad -\; e^T(t)\, P\, L\, \eta(t) \;+\; d^T(t)\, E^T\, P\, e(t) \\ &\quad +\; f^T(t)\, F^T\, P\, e(t) \;-\; \eta^T(t)\, L^T\, P\, e(t) \\ &\quad +\; e^T(t)\, C^T\, C\, e(t) \;+\; e^T(t)\, C^T\, \eta(t) \\ &\quad +\; \eta^T(t)\, C\, e(t) \;+\; \eta^T(t)\, \eta(t) \\ &\quad -\; \theta^2\, d^T(t)\, d(t) \;-\; \tau^2\, \eta^T(t)\, \eta(t) \leq 0 \end{aligned}$$

Here, the variable $Q = PL$ is introduced in order to "linearize" the bilinear matrix equation in (5-18). Now, equation (5-18) will be developed as an LMI to express the conditions outlined above, and a line search algorithm is used to achieve the minimum of $d(t)$ and $\eta(t)$.

Equation (5-18) may be expressed in matrix form as follows:

$$\begin{bmatrix} e(t) \\ d(t) \\ f(t) \\ \eta(t) \end{bmatrix}^{\top} \left(\begin{bmatrix} He\Big(PA-QC\Big) & P\,E & P\,F & Q \\ \star & 0 & 0 & 0 \\ \star & \star & 0 & 0 \\ \star & \star & \star & 0 \end{bmatrix} + \begin{bmatrix} C^TC & 0 & 0 & 0 \\ 0 & -\theta^2\,I & 0 & 0 \\ 0 & 0 & 0 & 0 \\ 0 & 0 & 0 & -\tau^2\,I \end{bmatrix} \right) \begin{bmatrix} e(t) \\ d(t) \\ f(t) \\ \eta(t) \end{bmatrix} \leq 0$$

$$\iff \quad \begin{bmatrix} e(t) \\ d(t) \\ f(t) \\ \eta(t) \end{bmatrix}^{\top} \begin{bmatrix} He\Big(PA-QC\Big) + C^TC & P\,E & P\,F & Q \\ \star & -\theta^2\,I & 0 & 0 \\ \star & \star & 0 & 0 \\ \star & \star & \star & -\tau^2\,I \end{bmatrix} \begin{bmatrix} e(t) \\ d(t) \\ f(t) \\ \eta(t) \end{bmatrix} \leq 0\,. \tag{5-18}$$

where $He\{.\}$ denotes the Hermitian part of $PA-QC$. For this resultant expression the term:

$$\begin{bmatrix} He\,(PA-QC)+C^TC & PE & PF & -Q \\ \star & -\theta^2 I & 0 & 0 \\ \star & 0 & 0 & 0 \\ \star & 0 & 0 & -\tau^2 I \end{bmatrix} \leq 0 \tag{5-19}$$

As indicated by the last expression in (5-19), the matrix inequality is singular, preventing the determination of matrices P and Q under these conditions. However, if the fault signal $f(t) \to 0$, the matrix inequality becomes solvable, as it is no longer singular. Thus, for $\forall f(t) \to 0$, the matrix inequality is expressed as:

$$\begin{bmatrix} He\,(PA-QC)+C^TC & PE & -Q \\ \star & -\theta^2 I & 0 \\ \star & 0 & -\tau^2 I \end{bmatrix} \leq 0 \tag{5-20}$$

5.2.4 Augmented system representation with added fault states

In this scenario, the fault is treated as an additional state in the system defined by many authors as fault models Besançon et al. (1996), Torres et al. (2014). The following approach is proposed for constructing an interval observer in a positive representation for the system described through the following analysis:
Given the following interval dynamic system:

$$\Upsilon^{I}_{d(t),\eta(t)} = \begin{cases} \dot{\underline{x}} = \underline{A}\underline{x}\,(t) + \underline{B}u\,(t) + E\underline{d}\,(t) \\ \\ \dot{\overline{x}} = \overline{A}\overline{x}\,(t) + \overline{B}u\,(t) + E\overline{d}\,(t) \end{cases} \tag{5-21}$$

The nominal dynamic system :

$$\Upsilon_{d(t),\eta(t)} \begin{cases} \dot{x} = Ax\left(t\right) + Bu\left(t\right) + Ed\left(t\right) \\ \\ \quad y\left(t\right) = Cx\left(t\right) + \eta\left(t\right) \end{cases}$$

is associated with the interval dynamic system described in (5-21) and is given by:

$$\underline{Ax}\left(t\right) + \underline{B}u\left(t\right) + E\underline{d}\left(t\right) \preceq Ax\left(t\right) + Bu\left(t\right) + Ed\left(t\right) \preceq \overline{A}\overline{x}\left(t\right) + \overline{B}u\left(t\right) + E\overline{d}\left(t\right) \tag{5-22}$$

This type of system, in its general form, is evaluated using methods proposed by Raïssi et al. (2010), Efimov et al. (2013). In this thesis, studies by Yang and Ma (2021); Cruz et al. (2023), on interval system concepts are taken into account, particularly considering that the fault directly impacts the system's behavior, which could influence the open-loop stability of the nominal system. The objective is to evaluate the uncertainties ΔA, ΔB, and ΔC present in the matrices, which represent the parametric uncertainties associated with the model. The goal is to identify these uncertainties in a way that does not affect the nominal system's behavior. Once complies the conditions for the nominal system described $\Upsilon_{d(t),\eta(t)}$ are satisfied and to assurer that the uncertainties do not affect the open loop stability over the nominal system the following lemma is proposed

Lemma 4. *For the nominal system described $\Upsilon_{d(t),\eta(t)}$, an interval observer is defined by its lower and upper bounds as follows:*

Lower bound:

$$\dot{\underline{\hat{x}}}(t) = A\underline{\hat{x}}(t) + Bu(t) + L\left(y(t) - C\underline{\hat{x}}(t)\right)$$

Upper bound:

$$\dot{\overline{\hat{x}}}(t) = A\overline{\hat{x}}(t) + Bu(t) + L\left(y(t) - C\overline{\hat{x}}(t)\right)$$

According to the positive representation:

$$\underline{\hat{x}}(t) \in \mathbb{R}^n \rightarrow \underline{X}(t) \in \mathbb{R}^{2n},$$
$$\overline{\hat{x}}(t) \in \mathbb{R}^n \rightarrow \overline{X}(t) \in \mathbb{R}^{2n}.$$

The interval observer is based on the following assumptions:

1. *Strong monotonicity conditions are satisfied, as described in Chapter 2.*
2. *The pair (A, C) is observable or detectable.*
3. *There is a positive representation for the matrix $A - LC$, where $A - LC \in \mathbb{R}^{n\times n}$ and $[A - LC] \in \mathbb{R}^{2n\times 2n}$, ensuring that it is Metzler and Hurwitz. If it is Metzler but not Hurwitz, a Jordan form transformation can be applied to transform the system.*

4. *The matrices A, B, C in positive representation are non-negative (that is, $\succeq 0$).*

5. *The initial conditions $\hat{x}(0)$ in positive representation are non-negative (that is, $\succeq 0$).*

6. *The input vector $u(t)$ in positive representation is non-negative (that is, $\succeq 0$).*

Proof. The estimation error dynamics for the interval observer are given by:

$$\underline{e}(t) = x(t) - \underline{\hat{x}}(t),$$
$$\overline{e}(t) = \overline{\hat{x}}(t) - x(t).$$

For this estimation interval error, we define the following Lyapunov quadratic function:

$$V(e(t)) = \underline{e}^T(t) P \underline{e}(t) + \overline{e}^T(t) P \overline{e}(t).$$

The stability conditions for the Lyapunov function to ensure that the estimation error converges asymptotically to zero are:

$$V(e(t)) > 0 \text{ and } \dot{V}(e(t)) \quad \leq 0.$$

The derivative of the Lyapunov function is:

$$\dot{V}(e(t)) = \underline{e}^T(t) P \dot{\underline{e}}(t) + \dot{\underline{e}}^T(t) P \underline{e}(t) + \overline{e}^T(t) P \dot{\overline{e}}(t) + \dot{\overline{e}}^T(t) P \overline{e}(t) < 0.$$

This can be expressed as:

$$\begin{bmatrix} \underline{e}\,(t) \\ \overline{e}\,(t) \\ d\,(t) \\ f\,(t) \\ \eta\,(t) \end{bmatrix}^T \begin{bmatrix} PA + A^T P - 2C^T Q^T & 0 & PE & PF & -Q \\ \star & PA + A^T P - 2C^T Q^T & -PE & -PF & Q \\ \star & \star & 0 & 0 & 0 \\ \star & \star & 0 & 0 & 0 \\ \star & \star & 0 & 0 & 0 \end{bmatrix} \begin{bmatrix} \underline{e}\,(t) \\ \overline{e}\,(t) \\ d\,(t) \\ f\,(t) \\ \eta\,(t) \end{bmatrix} < 0 \tag{5-23}$$

where $Q = PL$ and $P \succ 0$ is a positive-definite symmetric matrix.

Assuming the fault signal $f(t)$ must be equal to zero, the previous expression may be reduced to

$$\begin{bmatrix} PA + A^T P - 2C^T Q^T & 0 & PE & -Q \\ \star & PA + A^T P - 2C^T Q^T & -PE & Q \\ \star & \star & 0 & 0 \\ \star & \star & \star & 0 \end{bmatrix} \leq 0 \tag{5-24}$$

This ensures exponential convergence of the estimation error when the fault signal $f(t) = 0$. Thus, the solution of the matrix inequality ensures that the observer error of the interval will converge under fault-free conditions. □

5.2.5 Pseudocode for the Proposed Interval Observer

The following pseudocode outlines the positive-representation interval observer introduced in this section.

Algorithm 2 Positive Representation–Based Interval-Observer Design

Require: System matrices A, B, C, D, W
Ensure: Interval–state estimates $\left[\underline{\hat{x}}(t),\, \overline{\hat{x}}(t)\right]$

Read A, B, C, D, W ▷ Step 1
Verify observability of (A, C) ▷ Step 2
Compute observer gain L via an LMI optimisation 5-24 ▷ Step 3
$A_L \leftarrow A - LC$ ▷ Step 4
if A_L is Hurwitz **and** Metzler **then** ▷ Step 5
    goto Step 14
else▷ Step 6
    Compute similarity transform T from the Jordan form of A_L
    $A_{L1} \leftarrow TA_LT^{-1},\ B_1 \leftarrow TB,\ C_1 \leftarrow CT^{-1},\ W_1 \leftarrow TW$ ▷ Step 7
    Obtain a positive representation of $\left(A_{L1}, B_1, C_1, W_1\right)$ ▷ Step 8
    Design interval observer to get $\dot{\underline{Z}}(t)$ and $\dot{\overline{Z}}(t)$ ▷ Step 9
    Map back to original coordinates:
    $\dot{\underline{\hat{x}}}(t) = T^{-1}\dot{\underline{Z}}(t),\ \dot{\overline{\hat{x}}}(t) = T^{-1}\dot{\overline{Z}}(t)$ ▷ Step 10
end if
Obtain a positive representation of $\left(A_L, B, C, W\right)$ ▷ Step 11
Design interval observer to get $\dot{\underline{Z}}(t)$ and $\dot{\overline{Z}}(t)$ ▷ Step 12
Recover estimates in original coordinates:
5-14 $\dot{\underline{\hat{x}}}(t) = \dot{\underline{Z}}(t),\ \dot{\overline{\hat{x}}}(t) = \dot{\overline{Z}}(t)$ ▷ Step 13
return $\left[\underline{\hat{x}}(t),\, \overline{\hat{x}}(t)\right]$ ▷ Step 14

5.2.6 Proposed Estimation Interval Residue

In this section, we present the estimation interval residue. For this analysis, we consider the following assumptions.

1. The residue established between the measured state $y_m(t)$ and the interval states, defined by the lower and upper limits $\hat{y}^I(t) = \left[\underline{\hat{y}}(t), \overline{\hat{y}}(t)\right]$, must adhere to the concepts of the Subset Property and Monotonic Inclusion introduced in Definition 7 of Chapter 2 of this thesis, we propose that, given a measured state $y_m(t)$, the following condition must hold:

$$y_m(t) \subseteq \left[\underline{\hat{y}}(t), \overline{\hat{y}}(t)\right]$$

2. Based on the above condition, the monotonicity between the lower and upper limits of the interval estimation with respect to the measured state must satisfy the following relation:

$$\underline{\hat{y}}(t) \preceq y_m(t) \preceq \overline{\hat{y}}(t)$$

for all $t \to \infty$, even in the presence of uncertainties, perturbations, and noise.

In the context of conventional Fault Detection and Isolation (FDI) analysis, a false fault refers to a false alarm or incorrect detection of a fault when no actual fault has occurred. False faults can be caused by the following:

1. Sensor noise or disturbances that exceed the fault detection thresholds
2. Modeling errors or uncertainties in the system model used for fault detection
3. Fault signatures

To mitigate the impact of false faults in the FDI analysis, it is essential to use robust and consistent data collection and reporting methods to ensure accurate and complete information about FDI flows. Furthermore, using multiple sources and applying rigorous statistical methods can help identify and correct any discrepancies or inaccuracies in the data.
Based on the discussion above, the new concept of using interval observers and interval residues for FDI (Fault Detection and Isolation) analysis aims to enhance the reliability of fault detection while minimizing the occurrence of false detections. The residue-based interval approach, which is based on estimated interval states, allows for a more efficient threshold setting that reduces the detection of false faults (Samy and Gu, 2011). Based on the foregoing, the following analytical proposal is presented: Give the following system:

$$\begin{aligned} \dot{x}(t) &= Ax(t) + Bu(t) + \nu(t) \\ y(t) &= Cx(t) + \eta(t) \end{aligned} \tag{5-25}$$

An observer is defined for (5-25) as

$$\dot{\hat{x}}(t) = A\hat{x}(t) + Bu(t) + LCx(t) + L\eta(t) - LC\hat{x}(t) \tag{5-26}$$

and the dynamic estimation error $\dot{e}(t) = \dot{x}(t) - \dot{\hat{x}}(t)$ is given as:

$$\dot{e}(t) = (A - LC)\, e(t) + \nu(t) - L\eta(t) \tag{5-27}$$

An interval observer for the system (5-27) provides the following dynamic interval estimation error:

$$\begin{aligned} \dot{\underline{e}}(t) &= (A - LC)\, \underline{e}(t) + \underline{\nu}(t) - L\underline{\eta}(t) \\ \dot{\overline{e}}(t) &= (A - LC)\, \overline{e}(t) + \overline{\nu}(t) - L\eta(t) \end{aligned} \tag{5-28}$$

With $\nu(t)$ defined as a bounded disturbance signal:

$$\nu(t) \in [\underline{\nu}(t), \overline{\nu}(t)]$$

and $\eta(t)$ defined as a bounded noise signal:

$$\eta(t) \in \left[\underline{\eta}(t), \overline{\eta}(t)\right],$$

if $\| \overline{\nu}(t) - \underline{\nu}(t) \|$ and $\| \overline{\eta}(t) - \underline{\eta}(t) \|$ are uniformly bounded, then $\| \overline{x}(t) - \underline{x}(t) \|$ is also uniformly bounded. Furthermore, if $\nu(t) = \underline{\nu}(t)$ and $\overline{\eta}(t) - \underline{\eta}(t) = 0$ for $t \geq 0$, then $\| \overline{x}(t) - \underline{x}(t) \| \rightarrow 0$. Under these conditions, the relationship between (5-27) and (5-28) is equivalent because, by the arithmetic properties of the intervals, $\overline{e}(t) - \underline{e}(t) = e(t)$.

Based on the theory presented, the residual derived from the observers of the interval uses the estimated interval state $\hat{x}^I = [\underline{\hat{x}}(t), \overline{\hat{x}}(t)] \in \mathbb{IR}^n$ and the output state vector $x(t) \in \mathbb{R}^n$. This incorporates the following two estimation errors discussed in this study.

$$\begin{aligned} \underline{e}\,(t) &= \underline{\hat{x}}\,(t) - x\,(t) \\ \overline{e}\,(t) &= \overline{\hat{x}}\,(t) - x\,(t) \end{aligned} \tag{5-29}$$

The expressions stated in (5-29) are feasible under the conditions of monotonic inclusion. According to the theory presented, monotonic inclusion occurs when an interval observer is constructed based on a positive representation.

A residue generator $r(t)$ is defined as the relationship between

$$r\,(t) = y_m\,(t) - \hat{y}\,(t) \tag{5-30}$$

where $y_m(t)$ is the measured output state, that is, $y_m(t) = Cx(t)$ and $\hat{y}(t)$ is the estimated state, then an interval residue is proposed as:

$$\underline{r}\,(t) = C\underline{e}(t) = C\underline{\hat{x}}\,(t) - Cx\,(t) \tag{5-31}$$

$$\overline{r}\,(t) = C\overline{e}(t) = C\overline{\hat{x}}\,(t) - Cx\,(t) \tag{5-32}$$

Equations (5-31) and (5-32) fulfill the conditions of monotonicity, with the existence of an interval residue being ensured.

$$r^I\,(t) = \left[\ \underline{r}\,(t) \quad , \quad \overline{r}\,(t)\ \right] \tag{5-33}$$

Based on the logical proposition above, the following fault-detection rule is defined:

$$\text{Decision} \ : \begin{cases} \text{NF}, & \text{if } r(t) \in \Big[\underline{r}(t),\, \overline{r}(t)\Big], \\ \text{FE}, & \text{if } r(t) \notin \Big[\underline{r}(t),\, \overline{r}(t)\Big]. \end{cases}$$

where

$$NF : f(t) = 0$$

and

$$FE : f(t) \neq 0$$

5.3 Theoretical calculation of the minimum leak area

In this part we exploit the interval residual produced by the observer,

$$r^I(t) = \Big[\underline{r}(t),\, \overline{r}(t)\Big],$$

to derive a theoretical lower bound on the leak cross–sectional area that can be detected.

According to leak–flow models in Santos-Ruiz et al. (2018); Torres et al. (2014), the leakage discharge Q_l relates to the leak area A_l and the local piezometric head H_f via

$$Q_l = \lambda\sqrt{H_l}, \qquad \lambda = C_d\sqrt{2g}\, A_l,$$

where C_d is the discharge coefficient and g is the gravitational acceleration.

Because the observer returns an interval residual, a leak is declared whenever the leakage flow exceeds the residual width, i.e.

$$Q_l \ \geq \ \overline{r}(t) - \underline{r}(t). \tag{5-34}$$

Combining (5-34) with the expression for Q_l yields a lower bound on the detectable leak area:

$$A_l \ \geq \ \frac{\overline{r}(t) - \underline{r}(t)}{C_d\sqrt{2g\, H_l}}. \tag{5-35}$$

Equation (5-35) thus provides the *minimum leak area* that the interval observer can reliably detect using the interval residual $r^I(t)$.

5.4 Numerical Simulations

As outlined in Chapter Three, which describes the fluid model flowing through a pipeline, this chapter applies the interval observer design method to the fault detection and isolation (FDI) analysis. The analysis addresses two scenarios: the first treats the fault signal as an unknown input, while the second considers the fault as two additional states in the linearized system.

5.4.1 Fault as an unknown input

Given the following nonlinear model,

$$\Gamma_{\text{NLF}}: \begin{cases} \dot{\zeta}(t) = f(\zeta) + G\,\nu(t) + f_a(t), \quad \zeta(0) = \zeta_0, \\ \eta(t) = h(\zeta) + f_s(t), \end{cases} \tag{5-36}$$

This model is linearized according with that exposed in (3.2.2), hence the system model can be written as,

$$\Upsilon_{\text{LF}}: \begin{cases} \dot{x}(t) = Ax(t) + Bu(t) + f_a(t), \quad x(t_0) = x_0, \\ y(t) = Cx(t) + f_s(t)\,, \end{cases} \tag{5-37}$$

where $x(t) = \zeta(t) - \zeta^*$ is the *state*, $u(t) = \nu(t) - \nu^*$ is the *control input*, and $y(t)$ is the *output* of the system Υ_{L}. In addition, we consider $f_a(t)$ to represent the term of faults and $f_s(t)$ to be the fault signal of the sensors. The latter terms $f_a(t) = 0$ and $f_s(t) = 0$ are given in the nominal case. $A \in \mathbb{R}^{3\times3}$ and $B \in \mathbb{R}^{3\times2}$ are defined as Jacobian matrices of $f(\zeta) + G\nu$ with respect to ζ and ν, respectively. In addition, $C \in \mathbb{R}^{2\times3}$ is the Jacobian measurement matrix of $h(\zeta)$ with respect to ζ. Such Jacobian matrices are expressed as

$$A = \begin{bmatrix} -2\mu_1\zeta_{10} & -\dfrac{a_1}{\Delta z_1} & 0 \\ \dfrac{a_2}{\Delta z_1} & -\dfrac{a_2\lambda_1}{2\Delta z_1\sqrt{\zeta_{20}}} & -\dfrac{a_2}{\Delta z_1} \\ 0 & \dfrac{a_1}{L-\Delta z_1} & -2\mu_2\zeta_{30} \end{bmatrix}, \quad B = \begin{bmatrix} \dfrac{a_1}{\Delta z_1} & 0 \\ 0 & 0 \\ 0 & -\dfrac{a_1}{L-\Delta z_1} \end{bmatrix}, \quad C = \begin{bmatrix} 1 & 0 & 0 \\ 0 & 0 & 1 \end{bmatrix}. \tag{5-38}$$

With the system linearized and the leak considered as the fault signal $f_a(t)$. The fault signal is modeled from the parameter λ given as:

$$f_a = \lambda_1 \mathcal{H}_l\,(t - t_l)$$

The interval observer outlined in Section 5.2.1 is designed to detect a pipeline leak based on the data in Table **5-1**.

Here, L denotes the pipeline length; D the pipeline diameter; A_T the cross-sectional area; g the acceleration due to gravity; b the fluid velocity; and μ_1, μ_2 are coefficients related to

Table 5-1: Numeric values of the parameters.

Parameter	Numeric value	Units
L	132.56	m
D	0.105	m
A_T	0.0087	m^2
g	9.81	m/s^2
b	1250	m/s
μ_1	0.005	m^{-3}
μ_2	0.005	m^{-3}

the fluid's physical properties, with $H_{in} = 18m$ and $H_{out} = 6m$

The results obtained for the interval observer with the f_a appears as a leak is $t_{fault} = t_{leak} = 70sec$, and its is shown in the following figures.

The residue of the interval proposed through only the interval estimations of $\hat{Q}^I_{in}$ and $\hat{Q}^I_{out}$ is shown in Figure **5-2**.

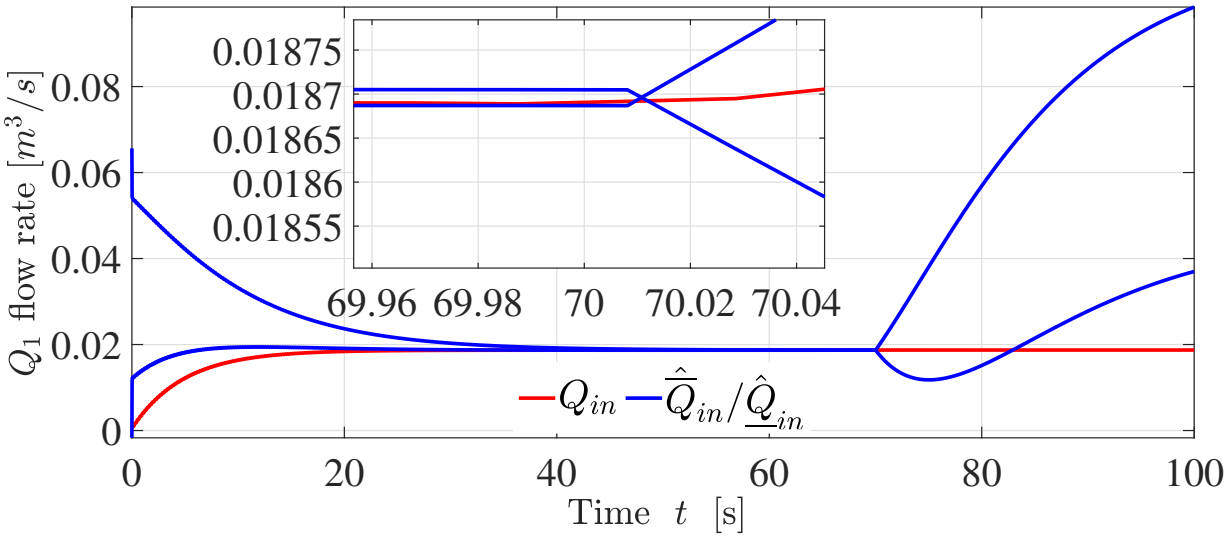

Figure 5-1: Inlet flow rate Q_{in} and interval estimate Q^I_{in}

As the figures demonstrate, the interval residual reacts immediately when the fault appears, and the threshold—tuned with the data in Figure 5-1—updates accordingly. The

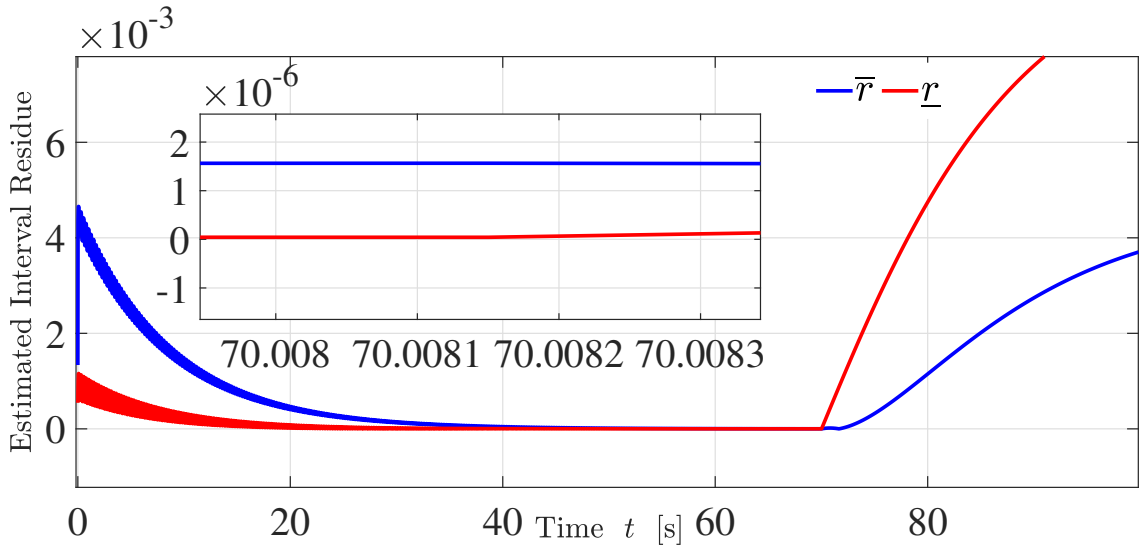

Figure 5-2: Estimated interval residue $\hat{r}^I$

detection algorithm is then activated whenever the following logical condition holds::

$$\begin{cases} \text{If } \underline{\hat{r}}(t) < 0 \quad \vee \quad \hat{\overline{r}}(t) > \alpha \quad \Longrightarrow 1 \\ \\ \text{If } \underline{\hat{r}}(t) > 0 \quad \vee \quad \hat{\overline{r}}(t) < \alpha \quad \Longrightarrow 0 \end{cases} \tag{5-39}$$

where 1 is fault condition and 0 is not fault condition, and $\alpha = 1.8 \times 10^{-6}$.

Remark 12. *Despite this, the observer gain L obtained for the interval observer ensures robustness against disturbances and measurement noise. This robustness is achieved because*

(i) the disturbances and noise are bounded with known limits, and

(ii) their positive representations remain non negative,

thereby upholding the analytical requirements for positive system behavior.

Sensitivity Analysis of Fault Impact on the interval residue

In this part, we analyze how treating the fault signal $f(t)$ as an unknown input affects the behavior of the interval residual for the estimated interval output states $\hat{Q}_{in}^{T}$ and $\hat{Q}_{out}^{T}$. As shown in Figures **5-1** and **5-2**, the sudden occurrence of a leak immediately triggers the detection threshold, indicating that the interval states are highly sensitive to faults. At the same time, the estimated interval states remain robust against both disturbances and noise. However, the width of the detection threshold depends on the leak's position along the pipeline: if the leak is located at certain points, the threshold can widen enough that a small leak becomes indistinguishable from other disturbances and goes undetected. This scenario can critically impair system performance. Conversely, if the threshold becomes too narrow, normal disturbances may be mistaken for a leak, producing false alarms. In other words, when the leak position causes the threshold to increase excessively, faults may be missed; when it causes the threshold to decrease too much, benign disturbances may trigger spurious leak alarms.

5.4.2 Augmented system representation with added fault states

In this section, the linearized system Υ_{LF} discussed in Chapter 3, Section 3.2.2, requires the incorporation of two new states into the A matrix. The first state, Δz_1, represents the position of the leak, and the second state, λ_1, corresponds to the leak size parameter. These states are static within the system dynamics, meaning that their time derivatives are zero, i.e., $\dot{\Delta} z_1 = 0$ and $\dot{\lambda}_1 = 0$. According to the exposed, the state matrices for the linearized system described in (4-1) are the following: The system to considered is the class of uncertain and perturbed systems in Υ_{F} in (4-31), with the states $x = [Q_1,\, H_2,\, Q_2,\, \Delta_z,\, \lambda]$. It should be noted that the position and magnitude of the fault are added to the state vector. Hence, the matrices of Υ_{F} as

$$A = \begin{bmatrix} -2\mu\zeta_{10} & -\dfrac{a_1}{\zeta_{40}} & 0 & -\dfrac{a_1\left(\nu_{10}-\zeta_{20}\right)}{\zeta_{40}^2} & 0 \\ \dfrac{a_2}{\zeta_{40}} & -\dfrac{a_2\zeta_{50}}{2\sqrt{\zeta_{20}}\zeta_{40}} & -\dfrac{a_2}{\zeta_{40}} & -\dfrac{a_2\left(\zeta_{10}-\zeta_{50}\sqrt{\zeta_{20}}-\zeta_{30}\right)}{\zeta_{40}^2} & -\dfrac{a_2\sqrt{\zeta_{20}}}{\zeta_{40}} \\ 0 & \dfrac{a_1}{L-\zeta_{40}} & -2\mu\zeta_{30} & \dfrac{a_1\left(\zeta_{20}-\nu_{20}\right)}{\left(L-\zeta_{40}\right)^2} & 0 \\ 0 & 0 & 0 & 0 & 0 \\ 0 & 0 & 0 & 0 & 0 \end{bmatrix}, \tag{5-40}$$

where the vector of equilibrium values is

$$\boldsymbol{\zeta} = \begin{pmatrix} \zeta_{1,0} \\ \zeta_{2,0} \\ \zeta_{3,0} \\ \zeta_{4,0} \\ \zeta_{5,0} \end{pmatrix}, \qquad \text{with} \quad \zeta_{1,0} = Q_1,\ \zeta_{2,0} = H_2,\ \zeta_{3,0} = Q_2,\ \zeta_{4,0} = \Delta_z,\ \zeta_{5,0} = \lambda_1.$$

with $\nu_{1,0}$ and $\nu_{2,0}$ are the equilibrium values of the input pressure heads, namely the upstream head H_1 and the downstream head H_3, respectively.

$$B = \begin{bmatrix} \dfrac{a_1}{\zeta_{40}} & 0 \\ 0 & 0 \\ 0 & -\dfrac{a_1}{L-\zeta_{40}} \\ 0 & 0 \\ 0 & 0 \end{bmatrix}, \quad C = \begin{bmatrix} 1 & 0 & 0 & 0 & 0 \\ 0 & 0 & 1 & 0 & 0 \end{bmatrix}. \tag{5-41}$$

Remark 13. *The method presented in Chapter 4 of this thesis for designing an interval observer has performance limitations. In equation 5-40, the augmented matrix A contains two zero rows, making it difficult to satisfy both LMI conditions* (4-24) *and* (4-25) *simultaneously—observability may be compromised, and no feasible solution is found. In contrast, the*

positive-representation approach directly yields an observer gain by requiring only the single LMI condition (5-24) *to be solved.*

Remark 14. *The position of the leak modifies the location of the system's poles; in extreme conditions, when $\Delta_z \to L$ (with L being the length of the duct) or $\Delta_z \to 0$, the matrix A tends to become singular and the system approaches marginal stability. Likewise, the observability and detectability properties may be compromised, since the corresponding matrices can lose rank. In the case of the interval observer, these circumstances increase the width of the estimation interval, which reduces the observer's sensitivity to detect faults when the leak is located at the duct's extremes, either at the beginning or at the end.*

Using the numerical data from Table **5-1**, the observer of the interval was incorporated, producing the following results.

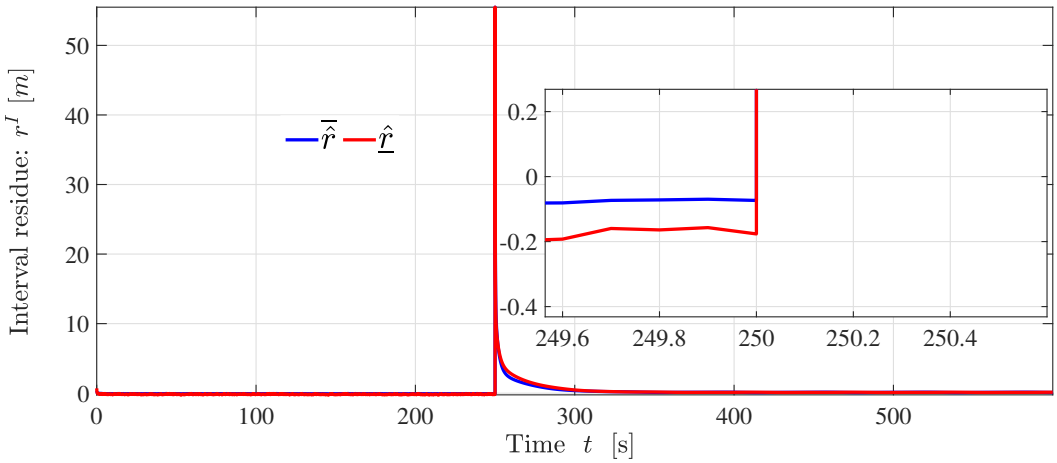

Figure 5-3: Proposed Interval residue

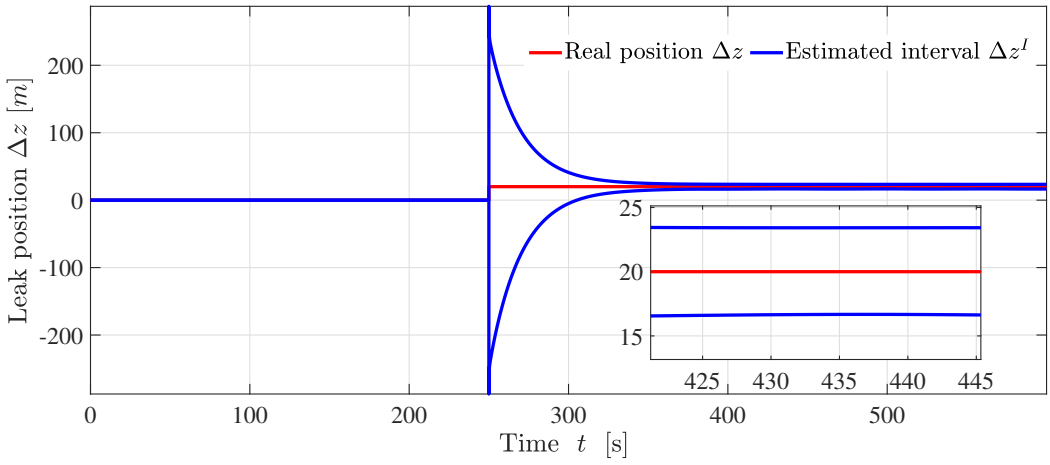

Figure 5-4: Leak position an interval leak position

According to Figure **5-3**, the residual interval effectively detects the occurrence of the fault, marking the detection phase in the FDI analysis. Figure **5-4** presents the actual leak position along with the interval estimates of the designed observer, representing the isolation phase. Lastly, Figure **5-5** demonstrates the reconstruction phase, achieved by estimating the fifth state by the observer of the interval.

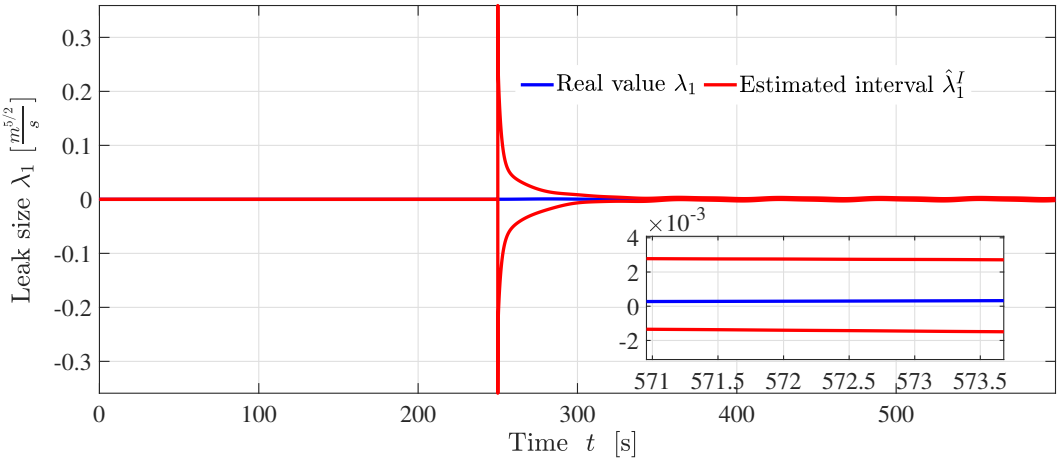

Figure 5-5: Leak size

Table 5-2: Parameters of the pilot pipeline and fluid Santos-Ruiz et al. (2018)

Parameter	Value
Pipeline diameter	4.86 cm
Pipeline length	112.22 m
Tested leak position Δz	39.99 m
Fluid kinematic viscosity, ν	8.03×10^{-7} $\frac{m^2}{s}$
Fluid density, ρ	996.59 $\frac{kg}{m^3}$
Gravity acceleration, g	9.79 $\frac{m}{s^2}$
Pressure wave speed, b	1250 $\frac{m}{s}$

5.5 Experimental data

Based on the design approach described and following the structure of the observer in an interval, an application is derived from the scenario discussed by Santos-Ruiz et al. (2018). In their work, the authors utilized an extended Kalman Filter (EKF) to propose an estimation method that incorporates pressure head and flow rate measurements at the end of the pipeline. These measurements inherently include sensor and process noise. The EKF performs detection and isolation within this system, using real-time information tested using a USB data acquisition device implemented in the MATLAB environment. The table 5-2 outlines the characteristics of the real pipeline model used in the design of the interval observer.

The results obtained under these conditions are as follows.

Figure **5-6** depicts the behavior of the interval residue, where fault detection is evident through the change observed around 70 seconds. These findings are consistent with those

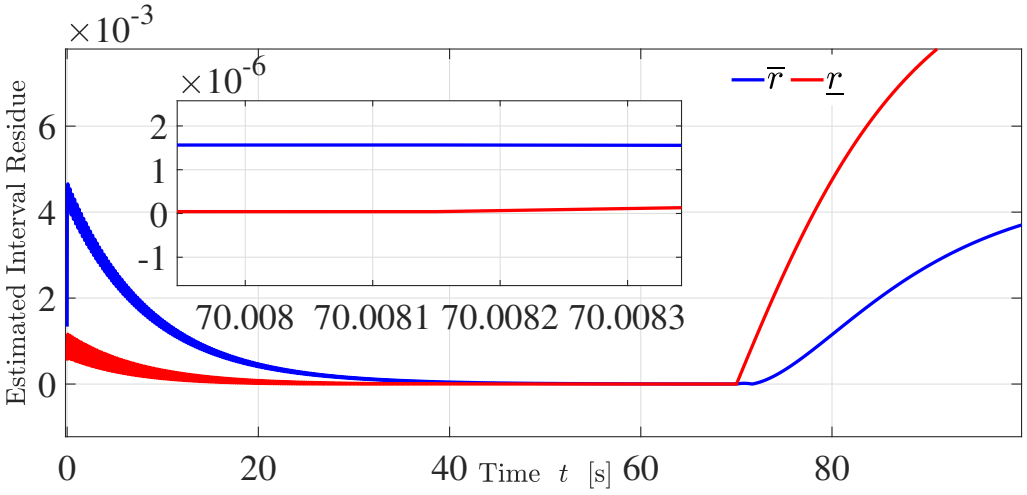

Figure 5-6: Interval Residue for the system with three states

reported by Santos-Ruiz et al. (2018). The results of the interval estimations confirm the monotonicity properties of the proposed interval observer.

5.5.1 Augmented system representation with added fault states

Similarly to the previous discussion, using the same experimental data provided by Santos-Ruiz et al. (2018) and the numerical data from Table 5-2, the interval observer proposed in this chapter was implemented. The results are presented in the following figures:

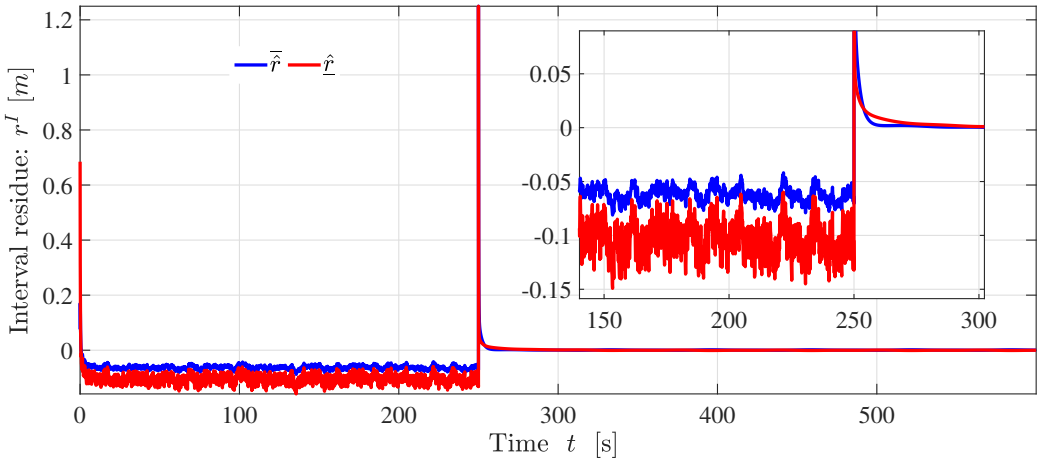

Figure 5-7: Interval residual for the augmented system

As shown in the figures, Figure **5-7** shows the residual interval, which indicates the detection of the leak at the time the leak occurred. Figure **5-8** presents the leak position, where

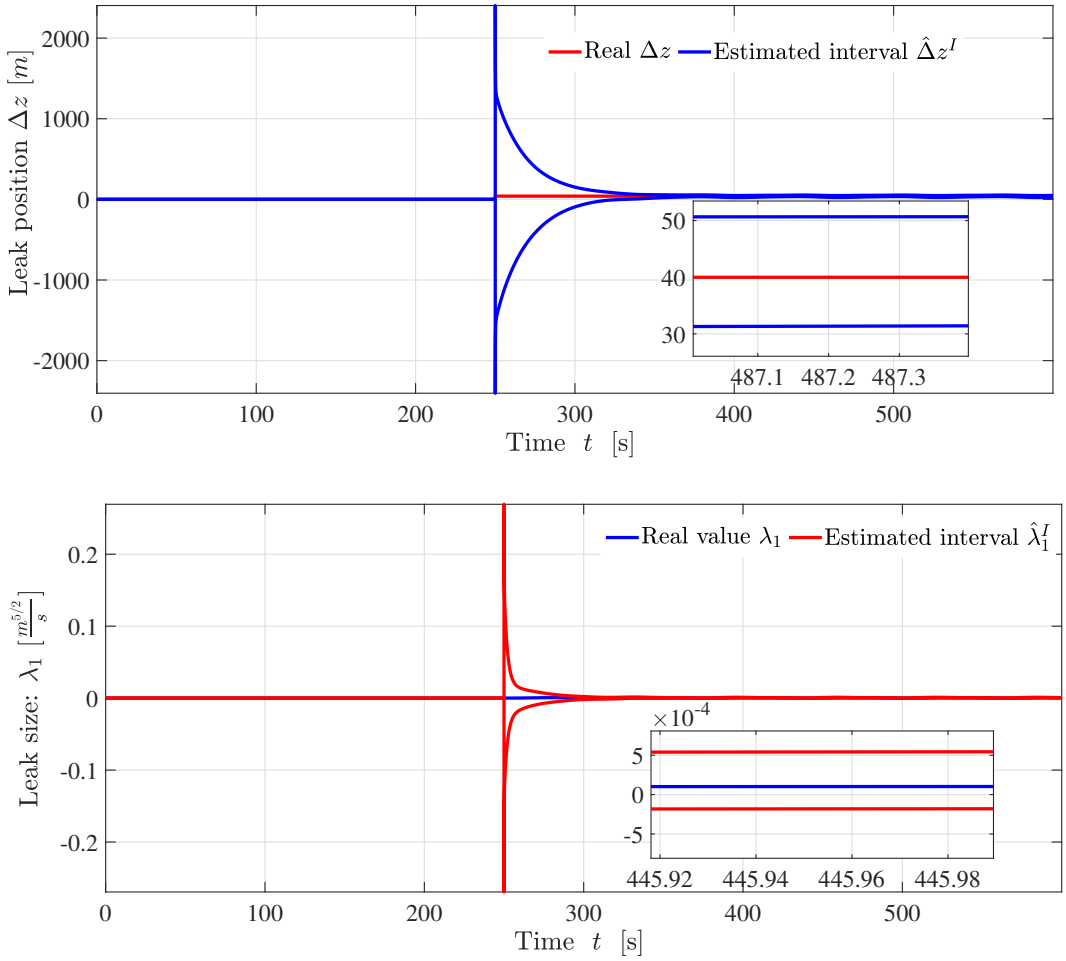

Figure 5-8: Leak position and size, and estimated intervals of position and size

the actual position was 40 meters, with the interval estimates centered on a mean value of approximately 40 meters. The mean interval value is given by:

$$w = \frac{\hat{\overline{\Delta}} z + \hat{\underline{\Delta}} z}{2} = \frac{50 + 32}{2} = 41m$$

When the actual position is 40 m, the interval estimation shows high accuracy. In the reconstruction phase, the interval estimate is also very close to the true value of λ_1, indicating good performance.

5.6 Detection of sequence faults through interval observer banks

This section outlines a procedure for detecting sequence faults, which is not yet extensively explored in the literature for the specific systems requiring study. For example, evaluating multiple leaks in a pipeline using analytical models (state observers) can be challenging. This difficulty arises due to the complex physical configuration described by the momentum equation and the continuous equation of the mathematical model for fluid movement in pipelines, as detailed in Chapter 4. When multiple leaks are present, pressure measurements become less definitive as the relationships between them are unclear. For more details, refer to Verde (2001). In response to this, other researchers have proposed experimental methods, such as Wang et al. (2019), to simplify complex analytical approaches. The primary goal of this section is to present a direct analytical method that utilizes inclusion techniques with interval estimations provided by interval observers.

5.6.1 Proposed Analytical Framework

To present this framework, the following lemma is provided:

Lemma 5. *Given two consecutive interval estimations:*

$$\begin{aligned} \hat{x}_i^I &= \left[\begin{array}{cc} \underline{\hat{x}}_{i=1} & \overline{\hat{x}}_{i=1} \end{array} \right] \\ \hat{x}_i^I &= \left[\begin{array}{cc} \underline{\hat{x}}_{i=2} & \overline{\hat{x}}_{i=2} \end{array} \right] \end{aligned} \tag{5-42}$$

for all $i = 1, \ldots, n$, where n denotes the interval observer scheme to be positioned along the duct and used as sensors for detecting one or more leaks. It must be ensured that there are necessary and sufficient conditions for the independence of the estimates provided by each interval observer relative to the other interval observers.

The following necessary and sufficient conditions are based on Definitions 3, 9, and 10 provided in Chapter 2 of this thesis. The necessary conditions are that the inclusion function exists for each interval estimation that is in relation with the estimated interval associated respectively with the input and output states:

$$\hat{x}_{input}^I = \left[\begin{array}{ccc} \underline{\hat{x}}_{input} & , & \overline{\hat{x}}_{input} \end{array} \right]$$

and

$$\hat{x}_{output}^I = \left[\begin{array}{ccc} \underline{\hat{x}}_{output} & , & \overline{\hat{x}}_{output} \end{array} \right]$$

The necessary conditions for representing a set of leaks are that each state pair indicates the presence of a specific leak through the interval hull union (see Chapter 2, Definitions

4 and 5), where one part of the pair is included within the other. The pairs considered are the input and output interval estimations. The sufficient condition for performing Fault Detection and Isolation (FDI) analysis on a sequence of leaks is that the logical intersection of two or more consecutive leaks must be zero.

Proof. Necessary conditions: The interval hull union ensures that one interval set is contained within another, as the union operation $\hat{x}^I_{\text{input}}$ and $\hat{x}^I_{\text{output}}$ are related through the containment of one within the other.

$$\hat{x}^I_{input} \cup \hat{x}^I_{output} \subseteq \hat{x}^I_{input} \underline{\cup} \hat{x}^I_{output}$$

Sufficient conditions: Given two sequences of leaks:

$$\hat{x}^I_{input} \mid_{leak \quad one} = \left[\ \underline{\hat{x}}_{input} \ , \ \overline{\hat{x}}_{input} \ \right] \underline{\cup} \hat{x}^I_{output} \mid_{leak \quad one} = \left[\ \underline{\hat{x}}_{output} \ , \ \overline{\hat{x}}_{output} \ \right]$$
$$\equiv \hat{x}^I{}_{leak \quad one}$$
$$and$$
$$\hat{x}^I_{input} \mid_{leak \quad two} = \left[\ \underline{\hat{x}}_{input} \ , \ \overline{\hat{x}}_{input} \ \right] \underline{\cup} \hat{x}^I_{output} \mid_{leak \quad two} = \left[\ \underline{\hat{x}}_{output} \ , \ \overline{\hat{x}}_{output} \ \right]$$
$$\equiv \hat{x}^I{}_{leak \quad two}$$

Once it is verified that

$$\hat{x}^I_{input} \mid_{leak \quad one} \subseteq \hat{x}^I_{output} \mid_{leak \quad one}$$

or

$$\hat{x}^I_{output} \mid_{leak \quad one} \subseteq \hat{x}^I_{input} \mid_{leak \quad one}$$

which results in a new set of intervals through the logical union operation described, and the same applies to the other leak.

$$\hat{x}^I_{input} \mid_{leak \quad two} \subseteq \hat{x}^I_{output} \mid_{leak \quad two}$$

or

$$\hat{x}^I_{output} \mid_{leak \quad two} \subseteq \hat{x}^I_{input} \mid_{leak \quad one}$$

□

In conclusion, the sufficient condition for ensuring the independent detection of two or more sequential leaks is that the intersection operation between the two resultant unions must be zero.

$$\hat{x}^I{}_{leak \quad one} \cap \hat{x}^I{}_{leak \quad two} = 0$$

An application for detecting sequential leaks is now presented. Using a MATLAB algorithm, the number of observers required to provide independent estimations along the duct was determined. The conduit analyzed with this method is a prototype with characteristics similar to those of the one located at the Institute of Engineering at UNAM Torres et al. (2014).

The physical characteristics of the pipeline are as follows:

Table 5-3: numerical values

Variables		
pipeline diameter	=	$\phi = 0.25\ m$
pipeline length: L	=	$132.56\ m$
transversal area:A_r	=	$\frac{\pi\phi^2}{4}$=$0.0491\ m^2$
leak area:A_f	=	$A_r/100$
velocity:v	=	$1250\ \frac{m}{s}$
upstream pressure head: H_{in}	=	$7\ m$
downstream pressure head: H_{out}	=	$1\ m$
friction factor: f	=	0.0181076

As shown in Table **5-3**, the observer bank of the interval will be placed at the following leak points to perform the FDI analysis. Table **5-4** indicates that, for the specified pipeline, it is feasible to use a bank of 9 Luenberger-type interval observers with positive representation. This setup will establish a simulated estimation threshold to ensure that each interval observer can detect one or more simultaneous leaks. This is accomplished through the interval threshold set for each observer and its designated placement along the pipeline.

Table 5-4: Interval observer banks

Interval observer number	1	2	3	4	5	6	7	8	9
leak position (meters)	10	20	35	70	90	100	110	120	130

Figure **5-9** shows the scenario in which two of the observer banks listed in Table **5-3** have detected a leak simultaneously at 10 and 100 meters. This figure illustrates how each specific interval observer performs leak detection using interval estimation.

In this section, the conditions for simultaneous leak detection using analytical methods through interval observer banks are discussed. This approach offers a novel alternative to perform Fault Detection and Isolation (FDI) analysis. By assigning each leak to a separate interval observer, the observer model consistently remains of fifth order, as each simultaneous leak is addressed individually.

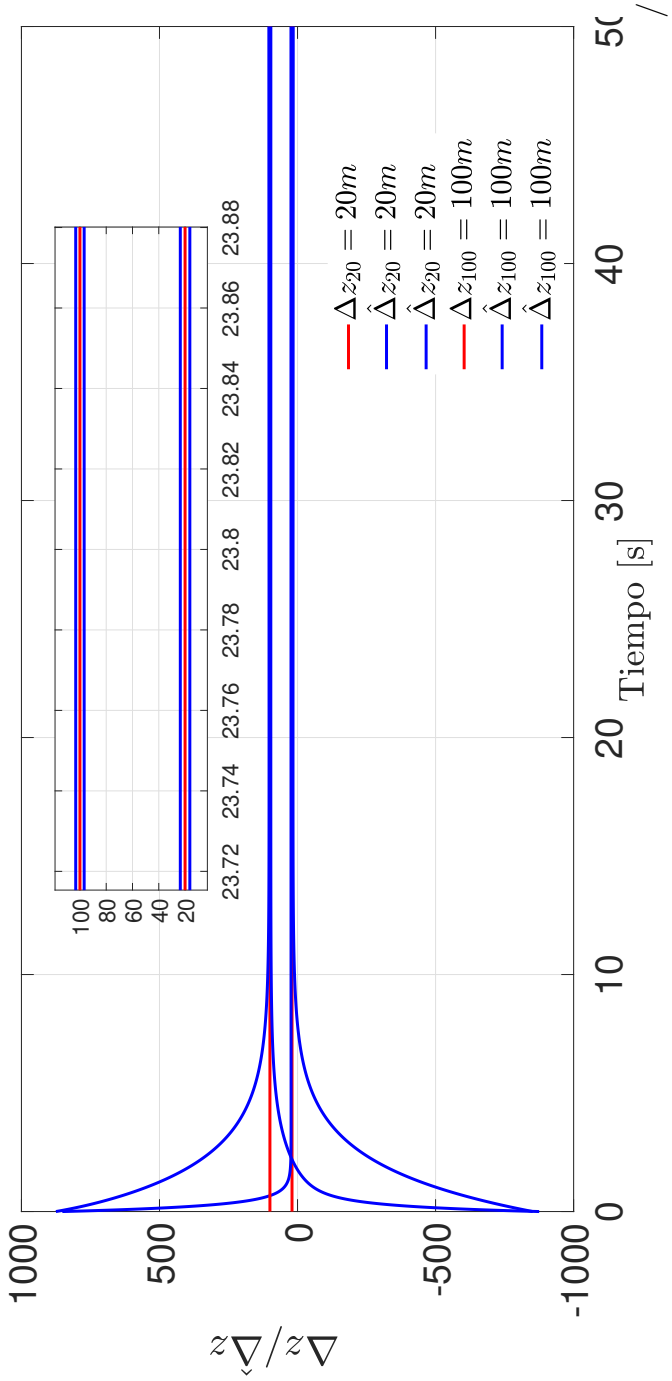

Figure 5-9: Simultaneous detection of two leaks

6 Conclusions and perspectives

This chapter summarizes the contributions of the thesis and provides recommendations for future work. Firstly, it will outline the main contributions and conclusions. Secondly, it will discuss future directions for this topic.

6.1 Main Conclusion

The main goal of this thesis is to develop and simulate an analytical FDI method using Interval Arithmetic theory, cooperative systems, and positive representations to detect, locate, and identify simultaneous faults (leaks) in a fluid transport pipeline. Specific objectives were set to propose observer designs in intervals based on a positive representation structure and cooperative systems. The validation of this design was applied to estimate a linearized pipeline model, which facilitates FDI analysis for leak detection and isolation. The positive representation of the interval observer can be tailored for plants subject to parametric uncertainties, disturbances, and noise.

- The study and analysis of analytical methods to define the existing FDI models applicable in fluid distribution networks, carried out in the development of this thesis, have allowed a deeper and more precise understanding of their functioning. Interval observers have been shown to improve performance and efficiency in fault detection, isolation, and reconstruction, especially in the case of pipeline leaks. This contributes to the advancement and continuous improvement of FDI analysis applied to the field of fluid distribution.

- This doctoral thesis addressed the analysis of the most widely used mathematical model to characterize the behavior of a fluid in a distribution network. The model is based on differential equations and encompasses all relevant physical properties governing fluid dynamics in distribution networks.

- Using the analytical properties of interval arithmetic theory, such as interval inclusion and compact sets, we developed an interval dynamic system from the linearized dynamic system derived from the non-linear model describing the flow of a fluid in a horizontal duct.

- The interval model describing the linearized system of fluid flow in a horizontal duct, along with the interval observer explicitly incorporating signals of disturbances and

noise, provides results that ensure a sufficient level of reliability for analyzing leak detection in ducts.

- This thesis achieved the development of a standardized fault diagnosis algorithm, based on interval arithmetic, by designing a positive representation interval observer. This algorithm was formulated as a Luenberger-type interval observer. It represents a significant advance in the ability to estimate fault detection, particularly leaks in ducts. The algorithm design relies on measurements of kinematic and kinetic characteristics of the fluid, such as flow rate, pressure, and velocity, to provide a good and precise assessment of the distribution system's condition. Implementing this algorithm not only improves the reliability of fault detection, but also promotes more effective management of the integrity of the duct network, thus enhancing operational safety and reducing the costs associated with unplanned fluid losses.

- The first interval observer is based on the positive representation and dissipativity conditions in order to estimate the state vector. Furthermore, a scheme of fault detection is proposed using a residual generator and adaptive thresholds. The method includes the design of the gains by means of Linear Matrix Inequalities. This interval observer is used to detect a leak in a pipeline when fluid is flowing through it.

- The second interval observer is designed to preserve the partial ordering between the estimations and state trajectories of the augmented plant based on cooperative systems. In addition, a fault detection and diagnosis scheme is added to detect, isolate, and reconstruct a leak. In addition, we incorporate a bank of observers to monitor the health of the pipeline model.

- The algorithm described above was evaluated using information from previous studies that had performed FDI analysis to detect leaks in pipelines, generating results consistent with those of those previous studies.

6.2 Future works

1. Based on the results obtained from the FDI analysis in pipelines, it is proposed to expand this study through additional experimental methods to validate and/or develop new analytical and simulation expressions.

   Specifically, the following recommendations are made for future work related to related areas of study in this doctoral thesis:

   - Develop robust interval estimation techniques for the isolation and reconstruction phase of the leak through analytical methods of interval optimization.
   - For the detection of two or more simultaneous leaks, it is possible to combine interval observers such as Luenberger, Unknown Inputs and Internal Observability (UIIO).
   - Propose new analytical methodologies of interval arithmetic to obtain an optimal bounded interval in FDI analysis, aiming to minimize the risk by excluding the presence of one or more false faults within the bounded interval.

2. It is expected that the analytical foundations presented in this doctoral thesis serve as a reference to motivate research groups in Colombia to join the international research community promoting applications of Interval Arithmetic in the field of Fault Detection and Identification (FDI).

.

Bibliography

Angeli, D. and Sontag, E. D. (2003). Monotone control systems. *IEEE Transactions on automatic control*, 48(10):1684–1698.

Avilés, J. D. and Moreno, J. A. (2014). Preserving order observers for nonlinear systems. *International Journal of Robust and Nonlinear Control*, 24(16):2153–2178.

Avilés, J. D. and Moreno, J. A. (2018). Interval observer design for nonlinear systems: Stability radii approach. *IEEE Access*, 6:52801–52813.

Besançon, G., Bornard, G., and Hammouri, H. (1996). Observer synthesis for a class of nonlinear control systems. *European Journal of control*, 2(3):176–192.

Besançon, G., Guillén, M., Dulhoste, J.-F., Santos, R., and Scola, I. R. (2013). Pipeline partial blockage modeling and identification. *IFAC Proceedings Volumes*, 46(11):730–735.

Brogliato, B., Lozano, R., Maschke, B., Egeland, O., et al. (2007). Dissipative systems analysis and control. *Theory and Applications*, 2:2–5.

Cacace, F., Germani, A., and Manes, C. (2015). A new approach to design interval observers for linear systems. *IEEE Transactions on Automatic Control*, 60(6):1665–1670.

Carrillo, J. A. C. et al. (2012). Método de detección y ubicación de fugas, en ductos de gran longitud, mediante velocidad de propagación de onda de presión negativa, en ductos con mediciones de presión multipunto.

Chaudhry, M. H. (2014). *Transient-Flow Equations*, pages 35–64. Springer New York, New York, NY.

Chow, E. and Willsky, A. (1984). Analytical redundancy and the design of robust failure detection systems. *IEEE Transactions on Automatic Control*, 29(7):603–614.

Cruz, E. C., Esmeral, J. I. S., and Velásquez, J. D. A. (2023). Open-loop stability analysis of interval dynamic systems. In *Workshop on Engineering Applications*, pages 92–103. Springer.

Cugueró-Escofet, M. A., Puig, V., Quevedo, J., and Blesa, J. (2015). Optimal pressure sensor placement for leak localisation using a relaxed isolation index: Application to the barcelona water network. *IFAC-PapersOnLine*, 48(21):1108–1113.

Deif, A. S. (1990). *Adv Matrix Theory Sci Eng*. CRC Press.

Delgado-Aguiñaga, J., Becerra-López, F., Torres, L., Besançon, G., Puig, V., and Magaña, M. J. (2020). Dynamic model for a water distribution network: Application to leak diagnosis and quality monitoring. *IFAC-PapersOnLine*, 53(2):16679–16684.

Delgado-Aguiñaga, J., Besancon, G., Begovich, O., and Carvajal, J. (2016). Multi-leak diagnosis in pipelines based on extended kalman filter. *Control Engineering Practice*, 49:139–148.

Delgado-Aguiñaga, J. A., Santos-Ruiz, I., Besançon, G., López-Estrada, F. R., and Puig, V. (2022). Ekf-based observers for multi-leak diagnosis in branched pipeline systems. *Mechanical Systems and Signal Processing*, 178:109198.

Drogkoula, M., Kokkinos, K., and Samaras, N. (2023). A comprehensive survey of machine learning methodologies with emphasis in water resources management. *Applied Sciences*, 13(22):12147.

Efimov, D., Raïssi, T., Chebotarev, S., and Zolghadri, A. (2013). Interval state observer for nonlinear time varying systems. *Automatica*, 49(1):200–205.

Fares, A., Tijani, I., Rui, Z., and Zayed, T. (2023). Leak detection in real water distribution networks based on acoustic emission and machine learning. *Environmental Technology*, 44(25):3850–3866.

Gao, Z., Cecati, C., and Ding, S. X. (2015). A survey of fault diagnosis and fault-tolerant techniques—part i: Fault diagnosis with model-based and signal-based approaches. *IEEE transactions on industrial electronics*, 62(6):3757–3767.

Gertler, J. (1997). Fault detection and isolation using parity relations. *Control Engineering Practice*, 5(5):653–661.

Gertler, J. (1998). *Fault Detection and Diagnosis in Engineering Systems*. Electrical Engineering & Electronics. CRC Press, 1 edition.

Hadroug, N., Hafaifa, A., Kouzou, A., and Chaibet, A. (2017). Dynamic model linearization of two shafts gas turbine via their input/output data around the equilibrium points. *Energy*, 120:488–497.

Isermann, R. (2005a). *Fault-diagnosis systems: an introduction from fault detection to fault tolerance*. Springer Science & Business Media.

Isermann, R. (2005b). Model-based fault-detection and diagnosis–status and applications. *Annual Reviews in control*, 29(1):71–85.

Jaulin, L. and Walter, E. (1993). Set inversion via interval analysis for nonlinear bounded-error estimation. *Automatica*, 29(4):1053–1064.

Karim, M. Z. A., Alrasheedy, A., and Gaafar, A. (2015). Compensated mass balance method for oil pipeline leakage detection using scada. *Int. J. Comput. Sci. Secur.(IJCSS)*, 9:293–302.

Khalil, H. K. (2002). *Nonlinear systems*. Prentice Hall, 3rd ed edition.

Khan, A., Xie, W., Zhang, L., and Liu, L.-W. (2020). Design and applications of interval observers for uncertain dynamical systems. *IET Circuits, Devices & Systems*, 14(6):721–740.

Khan, A. Q. (2010). *Observer-based fault detection in nonlinear systems*. PhD thesis, Duisburg, Essen, Univ., Diss., 2010.

Lorenzo Farina, S. R. (2011). *Positive Linear Systems -Theory and Applications*. John Wiley & Sons.

Meslem, N., Martinez, J., Ramdani, N., and Besançon, G. (2020). An interval observer for uncertain continuous-time linear systems. *International Journal of Robust and Nonlinear Control*, 30(5):1886–1902.

Moore, R. E. (1987). *Methods and applications of interval analysis*. SIAM studies in applied mathematics 2. LAP LAMBERT Academic Publishing, 1 edition.

Moore, R. E., Kearfott, R. B., and Cloud, M. J. (2009). *Introduction to interval analysis*. SIAM.

Navarro-Díaz, A., Delgado-Aguiñaga, J.-A., Begovich, O., and Besançon, G. (2021). Two simultaneous leak diagnosis in pipelines based on input–output numerical differentiation. *Sensors*, 21(23):8035.

Raïssi, T., Videau, G., and Zolghadri, A. (2010). Interval observer design for consistency checks of nonlinear continuous-time systems. *Automatica*, 46(3):518–527.

Raïssi, T., Ramdani, N., and Candau, Y. (2005). Bounded error moving horizon state estimator for non-linear continuous-time systems: application to a bioprocess system. *Journal of Process Control*, 15(5):537–545.

Roberson, J. A., Cassidy, J. J., and Chaudhry, M. H. (1998). Hydraulic engineering. Technical report.

Samy, I. and Gu, D.-W. (2011). *Fault Detection and Isolation (FDI)*, pages 5–17. Springer Berlin Heidelberg, Berlin, Heidelberg.

Santos-Ruiz, I., Bermúdez, J. R., López-Estrada, F. R., Puig, V., Torres, L., and Delgado-Aguiñaga, J. (2018). Online leak diagnosis in pipelines using an ekf-based and steady-state mixed approach. *Control Engineering Practice*, 81:55–64.

Shary, S. (2018). A note on definitions of the rank for interval matrices. *International Journal of Numerical Methods and Applications*, 17(2):91–96.

Sin, S. T. (2006). *Detección robusta de fallos utilizando análisis intervalar*. PhD thesis, Universitat Politècnica de Catalunya (UPC).

Sontag, E. D. (2007). The iss philosophy as a unifying framework for stability-like behavior. In *Nonlinear control in the year 2000 volume 2*, pages 443–467. Springer.

Torres, L., Verde, C., Carrera, R., and Cayetano, R. (2014). Algoritmos de diagnóstico para fallas en ductos. *Tecnología y ciencias del agua*, 5(4):57–78.

Verde, C. (2001). Multi-leak detection and isolation in fluid pipelines. *Control Engineering Practice*, 9(6):673–682.

Verde, C., Gentil, S., and Morales-Menéndez, R. (2013). *Monitoreo y diagnóstico automético de fallas en sistemas dinámicos*. Editorial Trillas.

Verde, C. and Visairo, N. (2001). Bank of nonlinear observers for the detection of multiple leaks in a pipeline. In *Proceedings of the 2001 IEEE International Conference on Control Applications (CCA'01)(Cat. No. 01CH37204)*, pages 714–719. IEEE.

Wang, X., Ghidaoui, M. S., and Lin, J. (2019). Identification of multiple leaks in pipeline iii: Experimental results. *Mechanical Systems and Signal Processing*, 130:395–408.

Willems, J. C. (1972a). Dissipative dynamical systems part i: General theory. *Archive for rational mechanics and analysis*, 45(5):321–351.

Willems, J. C. (1972b). Dissipative dynamical systems part ii: Linear systems with quadratic supply rates. *Archive for rational mechanics and analysis*, 45:352–393.

Yang, A. and Ma, S. (2021). Robust control for singular systems based on the uncertainty and disturbance estimator. *IEEE Access*, 9:109704–109717.